FACULTY OF ENGINEERING
AND ARCHITECTURE

Fourth and Fifth Generation District Heating Systems: Methodology, Design, and Development

Joseph Maria Jebamalai

Doctoral dissertation submitted to obtain the academic degree of
Doctor of Electromechanical Engineering

Supervisors

Prof. Jelle Laverge, PhD* - Prof. Lieven Vandevelde, PhD**

* Department of Architecture and Urban Planning
Faculty of Engineering and Architecture, Ghent University

** Department of Electromechanical, Systems and Metal Engineering
Faculty of Engineering and Architecture, Ghent University

April 2023

GHENT
UNIVERSITY

FACULTY OF ENGINEERING
AND ARCHITECTURE

Fourth and Fifth Generation District Heating Systems: Methodology, Design, and Development

Joseph Maria Jebamalai

Doctoral dissertation submitted to obtain the academic degree of
Doctor of Electromechanical Engineering

Supervisors
Prof. Jelle Laverge, PhD* - Prof. Lieven Vandevelde, PhD**

* Department of Architecture and Urban Planning
Faculty of Engineering and Architecture, Ghent University

** Department of Electromechanical, Systems and Metal Engineering
Faculty of Engineering and Architecture, Ghent University

April 2023

GHENT
UNIVERSITY

ISBN 978-94-6355-699-6
NUR 961, 978
Wettelijk depot: D/2023/10.500/31

Members of the Examination Board

Chair

Prof. Sabine Wittevrongel, PhD, Ghent University

Other members entitled to vote

Prof. Stefan Holler, PhD, HAWK University of Applied Sciences and Arts, Germany
Prof. Igor Krupenski, PhD, Tallinn University of Technology, Estonia
Prof. Steven Lecompte, PhD, Ghent University
Prof. Ivan Verhaert, PhD, Universiteit Antwerpen
Prof. Martijn van den Broek, PhD, Ghent University

Supervisors

Prof. Jelle Laverge, PhD, Ghent University
Prof. Lieven Vandevelde, PhD, Ghent University

Acknowledgment

It has been a wonderful six-year journey since I began my PhD in Belgium. When I was looking for a doctorate research opportunity in thermal systems, I was very interested in seeing one in district heating systems. Thank you Martijn van den Broek for selecting me to begin working in district heating systems. I worked on the EU H2020 HeatNet NWE project as well as a project with Comsof to develop design methodology for district heating systems. I'd like to thank all of the HeatNet project partners for their warm welcome and knowledge transfer from the pilot projects. Especially, I would like to thank the city of Kortijk, with whom I worked closely. I was also working on the Comsof project, specifically with Kurt and Wouter. During the early days of Comsof Heat, I had many meetings and brainstorming sessions with Kurt and Wouter. Thank you Martijn again, for your support and guidance during the early years.

I applied for Baekeland mandate funding through Comsof to conduct research on 4th and 5th generation district heating design features. Jelle Laverge, my academic supervisor, and Kurt Marlein, my industrial supervisor at Comsof, both contributed significantly to my success in the Baekeland mandate funding. They are the pillars of my successful PhD. I'd also like to thank Raf Meersman and Paul for making this research opportunity with Comsof possible. I'd like to thank Eline, Marc, and Elisa for guiding and assisting me with the application.

I would like to express my heartfelt gratitude to my academic supervisor, Jelle, for his unwavering support, guidance, and encouragement throughout my PhD journey. His knowledge, expertise, and commitment to excellence have been invaluable to me, and I could not have completed this research without his guidance and mentorship. I am grateful for the time and effort he dedicated to reviewing my work, providing constructive feedback, and challenging me to think critically about my research.

I wanted to take a moment to express my special thanks and deepest gratitude to my industrial supervisor, Kurt for all of his guidance and constant support throughout the journey. Your guidance and mentoring have been invaluable to my personal and professional development, and I feel incredibly fortunate to have had you as my supervisor. Thank you for always pushing me to do my best and encouraging me to pursue new opportunities. Your feedback has been insightful and has helped me in improving my work in ways that I never would have been able to do on my own. I am grateful for the time and effort you have invested in my development and for the opportunities you have given me to learn and grow. I truly feel that I have become a better person and professional under your guidance.

I'd also like to thank my co-supervisor, Lieven Vandevelde, for his assistance and advice. In addition, I'd like to thank the members of my thesis committee, Martijn van den Broek, Steven Lecompte, Ivan Verhaert, Stefan Holler, and Igor Krupenski, for their insightful feedback and constructive criticism, which helped me refine my research and improve the quality of my thesis. Their diverse perspectives and expertise in various fields have enriched and broadened my research.

I would like to thank my BFG research group colleagues as well as my Comsof colleagues for their support and insightful discussions. I'd like to thank Wouter D, Phillipe, Onne, Thomas De Praetere, Wouter VS, and Jonas VN in particular for their valuable input and assistance throughout my research.

My heartfelt gratitude goes to my family and friends for their unwavering support, encouragement, and love throughout my PhD journey. My heartfelt gratitude especially goes to my beloved wife, Gracia, for her consistent support and encouragement throughout the journey. Their belief in me has been a source of motivation and inspiration for me, and I could not have completed this research without their help. I am grateful for their sacrifices, patience, and understanding throughout the PhD process.

Finally, I'd like to thank the funding agency, Vlaio, for their financial support, which has allowed me to continue my research and complete my PhD. Their assistance has been critical in providing me with the resources and opportunities I needed to conduct my research. I would like to extend my gratitude to Leiedal who have contributed to this case study. I'd also like to thank Tom Prinze and Jullio for a number of technical discussions about district heating systems.

In conclusion, I would like to express my heartfelt appreciation to all those who have contributed to my academic journey and helped me to achieve this milestone. Thank you for all of your help, advice, and encouragement.

Table of Contents

Nomenclature

Abbreviations

2G 2nd Generation

3G 3rd Generation

3GDH 3rd Generation District Heating

4GDH 4th Generation District Heating

5GDH 5th Generation District Heating

CHP Combined Heating and Cooling

DC District Cooling

DH District Heating

DHC District Heating and Cooling

DHS District heating system

DHW Domestic Hot Water

EU European Union

GIS Geographic Information System

NOMENCLATURE

HIU Heat Interface Unit

HLV Heat load variation

ILP Integer Linear Programming

KPI Key Performance Indicator

LNG Liquefied Natural Gas

LTDH Low Temperature District Heating

MILP Mixed-Integer Linear Programming

NP complete Nondeterministic Polynomial-time Complete

PN Pressure Number

POC Proof-Of-Concept

PUR Polyurethane

PV Photo Voltaic

PV-T Photo Voltaic Thermal

TES Thermal Energy Storage

ULTDH Ultra-Low Temperature District Heating

Greek letters

ϵ Pipe roughness

λ_g Ground thermal conductivity (W/(m.K))

λ_i Coefficient of thermal conductivity for the PUR insulation

μ Dynamic viscosity $(kg/(m.s)$

ν Pump efficiency

ρ Fluid density (kg/m^3)

Parameters

Δh Head loss (m)

ΔP Pressure loss

ΔT Temperature difference between the supply and return pipes

ϵ/D_h Relative pipe roughness

A_j Internal area of pipe j (m^2)

C Pipe roughness coefficient

C^i Distance between the center lines of the two pipes (m)

c_p Fluid specific heat capacity (KJ/kg.K)

COP Coefficient of Performance

D Half the distance between the centres of the pipes (m)

D_c Outer diameter of the casing pipe (m)

D_i Internal diameter of pipe (m)

d_o Outer diameter of the service pipe (m)

D_{PUR} Diameter of the insulation material (m)

$E_{peak,m}$ Monthly peak heat demand (kWh)

f Darcy friction factor

g Local acceleration due to gravity, 9.81 m/s^2

NOMENCLATURE

G_d Daily variation

H Depth between the ground surface and the centre of the pipe (m)

h_f Head loss (m)

h_m Head loss due to bends, elbows, tees and valves

k Loss coefficient

L Pipe length (m)

LF Thermal load factor

m Mass flow rate (kg/s)

N Cumulative number of homes at each building demand point in the network

N_i Total number of homes connected to the respective pipe node

n_i Total number of hot water taps connected to the respective pipe node

P_a Annual average heat load (W)

P_d Daily average heat load (W)

P_h Hourly average heat load (W)

P_{pump} Pump power (kW)

Q Heat flow throw pipe (kW)

Q_f Heat loss of the supply pipe (W/m)

Q_r Heat loss of the return pipe (W/m)

$Q_{\mathbf{total}}$ Overall heat loss (W/m)

$Q_{CDHW,i}$ Cumulative domestic hot water peak load demand at node i (kW)

$Q_{CSH,i}$ Cumulative space heating peak load demand at node i (kW)

$Q_{DHW,i}$ Domestic hot water load at node i after applying simultaneity factor (kW)

Q_{el} Electricity required for the heat pump (kW)

Q_{heat}, n Heat required from the low temperature network (kW)

Q_{loss} Total heat loss for twin pipes (W/m)

$Q_{peak,DHW}$ Peak heat demand of domestic hot water (kW)

Q_{peak} Hourly peak heat demand (kW)

$Q_{SH,i}$ Space heating load at node i after applying simultaneity factor (kW)

Q_{TES} Thermal energy storage capacity

$Q_{total,i}$ Total heat load at node i after applying simultaneity factor (kW)

R_h Insulance of the heat exchange between the flow and return pipes

R_i Insulating material's insulance

r_i Inner pipe diameter (m)

r_o Outer pipe diameter (m)

R_s Soil's insulance

Re Reynolds number

NOMENCLATURE

$SF_{DHW,i}$ Domestic hot water simultaneity factor

$SF_{SH,i}$ Space heating simultaneity factor

t Total number of hours (h)

T_f Supply pipe temperature (K)

T_g Ground temperature (K)

T_H High temperature of storage tank (K)

T_L Low temperature of storage tank (K)

T_r Return pipe temperature (K)

T_s Soil temperature (K)

T_{avg} Average temperature of supply and return temperatures (K)

U_1 Heat loss coefficient from pipe (supply or return) to ground (W/mK)

U_2 Heat loss coefficient from supply pipe to return pipe (W/mK)

V Volume of storage (m^3)

V Volumetric flow rate (m^3/s)

v Mean flow velocity (m/s)

v_j Fluid velocity of pipe j (m/s)

Z Distance from the surface to the middle of the pipe (m)

Z_c Corrected depth z value that takes into account the soil surface transition insulance (m)

Summary

Global warming and climate change are one of the most pressing issues that compels the European Union (EU) to take action against carbon emissions. Additionally, the EU's excessive reliance on fossil fuels currently poses a threat to its energy security. Beginning with the EU's current energy supply scenario, Chapter 1 shows how dependent EU nations are on both energy and natural gas. The majority of the energy used in the EU comes from hydrocarbon sources. The EU currently relies heavily on oil, petroleum, and natural gas for its energy needs. Therefore, it is essential to quicken the transition to renewable energy for increased energy security, particularly given the current geopolitical environment. In the EU, heating and cooling account for 50% of all energy demand, with fossil fuels making for 75% of all energy use. So, to attain climate neutrality in Europe by 2050, the heating and cooling sector must be decarbonized, notably in the built environment.

District heating and cooling (DHC) networks play an important role in the decarbonization of the heating and cooling sector. A district heating network's design, dimensioning, and cost estimation present numerous difficulties. It takes a lot of time and effort to manually create a network layout, especially for large networks. Customized spreadsheets enable automatic hydraulic calculations and pipe selection, but they are not appropriate for big networks and can be error-prone when used improperly. Another spreadsheet is generally used to estimate the cost of network deployment. In short, the different design aspects typically require different software tools, and the process is usually not well integrated. This increases the cost and duration of the design process. Chapter 2 discusses solutions to the challenges stated above provided by an automated, geographic information system (GIS)-based planning tool. The district heating network dimensioning needed for a feasibility study is included in this tool, which was created as a plug-in to a GIS program. It also includes automated and optimized network routing algorithms. The tool was demonstrated using a case study of a neighborhood in Nijmegen, illustrating the impact of various design factors, such as network pressure level and substation size, on overall network dimensions, cost, and performance. The effects of several future heat demand scenarios on network costs and performance were evaluated through simulation.

SUMMARY

Future district heating networks must be adaptable enough to handle changes in heat production and heat load brought on by more intermittent renewable energy sources. For such flexibility, thermal energy storage (TES) is a tried-and-true, effective, and economical technology. In modern district heating systems, the most typical TES layout is a central hot water storage tank close to the source. Although this architecture offers flexibility and lowers peak load capacity, it has no effect on the network's peak transport capacities because heat must still be delivered from the source point during periods of high demand. The advantages of adding thermal storage tanks to distribution networks to balance local heat loads and reduce network peak transport capabilities are examined in Chapter 3. Using publicly available street-level gas consumption statistics, building heat demand information is extracted, and the right heat demand profiles are selected based on the kind of building. With the help of Comsof Heat, an automated district heating network routing and planning tool, a case study comparing centralized and distributed storage is conducted. The impact of these storage configurations on overall network costs is contrasted, and several scenarios with various storage volumes are investigated. According to the case study findings, centralized storage can lower network investment costs overall by 4%, substation-level storage can lower costs by 5%, and building-level storage can lower costs as much as 7% for the specified inputs.

Due to the growing need to include distributed waste heat and renewable energy sources, district heating systems are becoming decentralized. District heating systems are increasingly reliant on a variety of sources. With several sources, efficient routing of the district heating network is difficult. In order to select the most affordable route and source allocation for the building demand points, optimization is required. Using a combination of assignment and routing algorithms, Chapter 4 presents a method for automated routing and design of multi-source district heating networks. The developed method is used in Comsof Heat, a GIS-based district heating network planning and dimensioning tool, as a proof of concept. A case study with a municipality from Belgium is presented to illustrate the devised technique employing Comsof Heat. The effects on network expenses of various scenarios with various potential source options and building demand points will be compared. Based on the following factors: source investment cost, energy production cost, carbon cost, or combinations of the above, the tool is used to choose the best energy sources out of the many options shown. The chosen energy sources are then connected to the building's demand locations via network routing. In order to determine how design decisions affect costs and CO2 emissions, all of the simulated instances are compared at the end.

Building-side heat pumps and ultra-low-temperature systems are being tested in pilot projects, and district heating systems have evolved from steam systems (first generation) to low-temperature water-based systems (4th generation) (5th generation). Future (4th and 5th generation) district heating and cooling (DHC) networks will likely include distributed low-temperature sources, combined DHC systems, integrated heat and cold storage, and heat pumps on the building side, among other noteworthy characteristics. There are numerous difficulties in designing large-scale DHC networks with all of these properties. A technique for designing 3-pipe DHC networks and ultra-low temperature DHC networks employing a ring network structure will be discussed in Chapter 5 along with a comparison of the expenses of their respective networks. The developed method is employed as a proof of concept in the DHC design tool, Comsof Heat, and a case study is created to design, compare, and analyse the impact on the network cost of these two configurations. The results of the case study show that the cost of deploying a network for ultra-low temperature DHC rings is roughly 23% higher than for third-generation rings. Additionally, the availability of a free low-temperature waste heat source is a prerequisite for the economic viability of fifth generation ultra-low temperature networks.

DHC networks offer the supply-side flexibility to adapt and change over time, which is one of their key benefits. More and more low-grade energy sources can be used as building energy efficiency increases. In order to increase the heat and meet the energy needs of the buildings, heat pumps are frequently utilized in conjunction with low-grade energy sources. Building-side distributed heat pumps and district heating networks have recently been combined, which improves the network's energy efficiency. With this arrangement, a two-pipe network configuration can be used to supply both heat and cold. The number of central and room air conditioners installed increased by more than 50 times between 1990 and 2010 in the European Union, indicating a huge growth in the energy demand for space cooling during the 1990s. Furthermore, across Europe over the past 15 years, cooling degree days have grown while heating degree days have declined. This demonstrates how crucial space cooling is becoming. The arrangement of low-temperature water being circulated in the network and a building-side heat pump to raise or lower the temperature to the desired level is studied in Chapter 6 and compared to conventional district heating networks. While having a sustainable solution and greater energy efficiency is helpful for the environment, it's also critical to investigate the costs and primary energy usage. Therefore, Comsof Heat, an automated GIS-based district heating and cooling planning tool, is used to design the aforementioned configuration, and the costs of the network will be determined. The design and cost of this configuration are contrasted with those of conventional district heating networks in a case study location. The impact of various design factors is examined, and a variety of scenarios, including various electricity costs and coefficients of performance (COP), are analyzed. If a low temperature waste heat source is available, the overall cost of the ultra-low temperature district heating (ULTDH) network is 16% less than the typical network design throughout the course of the network's 35-year lifespan.

Samenvatting

De opwarming van de aarde en de klimaatverandering vormen één van de meest prangende kwesties die de Europese Unie (EU) dwingen om actie te ondernemen tegen koolstofemissies. Bovendien bedreigt de buitensporige afhankelijkheid van fossiele brandstoffen momenteel de energiezekerheid van de EU. Uitgaand van het huidige scenario van de EU voor energievoorziening, toont Hoofdstuk 1 hoe afhankelijk de EU-landen zijn van zowel energie en van aardgas in het bijzonder. Het grootste deel van de energie die in de EU wordt gebruikt, is afkomstig van koolwaterstofbronnen. De EU is momenteel sterk afhankelijk van aardolie, stookolie en aardgas voor haar energiebehoeften. Het is dan ook essentieel om de overgang naar hernieuwbare energie te versnellen voor meer energiezekerheid, vooral gezien de huidige geopolitieke situatie. In de EU zijn verwarming en koeling goed voor 50% van de totale energiebehoefte, waarbij 75% van al het energieverbruik op rekening komt van fossiele brandstoffen. Om tegen 2050 klimaatneutraliteit te bereiken in Europa, moet de verwarmings- en koelingssector dus koolstofvrij worden gemaakt, met name in de bebouwde omgeving.

Netwerken voor stadsverwarming en -koeling (DHC) spelen een belangrijke rol bij het koolstofvrij maken van de verwarmings- en koelingssector. Het ontwerp, de dimensionering en de kostenraming van een stadsverwarmingsnetwerk leveren tal van moeilijkheden op. Handmatig een netwerklay-out te maken kost veel tijd en moeite om, vooral voor grote netwerken. Er zijn aangepaste spreadsheets die automatische hydraulische berekeningen en pijpselectie mogelijk maken, maar die zijn niet geschikt voor grote netwerken en kunnen foutgevoelig zijn bij onjuist gebruik. Om de kosten van netwerkimplementatie te schatten wordt doorgaans dan weer een andere spreadsheet gebruikt. Kortom, de verschillende ontwerpaspecten vereisen doorgaans verschillende softwaretools en het proces is meestal niet goed geïntegreerd. Dit verhoogt de kosten en de duur van het ontwerpproces. Hoofdstuk 2 bespreekt oplossingen voor de bovengenoemde uitdagingen die een geautomatiseerd, op een geografisch informatiesysteem (GIS) gebaseerd planningshulpmiddel biedt. Dimensionering van het stadsverwarmingsnetwerk, nodig voor een haalbaarheidsstudie, is onderdeel van deze tool, die is gemaakt als een plug-in voor een GIS-programma. Hij bevat ook algoritmen voor geautomatiseerde en geoptimaliseerde routering van het netwerk. De tool werd gedemonstreerd aan de hand van een casestudie van een wijk in

Nijmegen, waarbij werd geïllustreerd wat de impact is van verschillende ontwerpfactoren, zoals het netwerkdrukniveau en de grootte van de substations, op de algehele netwerkafmetingen, kosten en prestaties. De effecten op netwerkkosten en -prestaties van verschillende toekomstige scenario's m.b.t. warmtebehoefte werden geëvalueerd door middel van simulatie.

Toekomstige stadsverwarmingsnetwerken moeten voldoende aanpasbaar zijn om veranderingen in warmteproductie en warmtebelasting aan te kunnen als gevolg van meer intermitterende hernieuwbare energiebronnen. Voor dergelijke flexibiliteit is warmte- en koudeopslag (WKO) een beproefde, effectieve en economische technologie. In moderne stadsverwarmingssystemen is de meest courante WKO-lay-out een centrale warmwateropslagtank dicht bij de bron. Deze architectuur biedt weliswaar flexibiliteit en verlaagt het piekvermogen, maar ze heeft geen effect op de piektransportcapaciteiten van het netwerk, omdat in periodes van grote vraag hoe dan ook warmte vanuit het bronpunt moet worden geleverd. De voordelen van het toevoegen van thermische opslagtanks aan distributienetwerken om lokale warmtebelastingen op te vangen en capaciteiten van het netwerk voor piektransport te verminderen, worden onderzocht in hoofdstuk 3. Uit de vrij beschikbare statistieken over gasverbruik op straatniveau wordt informatie over de warmtevraag van gebouwen gehaald en worden de juiste warmtevraagprofielen geselecteerd in functie van het soort gebouw. Met behulp van Comsof Heat, een geautomatiseerde routerings- en planningstool voor stadsverwarmingsnetwerken, wordt een casestudie uitgevoerd die gecentraliseerde en gedistribueerde opslag vergelijkt. De impact van deze opslagconfiguraties op de totale netwerkkosten

wordt afgewogen en diverse scenario's met verschillende opslagvolumes worden onderzocht. De bevindingen van de casestudy tonen aan dat gecentraliseerde opslag de investeringskosten van het netwerk globaal met 4% kan verlagen, dat opslag ter hoogte van de substations de kosten met 5% kan verlagen en dat opslag op ter hoogte van gebouwen de kosten met wel 7% kan verlagen voor de gespecificeerde inputs.

Vanwege de groeiende behoefte om gedistribueerde verlieswarmte en hernieuwbare energiebronnen op te nemen, worden stadsverwarmingssystemen gedecentraliseerd. Stadsverwarmingssystemen steunen in toenemende mate op verschillende bronnen. Met meerdere bronnen is een efficiënte routering van het stadsverwarmingsnet lastig. Om de voordeligste route en bron te selecteren die aan warmte-afnamepunten in gebouwen kan toegewezen worden, is optimalisatie nodig. Met behulp van een combinatie van toewijzings- en routeringsalgoritmen, presenteert Hoofdstuk 4 een methode voor geautomatiseerde routering en ontwerp stadsverwarmingsnetwerken met meerdere bronnen. De ontwikkelde methode wordt gebruikt als een proof of concept in Comsof Heat, een GIS-gebaseerde plannings- en dimensioneringstool voor stadsverwarmingsnetwerken. Een casestudy rond een gemeente uit België wordt gepresenteerd om de ontwikkelde techniek te illustreren met gebruik van Comsof Heat. De effecten op de netwerkkosten van diverse scenario's met verschillende mogelijke opties op het vlak van bronnen en warmte-afnamepunten in gebouwen worden vergeleken. Op basis van factoren zoals investeringskost voor een bron, energieproductiekost, koolstofkost of combinaties van bovenstaande, wordt de tool gebruikt om de beste energiebronnen te kiezen uit de vele getoonde opties. De gekozen energiebronnen worden vervolgens via netwerkroutering verbonden met de afnamelocaties van het gebouw. Om te bepalen hoe ontwerpbeslissingen de kosten en CO2-emissies beïnvloeden, worden alle gesimuleerde gevallen aan het einde vergeleken.

In proefprojecten worden testen gedaan met warmtepompen ter hoogte van gebouwen en ultra-lage-temperatuursystemen, en stadsverwarmingssystemen zijn geëvolueerd van stoomsystemen (eerste generatie) naar lage-temperatuursystemen op basis van water (4e en 5e generatie). Naast andere opmerkelijke eigenschappen zullen dergelijke netwerken voor stadsverwarming en -koeling (DHC) in de toekomst waarschijnlijk gekenmerkt worden door het gebruik van gedistribueerde lagetemperatuurbronnen, gecombineerde DHC-systemen, geïntegreerde warmte- en koudeopslag en warmtepompen aan de kant van het gebouw. Er zijn tal van moeilijkheden bij het ontwerpen van grootschalige DHC-netwerken met al deze eigenschappen. Een techniek voor het ontwerpen van 3-pijps

DHC-netwerken en ultra-lage temperatuur DHC-netwerken die gebruik maken van een ringnetwerkstructuur, zal worden besproken in hoofdstuk 5, samen met een vergelijking van de kosten van de respectieve netwerken. De ontwikkelde methode wordt gebruikt als een proof of concept in de DHC-ontwerptool, Comsof Heat, en er wordt een casestudy gemaakt om deze twee configuraties te ontwerpen, te vergelijken en de impact te analyseren op de netwerkkosten. De resultaten van de casestudy laten zien dat de kosten voor het uitrollen van een netwerk voor DHC-ringen met ultralage temperatuur ongeveer 23% hoger zijn dan voor ringen van de derde generatie. Bovendien is de beschikbaarheid van een gratis lagetemperatuurverlieswarmtebron een voorwaarde voor de economische levensvatbaarheid van ultralagetemperatuurnetwerken van de vijfde generatie.

DHC-netwerken bieden de flexibiliteit aan de toevoerzijde om zich doorheen de tijd aan te passen en te veranderen, wat een van hun belangrijkste voordelen is. Naarmate de energie-efficiëntie van gebouwen toeneemt, kunnen steeds meer laagwaardige energiebronnen worden gebruikt. Om de warmte te verhogen en te voorzien in de energiebehoefte van de gebouwen, worden warmtepompen vaak gebruikt als aanvulling bij laagwaardige energiebronnen. Decentrale warmtepompen ter hoogte van gebouwen en stadsverwarmingsnetwerken zijn onlangs gecombineerd, wat de energie-efficiëntie van het netwerk verbetert. Met deze opstelling kan een tweepijpse netwerkconfiguratie worden

gebruikt om zowel warmte als koude te leveren. Het aantal installaties van centrale airconditioners en kamerairconditioners is tussen 1990 en 2010 met meer dan 50 keer toegenomen in de Europese Unie, wat wijst op een enorme toename van de vraag naar energie voor ruimtekoeling in de jaren negentig. Bovendien is in heel Europa de afgelopen 15 jaar het aantal dagen waarbij er behoefte is aan koeling toegenomen, terwijl het aantal dagen waarbij er behoefte is aan verwarming is afgenomen. Dit toont aan hoe cruciaal ruimtekoeling aan het worden is. In Hoofdstuk 6 wordt de opstelling bestudeerd waarbij water met een lage temperatuur circuleert in het netwerk met een warmtepomp aan de kant van het gebouw om de temperatuur tot het gewenste niveau te verhogen of te verlagen. Dit wordt ook vergeleken met conventionele stadsverwarmingsnetwerken. Hoewel het realiseren van een duurzame oplossing en een grotere energie-efficiëntie nuttig zijn voor het milieu, is het ook cruciaal om de kosten en het primaire energieverbruik te onderzoeken. Daarom wordt Comsof Heat gebruikt om de bovengenoemde configuratie te ontwerpen, waarbij ook de kosten van het netwerk worden bepaald. Het ontwerp en de kosten van deze configuratie worden getoetst aan die van conventionele stadsverwarmingsnetwerken in een locatie van de case studie. De impact van verschillende ontwerpfactoren wordt onderzocht en verschillende scenario's, met o.a. verschillende elektriciteitskosten en prestatiecoëfficiënten (COP), worden geanalyseerd. Als er een verlieswarmtebron met lage temperatuur beschikbaar is, zijn de totale kosten van het ultra-lage temperatuur stadsverwarmingsnetwerk (ULTDH) 16% lager dan het typische netwerkontwerp gedurende de 35-jarige levensduur van het netwerk.

List of Figures

List of Tables

Chapter 1

Introduction

Contents

Global warming and climate-related events have caused more than €487 billion in financial losses, and over 138,000 people lost their lives between 1980 and 2020 in the European Union (EU) [1]. So, it is highly important to take measures against carbon emissions to reduce climate change. Our current energy system is one of the key contributors to carbon emissions, and it needs to be addressed in a way that ensures energy security.

This chapter introduces the context of why district heating and cooling networks should be an essential part of the future energy system. The chapter discusses the relevance and contribution of this technology to ensure energy security and reduce carbon emissions.

The problem statement section explains the current status of the EU's energy system and its dependence on fossil fuels that are imported from other countries. It also points out district heating and cooling networks as one of the possible solutions to move towards a self-sufficient green energy system. Next, different generations and configurations of district heating and cooling systems are described in the section on thermal energy networks. Then, the challenges are presented based on a literature review and the scope of this thesis is defined. Based on the identification of research gaps, the aim and objectives of this thesis are defined. As a result, the novelty and contribution of this thesis can be distinguished. Finally, the organization of this thesis is clarified.

1.1 Problem Statement

The EU is currently facing two major energy challenges. The first is energy insecurity because of fossil fuel dependence and the ongoing geopolitical situation. The second concern is climate change caused by carbon emissions. Both challenges are linked to the fossil fuel based energy supply. Hence, the key challenge is to adopt and integrate renewable energy sources into our current energy system.

1.1.1 Energy supply

The EU mainly relies on hydrocarbon sources for its energy supply for heating, electricity, transport, and industry. Oil, petroleum, and nat-

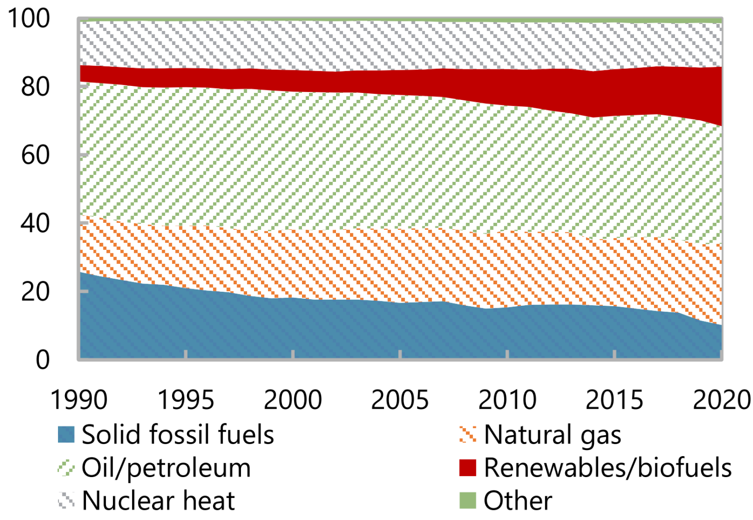

Figure 1.1: The energy supply of EU by source [2].

ural gas all play important roles in the EU's current energy supply, as illustrated in Figure 1.1. For the past 30 years, the renewable energy transition was not fast enough to offset the petroleum and natural gas usage. The natural gas sector accounted for a quarter of EU's greenhouse gas emissions in 2020 [3]. Yet, natural gas dominates the energy system, representing 21.5% of EU's primary energy consumption and it is used for 38% of the heat production in EU [3]. Clearly, the energy supply composition can be improved and a switch in the used energy sources is necessary.

The obvious solution would be to switch from fossil fuel based energy systems to low carbon energy systems. However, it is not easy since this also requires a transition in the underlying infrastructure. For example, natural gas grids are developed over several years with significant investments.

Utilizing waste heat, increasing renewable heat and electricity, and electrification are key to decarbonize the energy sector. Utilizing waste heat will help reduce primary energy consumption. A study by Heat Roadmap Europe [4] indicates that the available excess heat (from industry and electricity generation) within a reasonable distance can cover 31% of total building heat demands in the EU. This means that there is huge potential for reducing primary energy consumption by utilizing waste heat and thereby reducing carbon emissions. However, in order to utilize this excess heat, the infrastructure (thermal network) to transport the excess heat from available locations to the end-use buildings is necessary.

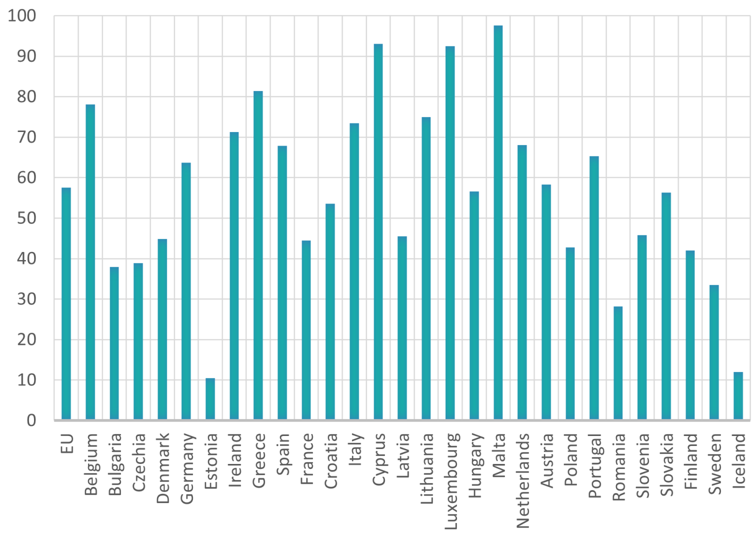

Figure 1.2: The energy dependency rate of EU countries (% of net imports in gross available energy in 2020) [5].

1.1.2 Achieving self sufficiency

Figure 1.2 shows the energy dependency rate, and Figure 1.3 shows the natural gas import dependency of EU countries. The energy dependency rate shows how much an economy relies on imports to meet its energy needs. The EU has a dependency rate of around 58 percent, which means that imports meet more than half of the EU's energy demands [5]. The natural gas share of the EU remains high (about 25%) in the overall energy mix, and its dependency rate is alarmingly high (about 83%) [6]. Therefore, it is crucial to accelerate the renewable energy transition for better energy security, especially with the current geopolitical situation.

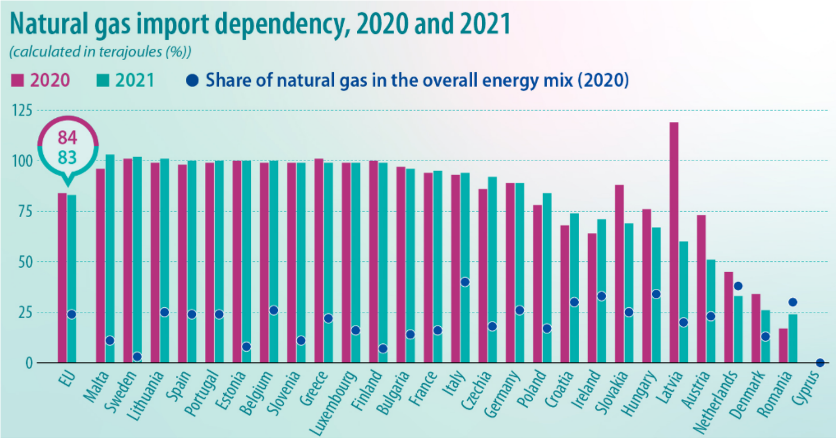

Figure 1.3: The rate of EU countries' reliance on natural gas imports in 2020 and 2021 [6].

European governments are already taking steps in the right direction. In the last two years, 19 European governments have increased their ambition of decarbonisation strategy, with a few of them aiming to generate almost all of their electricity from renewable sources by 2030 [7]. In contrast, EU countries are also still building or planning to build €87 billion worth of natural gas infrastructure in a continued expansion of pipelines and LNG (Liquefied Natural Gas) terminals [8]. These investments may be beneficial in the short term, but they may be obsolete in the medium to long term.

Hence, investing in the right technologies is key to accelerate the renewable energy transition. Renewable energies such as solar and wind fluctuate and are very hard to predict, causing challenges to balance supply and demand. According to the International Energy Agency, these could generate nearly 70% of all electricity globally by 2050 [9]. In the case of renewable heat, for example, solar energy is mostly available during the summer (the hotter seasons) in contrast to the heat demands during the winter (the colder seasons). In order to balance demand and supply, storage systems are often necessary to offset these imbalances.

Incorporating a high share of variable renewable sources in the electricity

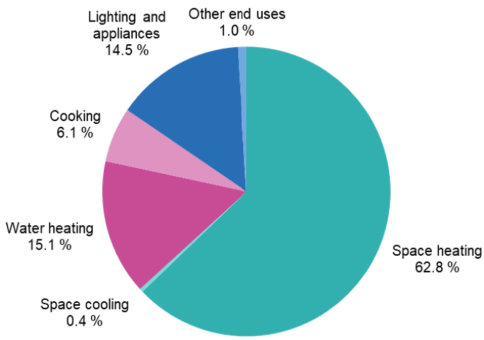

Figure 1.4: A typical EU household's energy composition [11].

grid will cause more fluctuation, so it will require additional flexibility in the system. If electricity and thermal grids are linked, thermal grids could help increase flexibility while also decarbonizing the building energy sector. Heat pumps will play a key role in future energy systems, helping to bridge electricity and heat grids with relatively high energy efficiency. Luc et al. [10] studied the sector coupling of the power and heat sectors, and they identified it as an important strategy for mitigating emissions.

1.1.3 Energy demand of heating and cooling sector

Heating and cooling account for half of total energy demand in the EU, with fossil fuels accounting for 75% of total energy consumption [12]. Residential heating and cooling demand accounts for 54% of total demand, followed by industry (24%), and services (21%) based on 2015 data [12]. Households accounted for 27% of total EU energy consumption [11]. The majority of household energy consumption (78%) was used for heating (space and water heating), as shown in Figure 1.4.

On further looking into the supply side, the residential sector accounts for most EU gas demand (40%), followed by industry and gas use for power generation. Natural gas has the highest share (32%) in household's energy usage as shown in Figure 1.5. This is understandable since around 40% of European households are connected to the gas network [3]. However, this has to be changed. Decarbonization of the heating and cooling sector, especially in the built environment, is key to achieve climate neutrality in Europe by 2050.

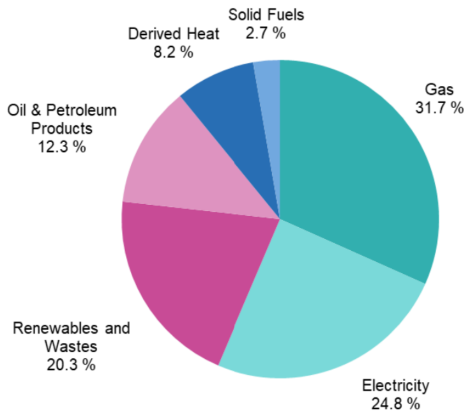

Figure 1.5: The proportion of fuels used for heating in EU households [11].

1.1.4 Reducing carbon emissions

Thermal network is one of the most cost-efficient ways to reduce carbon emissions in the heating and cooling sector when used in combination with carbon free source. Studies that modelled the role of thermal networks in the EU energy system stated that they could help in achieving EU 2050 carbon emission reduction targets at a lower cost compared to other alternative strategies [13]. Thermal networks are an essential part of future energy systems. Many of the low carbon heat sources and waste heat can only be used if there is a network infrastructure to distribute the heat. Thermal networks are fuel agnostic and can be heated with any fuel type. The carbon emissions from thermal networks are largely dependent on the source that supplies heat to the network. Therefore, it is possible to progressively decarbonize the heat supply over time as the networks are not tied to a single heat source.

Thermal networks distribute heat from a centralized heat source to the buildings of a city through pipe networks. These are generally some of the most efficient ways to heat homes, as they benefit from large-scale heat generation and can use industrial waste heat. Thermal networks have long been used in countries that are at the forefront of reducing carbon emissions, such as Sweden and Denmark [14]. Thermal networks are very common in Denmark and Sweden, as more than half of all space heating in the countries is supplied by these networks [14]. In Denmark, heat networks supply heat to almost 64% of all households for their space heating and hot tap water needs [15]. In Copenhagen (the capital of Denmark), the heat network is one of the world's largest, supplying 98% of the city's heating requirements through 1500 km of pipe network [16]. Thermal networks are the backbone of these countries' energy transition, delivering heat and balancing their renewable electricity fluctuations. Initially, these networks were fed by fossil fuels, and the heat sources were decarbonized over time using low carbon sources such as biomass, waste heat, solar, etc. Heat pumps, electric boilers, and thermal storage tanks are increasingly used to balance demand swings in the system. These forerunner countries are demonstrating that thermal networks will undoubtedly aid in the reduction of carbon emissions.

1.2 Thermal energy networks

Thermal energy networks, also known as district heating (DH) / district cooling (DC) networks, consist of pipe networks between the buildings of a city and one or more centralized or decentralized heating/cooling sources to fulfil heat/cold demand. They allow for easy replacement of the energy source, which can be combined heat and power (CHP) plants, waste-to-energy plants, and various other industrial surplus heat sources, as well as several renewable energy sources. Therefore, DH/DC systems have an important role to play in future energy systems that can provide sustainable and green energy to cities. Figure 1.6 depicts the basic layout of a district heating network.

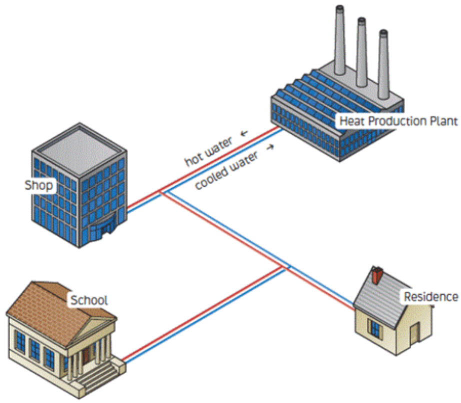

Figure 1.6: A simple district heating system [17].

1.2.1 The Evolution of District Heating Systems

District heating system designs are constantly being improved by reducing distribution losses, increasing energy efficiency, and integrating different energy sources and storage. The initial systems provided steam through pipes in concrete ducts. Those evolved into pressurized hot water distribution systems through pipes. The supply and return temperatures of the networks are drastically reduced to improve energy efficiency as we reach 4th generation district heating (4GDH) systems. Most of the DH networks operating currently are either 2nd generation (2G) or 3rd generation (3G) systems. Third-generation district heating (3GDH) systems have various drawbacks, such as high network operating temperatures, high distribution losses, the inability to utilize low temperature waste heat and renewable energy sources, a one-way heat supply, the disconnection between heating and cooling networks, etc., and hence can be further developed to move towards the future of sustainable energy systems. Figure 1.7 illustrates the evolution of DH systems.

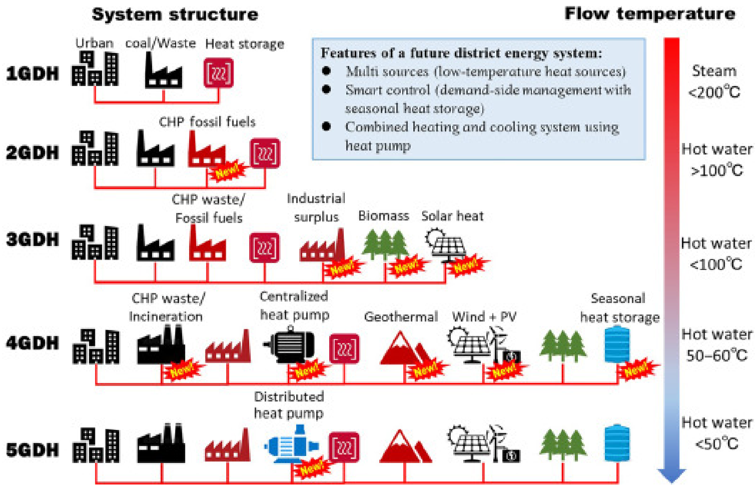

Figure 1.7: District heating system evolution: 1st to 5th generation [18].

1.2.2 4th generation district heating (4GDH) system

Lund et al. [19] defined 4GDH as well as its relationships to district cooling and the concepts of smart energy and smart thermal grids. They aim to decrease grid losses, exploit synergies, and thereby increase the efficiencies of low-temperature production units in the system. The key challenges of the 4GDH system that can be addressed are:

- Ability to supply low-temperature heat for space heating and domestic hot water to both existing and new buildings
- Ability to distribute heat in networks with low grid losses
- Ability to recycle heat from low-temperature waste heat and integrate renewable heat sources such as solar and geothermal heat
- Ability to be an integrated energy system (synergy with other grids)
- Ability to ensure sustainable planning, cost, and motivational structure in relation to operation as well as to investments

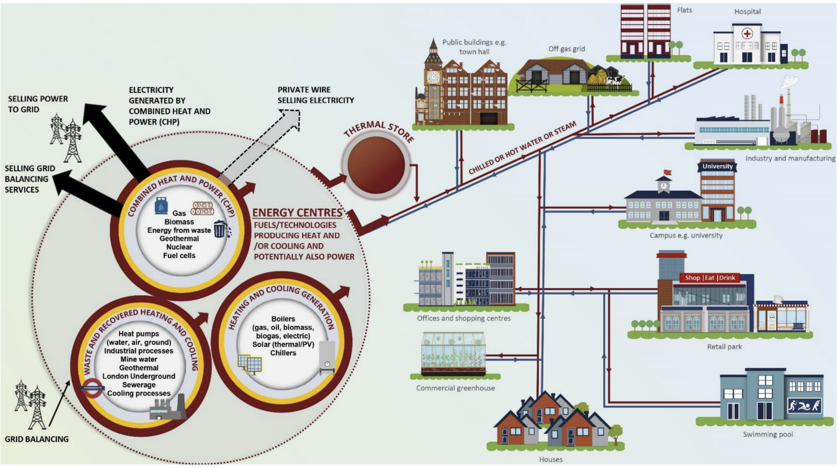

Figure 1.8: The fourth generation district heating network [20].

Currently, 4GDH is an advanced concept that has the focus on reducing heat losses and costs by lowering network temperature levels and creating synergy between buildings' heating and cooling demands. This will result in better utilization of low temperature waste heat and renewable sources. However, 4GDH networks have challenges connecting with existing or old buildings since they have high temperature requirements for heat demand. This can be addressed by the integration of other technologies such as heat pumps, boilers, etc.

4GDH systems can include any centralized and / or decentralized heating and cooling plants, combined heating and cooling (CHP) plants, heat and cold storage, industrial surplus heat and renewable sources as shown in Figure 1.8. Unlike other generation DH systems, the heat can either be extracted from or delivered to the 4GDH grid, in so-called two-way DH systems. The consumers who both extract and deliver heat into the system are called prosumers. This feature opens the way for adding distributed sources such as small scale solar thermal systems and heat pumps in the 4GDH networks, which will increase the utilization of low-temperature waste and renewable heat [21, 22]. It however introduces new challenges in the design complexity, integration, and management of 4GDH systems. Furthermore, when the 4GDH network scales with an increasing number of distributed capacities or prosumers in the system, a new scientific challenge is the development of a highly stable and reliable network that operates even in the most extreme conditions. Therefore, the size and location of storage will be critical when designing the network [19].

4GDH systems allow energy systems to include more distributed renewables in the networks, and the integration of seasonal thermal storage further enhances their flexibility. They also help to balance electricity grids by integrating them through heat pumps, electric boilers, and CHP plants. The vision of 100 percent sustainable energy supply is only possible by integrating different grids into one energy system in order to balance the renewable energy fluctuations. This integrated, holistic approach including more sectors (electricity, heating, cooling, industry, buildings, and transportation) is characteristic of so-called smart energy systems [23]. The 4GDH network can play a dominant role in the smart energy supply to EU cities since heating and cooling account for almost half of the EU's energy consumption. Thus, 4GDH networks are one of the ways to achieve 100% sustainable energy supply with the integration of different energy systems. However, there are many challenges, such as highly complex design and planning, high investment costs to overcome in order to achieve this feat.

1.2.3 5th generation district heating (5GDH) system

5GDH networks aim to combine the advantages of a centralized energy distribution system with low heat losses in energy supply. This is achieved by providing very low temperature water (10–25°C) through the centralized supply, which is then heated up by decentralized heat pumps, as shown in Figure 1.9. The cold water sources, ring network topology, multi-purpose heat pumps, and smart control system form the basis of the 5GDH network. This kind of network already exists in Switzerland, Germany, Italy, and the Netherlands. This concept is also suitable for district cooling since cold water is circulated through the pipes. The advantages of this system are the possibility of using low-cost pipe materials and a significant reduction in insulation thickness.

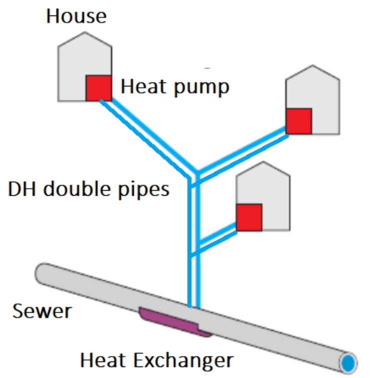

Figure 1.9: A simple 5th generation district heating network [24].

In case of heat demand, the circulation pump of the building extracts water from the hot pipe, uses it in a heat pump to reach the temperature suitable to provide heating, and then discharges the cooled water back to the cold pipe. In case of cooling demand, the reverse occurs. This system requires complex regulation of both the distribution network and consumer substations. This type of system requires two pipes but can provide both heating and cooling.

5GDH systems can also utilize renewables and create synergy with other grids, which makes them smart systems. Heat sources of the 5GDH can be integrated locally from a variety of potential sources. It is also possible to integrate domestic hot water production with solar thermal or hybrid photovoltaic thermal (PV-T) panels, which can provide both electric and thermal power. 5GDH networks provide users the possibility of returning heat and/or cold to the district heating ring. This enables bidirectional exchange, requiring high-cost smart meters and efficient control to manage prosumers. 5GDH networks can bridge the thermal and electric grids via heat pumps and storage.

In the Netherlands, the city of The Hague developed a district heating concept using sea water as a source, combined with heat pumps and a heat exchanger [25]. In the summer, the temperature of the seawater reaches 11 °C, and only the heat exchanger is used. In winter, when the seawater temperature drops below 4°C, an ammonia-based heat pump is used to heat it up to 10°C and feed the water into the district heating network ring. It is then further heated up by individual heat pumps on the building side.

Heat pumps play a vital part in 5GDH systems. The inclusion of heat pumps in the grid provides flexibility to handle different temperature levels and even allows for the use of very low-temperature heat sources such as sea water, sewage waste heat, data centers, and so on. It can also act as a technique to exchange heat between heating and cooling. This process is called heat balancing. An example of heat balancing is the use of heat extracted from a supermarket to heat a nearby building. In this example, the supermarket is cooled and the building is heated without using much external energy. Heat balancing in 5GDH networks requires synergy between heating and cooling loads, which should be considered during the design phase. This is one of the unique features that distinguishes 5GDH from the state-of-the-art approach.

A 4GDH (60°C supply) system requires 11% more primary energy than 5GDH networks, while a 3GDH (90°C supply) system requires 112% more primary energy [25]. The estimated thermal losses of the 5GDH networks in Hamburg are 2%, while the estimated losses are 19% and 25% respectively, if the same amount of energy is delivered through the 4G and 3G district heating networks [25].

1.2.4 District cooling system

The global cooling market has several different applications [26]:

- Space cooling for comfortable indoor temperatures
- Food supply chain: to preserve food quality
- Industrial processes: To secure product quality in data centres, breweries, and dairies
- Special uses: soil freezing; creating ice for ice rinks; liquid methane for LNG transports; etc.

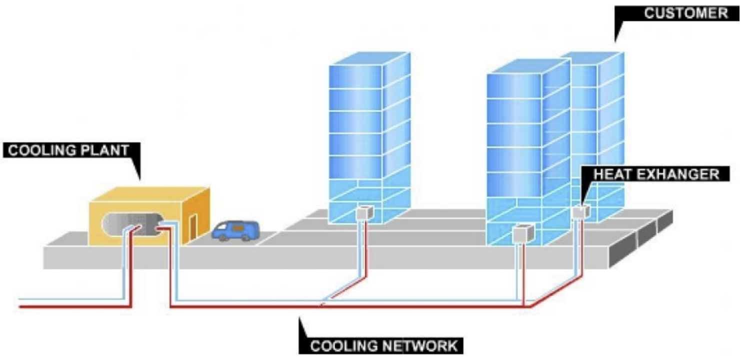

Figure 1.10: A district cooling network [27].

District cooling is normally used for space cooling in the buildings. As shown in Figure 1.10, it is similar to district heating systems, with distribution pipes supplying cold water from a centralized chiller plant to buildings. The alternative is individual cooling devices, which are normally purchased at a low cost but have high operating costs due to their low energy efficiency. On the other hand, district cooling has a high investment cost but a low operating cost. Therefore, at a particular volume of cooling demand, the overall cost of district cooling will be cheaper than individual cooling.

1.2.4.1 Cooling sources

The cooling source can be sea water, lake water, river water, ground source water, or the ambient air. Vapour compression or absorption chillers can be used in case of high source temperature. These chillers can generate additional cooling during the warmer months. Examples of cooling sources are:

- Free cooling: Sea water, lake water etc.
- Waste cold: LNG terminal etc.
- Vapor compression, absorption, or electrical chillers
- Cooling tower: Evaporative cooling with air

- Heat pumps: Ground, air, or water source

1.2.4.2 Cold distribution technology

In district cooling, the cold carrier is pressurized chilled water. District cooling pipes exist with and without insulation. In hot areas like the Middle East, district cooling pipes with insulation are used to avoid heat gain. In district cooling, a cold loss is the heat gain from the ground, which increases the supply temperature of the cold carrier pipe. Uninsulated pipes, on the other hand, are used for district cooling, particularly for large diameter pipes. In comparison to heat losses, cold losses are smaller because of the smaller temperature difference between the supply pipe and the ambient air. However, due to the small temperature difference, the pipe diameters are significantly larger for district cooling, resulting in greater cold losses. The typical distribution losses are below 10% in areas of high cold density and over 10% in areas of low cold density [26]. In the Helsingborg district cooling system during 2009, the distribution heat losses were 15% with a linear cold density of 3.4 GJ/m [26]. The linear cold density is the total cold demand divided by the total length of pipe in the network.

The typical supply and return temperatures for district cooling are 6°C and 16°C respectively [26]. Water should not freeze in severe winter areas, so all substations should have a mandatory bypass to keep water flowing when there is no cold demand. Another option is to install electric heating wire in the pipes. In the case of uninsulated pipes, they should be buried deeper than DH pipes in order to avoid freezing of water in cold winter areas and heat gains in hot summer areas.

1.2.4.3 Difference with DH systems

- Since the temperature difference is low compared to district heating, the pipes are wider and more expensive, which makes district cooling only feasible if the linear cold density is high enough.
- There are options to go with either insulated or uninsulated pipes based on the local ambient temperature conditions.

- Freezing of water in the pipes during the harsh winter should be avoided.
- Due to high viscosity from the low temperature and friction losses that produce heat works against the cooling capacity, pumping costs are significant compared to district heating.

1.3 Challenges and Scope

This thesis aims to address a number of challenges posed by DH network design, especially 4th and 5th generation district heating systems integrated with thermal energy storage (TES). There are several research and pilot projects ongoing in the field of 4GDH and 5GDH in order to prove their potential and viability. Since 4G/5GDH systems are not yet mature, there are many in-house stand-alone models being developed to address several individual aspects of the 4G/5GDH concept by different researchers. However, the integrated DH network design methodology and design automation are not addressed. In order to have a future-proof design for a DH system, a number of challenges need to be overcome, and they are presented in this section.

1.3.1 Automation of district heating network design

With increasing technological advancements, automation is helping with increased productivity, more efficient use of resources, better product quality, improved safety, reduction of human errors, and reduced time and effort in various sectors [28]. However, district heating networks are still often designed manually with the help of custom-made spreadsheets [29]. The network routing is also often drawn manually, which takes a lot of time, skilled people, and domain-specific knowledge. Yet, the design can be suboptimal and error-prone. Especially for large networks, designing a network layout manually is complex and time-consuming. Moreover, the current custom-made spreadsheets that are used for pipe selection and hydraulic calculations are not scalable. The network deployment costs are also typically calculated using yet another spreadsheet. In short, different design aspects typically require different software tools, and the process is usually not well-integrated. This makes the design process expensive and time-consuming.

Many papers in the literature [22, 30, 31, 32] study several individual aspects of 4G/5GDHC networks using their in-house model, but there are no integrated tools available to design 4G/5GDHC systems. However, commercial tools such as NetSim, Termis, Neplan, and sisHYD are available to design traditional district heating and cooling systems by drawing the network routes manually. Among them, NetSim and Termis are the most widely used commercial software for heat networks. The strength of NetSim [33] is that it has many technical features such as hydraulic balance, temperature and pressure drop calculation, and pipe and pump sizing. The drawback of this software is that the network has to be drawn manually. It is based on the simulation tool LicHeat, which is also used for the Termis software. Termis [34] is a hydraulic modeling tool that simulates heat network flow, pressure, and thermal behavior. One of the main advantages of Termis is that it can be used for real-time monitoring and to optimize production. Termis is more of an operating tool for managing district heating networks than a design tool. It has temperature, pump, and pressure optimizations. The limitation of the Termis software is that the routing is not automated. Even in the case of state-of-the-art DH system design, no well-integrated software tool with automated routing exists.

Therefore, it is important to automate and integrate all the design steps, such as network routing, network pipe dimensioning, pressure calculations, and network deployment cost calculations.

1.3.2 Optimal design of district heating networks

The design process of district heating systems involves technology selection, routing of pipes from the heat source to the end users, dimensioning of pipes based on design constraints, network deployment cost estimation, and investment analysis. In the case of centralized single-source networks, it is relatively simple to design the network using the estimated winter peak heat demand for the entire network. It was largely the case before, but the current networks have to deal with multiple distributed sources. With many of these sources and TES systems at different locations, the design process already gets quite complicated. Furthermore, future energy systems will consist of more fluctuating renewable energy sources, so a more robust design is required.

Mehleri et al., [31] presented a mixed-integer linear programming (MILP) model for the optimal design of distributed energy systems that satisfy the heating and power demand at the small neighbourhood level. The aim is to select the optimal system components among several technologies, including the optimal heating pipeline network that allows heat exchange between different nodes. They used the annualized overall investment cost and the annual operating cost of the system as objective functions. They analysed several scenarios with different technologies for 10 buildings in Greece. This model deals only with the design of distributed systems such as micro-CHP, photovoltaic (PV) plants, etc. in a small neighbourhood with 10–20 buildings.

Vesterlund and Dahl [35] described a new process integration method for modelling complex district heating systems containing loops. This method makes it possible to analyse how loops and bottlenecks affect the behaviour of the network, as well as the distribution path of the thermal energy in it. In this model, a district heating system with a complex design, including loops in Kiruna (Sweden) is used as an example. They used two different softwares to model the DH system: the physical model of the network was built in the Simulink/Matlab environment, and the ReMIND software was used to optimize the required heat production. This model uses the existing network to optimize the heat generation in the network to achieve operating cost minimization.

Wang et al., [32] proposed the hydraulic performance optimization problem of a meshed DH network with multiple heat sources. They adopted the General Reduced Gradient algorithm to minimize total pump power through optimizing the pump frequencies and substation valve openings of the DH network. Though they deal with multiple heat sources, the focus is on operational optimization and not on design aspects.

Different possible network topologies, such as branched, ring, and mesh are available to connect the heat sources with end-user buildings. Each of them has their own advantages and disadvantages, and it is up to the network designer to choose based on the project objectives. It is also difficult to make a decision unless the costs and benefits of various scenarios are weighed. Hence, an automated design method is necessary to design thermal networks with multiple sources and the possibility of choosing different network topologies.

1.3.3 Integration of thermal energy storage

The relevance of using thermal energy storage (TES) systems in DH networks is increasing rapidly since the share of fluctuating renewable energy sources is increasing. TES systems are seen as an essential component in a future energy system since they provide flexibility and stability to the grid. The difficulty arises in determining how to size the storage and where to locate it, as it can be centrally located or distributed across the network. The storage size and location decisions are based on the desired objectives. The objectives can be minimization of network investment costs, maximization of energy utilization, etc.

The integration of TES will result in increased utilization and reduced peak power requirements from energy sources. The effect of these results is variable based on the storage size and location. These factors are also weighing on the storage costs. Therefore, it is important to have a design method that is capable of analysing the impact of TES in district heating systems.

1.3.4 Selection of suitable DH network design

The current state-of-the-art network is 3GDH system, which are evolving over time. Currently, 4GDH networks are gaining momentum due to their low network heat losses and the possibility to integrate low-temperature waste heat and renewable energy sources.

5GDH networks are in the pilot phase, and some argue that this network will be more efficient than 4GDH networks. Pellegrini and Bianchini [25] reviewed the literature about 5GDH networks. They analyse the benefits and drawbacks in comparison with the alternatives currently used to heat and cool at the district level. Some argue that it is not cost-efficient, and having decentralized energy source or booster in every end-user building is not ideal. Hence, it is not an easy task to select a network configuration.

An automated network design tool that is capable of designing 4G and 5GDH networks and estimating the network costs would help in comparing these network designs.

1.3.5 Integration of prosumers in the network

Prosumers are consumers who can also put heat back into the network. They are negligible in the current energy systems, but that might change if more heat pumps are installed in end-user buildings. So, the future network design should be able to support prosumers in the network, and it is very complex to design and operate two-way network flows.

Sameti and Haghighat [30] apply a mathematical programming procedure to model the optimal design and planning of a new district that satisfies two potential features of a future energy system: energy reciprocity and on-site generation. Their model aims to investigate the effect of energy exchange among the buildings as well as to find the best way to select the equipment among various candidates (capacities), the pipeline network among the buildings, and their electrical connections. The distributed energy supply consists of heating, cooling, and power networks, several CHP technologies, a solar array, chillers, and auxiliary boilers. They use an in-house MILP model to solve the optimization problem. The drawback of this model is that the pressure drop of the thermal network is not considered. Furthermore, it is not linked with a GIS tool, and due to the required manual efforts, it is not scalable.

Brange et al. [22] evaluated the potential of a contribution from small-scale prosumers to district heating based on excess heat and their environmental impact in an area with diverse building types. The results were developed through a case study performed on Hyllie, an area under construction in Malmo, Sweden. The temperature of the excess heat was either raised with a heat pump or directly used in the district heating networks. They concluded that the potential for excess heat production by prosumers is fairly large, ranging from 50 to 120 percent of annual heat demand in Hyllie. This research was done using NetSim, a commercial tool to design district heating networks. There are several small-scale manual studies regarding prosumers, but the key challenge remains a design method for a large-scale network with prosumers.

1.3.6 Scope

Addressing all of these challenges in a single PhD would be too much to cover. Therefore, the scope of this thesis needs to be limited. The following research gaps are identified:

- An automated and integrated district heating network design method that provides routing, pipe sizing, and cost estimation.
- Impact of integrating TES centrally and at distributed locations in thermal networks on network cost.
- Optimal design of district heating networks with multiple distributed sources using different network topologies, such as branched and ring topology.
- How to design 5GDH networks? Is 5GDH network economically viable when compared with the current state-of-the-art network?

This thesis focuses on the optimal and automated design aspects of thermal networks incorporating multiple sources, different network topologies, thermal energy storage, and distributed heat pumps at end user buildings. Though distributed heat pumps can be considered prosumers, the energy exchange aspect of prosumers with the network will not be covered as part of this PhD.

1.4 Aim and Objectives

The aim of this thesis is to develop an automated and integrated design method for district heating networks incorporating multiple sources, different network topologies such as branched and ring topology, thermal energy storage, and distributed heat pumps. This thesis also aims to solve the research challenges that form the fundamental issues in the development of well-integrated tool that is capable of designing DH networks using automated network routing algorithms. The research questions relevant to this aim are: what will be the impact of integrating storage, where to place the storage, is there a cost optimum while sizing the storage, how to design distributed multi-source networks, is a ring topology network cost efficient compared to a branched topology, how to design 5GDH networks, and will 5GDH networks be economically viable?

The first objective of this thesis is to develop an automated design framework that is capable of designing the current state-of-the-art DH network. This is accomplished by developing a district heating network model integrated within Comsof's existing automated network routing algorithms. This design framework is applied to a case study to analyse the resulting designs. Furthermore, a parametric study is done to analyse the effect of different network design parameters on network cost and performance.

The next objective is to develop and integrate a TES model within the above-mentioned design framework. This makes it possible to easily vary design variables and obtain the resulting design. Design choices include the location of storage, such as centralized or distributed, storage size, and storage type (seasonal, daily). This is implemented as a proof-of-concept (POC) in Comsof Heat, a GIS-based DH network planning and dimensioning tool developed as a result of objective 1. This is further applied to a case study to compare centralized and distributed storage. The effect of these storage configurations on the total network costs is studied, and multiple designs with different storage sizes will be compared.

Developing a method to design multi-source district heating networks is the next big objective of this thesis. Optimization is necessary to identify the most cost-efficient route and source allocation to the end-user buildings. A design method based on the combination of assignment and routing algorithms is developed for the automated routing and designing of multi-source DH branched networks. This method is implemented as a POC in the DH network design tool, Comsof Heat. This tool is able to select the best energy sources out of the given possibilities based on the following objective functions: source investment cost, energy production cost, carbon emissions cost, or combinations of the above. It is also able to select the best end-user buildings for the given input power of the energy sources. Moreover, the tool optimally connects the selected sources with end-user buildings. A Belgian municipality is chosen for a case study to design a multi-source DH network with different possible source options. The case study is used to investigate the effect of design choices on costs and carbon emissions.

Furthermore, the design method is also be capable of designing multi-source networks in a ring topology. This is implemented as a POC in the DH network design tool, Comsof Heat. In a case study, these results are compared with those of 5GDH networks.

Lastly, a method to design 5GDH networks is developed and integrated with the design framework. This method is also implemented as a POC in Comsof Heat. A city in the United Kingdom is used as a case study to design 5GDH networks and compare the results to traditional networks.

1.5 Organization of thesis

There are five chapters between the Introduction and the Conclusion chapters. **Chapter 1** and **Chapter 7** presents the introduction and conclusions of this thesis.

Chapter 2 explains the method to automate the design process by combining routing algorithms and a district heating network model. This method is explained using a case study of a city in the Netherlands. The design steps such as network routing, clustering of buildings, and pipe dimensioning are described as part of the district heating network model. The effect of different design parameters such as network pressure level and substation size on network dimensioning, cost, and performance is studied. Moreover, network designs are made with future heat demand scenarios to analyse their impact on network cost and performance.

Chapter 3 describes the development and integration of a TES model with the developed district heating network design framework explained in Chapter 2. This chapter investigates the benefits of placing thermal storage tanks in the distribution networks and compares the results with the centralized storage design. A case study is developed to compare the centralized and distributed locations for different storage sizes. The effect of these storage configurations on total network cost is compared, and an important conclusion about distributed storage is drawn in this chapter.

In **Chapter 4**, the development of a branched multiple source design method using a combination of assignment and routing algorithms is explained. A capacity allocation strategy is used to match the substation (energy centre) with the energy sources. A municipality from Belgium is used as a case study to demonstrate the developed method using Comsof Heat. Different possible energy source options and building demand points are studied, and their impacts on network costs are compared. The tool is used to select the best energy source for the given objective function combinations. Finally, all the network designs are compared to study the effect of design choices on costs and CO_2 emissions.

Chapter 5 presents the development of a ring topology multiple source design method using the ring network algorithms. A method to design 3-pipe DHC ring networks will be presented, and a case study is developed to compare this design configuration with 5GDH networks in terms of network cost. Furthermore, the designs will be made with and without the availability of a free low-temperature waste heat source.

Chapter 6 describes the method for designing 5GDH networks with distributed heat pumps at each end-user building. The COP of the heat pumps at the building demand points can be configured separately for space heating, domestic hot water, and space cooling. A case study of a city from the UK will be used to study this configuration and compare the design and cost with traditional district heating systems. The tool will calculate the electricity required for heat pumps at the building and system level, and is useful to test the electricity grid loading.

1.6 Novelty and Contribution

This thesis presents an automated design optimization method for different DH network configurations developed using an adapted version of existing routing algorithms developed by Comsof. Comsof Heat, a GIS-based DH network design tool, is developed by Comsof based on this method. The routing algorithms used in this thesis were not developed as part of this PhD. For this thesis, DH design optimization model/algorithm are developed on top of these existing routing algorithms. The research gap, lack of automated DH network design in the literature is bridged by combining the existing automated routing algorithm with the newly developed DH network design optimization model/algorithm. Combining these algorithms is powerful since it saves a significant amount of time, effort, and manpower in the design process.

One of the added values of an integrated TES model with the automated design framework is that different storage location and size scenarios can be performed quickly and easily, even for large networks. This helps to find the optimal storage size and location for a specific case. Furthermore, most of the studies in the literature are rather small, and the existing models are not scalable to handle large networks. The developed method is very scalable, and one can even perform studies for a whole city with over 200,000 buildings.

Another valuable contribution of this thesis is the integrated optimization algorithm/method to design branched and ring multi-source networks. It is scalable with both the number of energy sources and end-user buildings. This will help reduce the design complexity of distributed renewable energy sources in future DH networks. The development of a 5GDH network configuration in this tool is also useful to compare techno-economic results between different network design configurations.

As a final contribution, all of the above-stated methods are implemented in Comsof Heat as a POC version. All POC implementation other than

Chapter 2 is implemented in Comsof Heat as part of this thesis work. Chapter 2 POC is created using Excel as part of the thesis and Comsof developers implemented it in Comsof Heat. These are already screened and included in the main product, Comsof Heat by Comsof. As a result, all of the features and configurations developed as part of this PhD are now available in the commercial software tool Comsof Heat. They are also already being used by a number of consulting companies, cities, and universities. These methods will help in designing the future DH networks in Belgium and other greenfield countries. Moreover, they will make the design process easier and more cost-efficient. Table 1.1 describes the contribution of each chapter to the methods and POC implementation. The novelties and contributions of each chapter are summarized below:

Table 1.1: Contribution to methods and POC implementation chapterwise

Contribution	**Method**	**POC**
Chapter 2: State-of-the-art DH design	Yes	No
Chapter 3: Thermal energy storage model	Yes	Yes
Chapter 4: Multi-source branched DH design	Yes	Yes
Chapter 5: Multi-source ring DH design	Yes	Yes
Chapter 6: 5GDH design	Yes	Yes

- Chapter 2: An automated design framework for optimal DH network design
- Chapter 3: A tool for the design optimization of TES in the district heating network
- Chapter 4: An integrated design optimization algorithm/method for branched multi-source networks
- Chapter 5: An integrated design algorithm/method for ring topology based multi-source networks
- Chapter 6: A design tool for optimal design and cost estimation of 5GDH networks

- In Chapter 2, 3, 4, 5, & 6, the developed method are applied to case studies in Belgium, the Netherlands, and the UK

Chapter 2

District Heating Network Design Methodology

Contents

This chapter is largely based on **Maria Jebamalai, J.**, Marlein, K., Laverge, J., Vandevelde, L., & van den Broek, M. (2019). An automated GIS-based planning and design tool for district heating: Scenarios for a Dutch city. Energy, 183, 487–496., DOI: 10.1016/j.energy.2019.06.111.

A district heating network's design, dimensioning, and cost estimation present numerous difficulties. It takes a lot of time and effort to manually create a network layout, especially for large networks. Customized spreadsheets enable automatic hydraulic calculations and pipe selection, but they are not appropriate for large networks and can be error-prone when used improperly. Another spreadsheet is generally used to estimate the cost of network deployment. In short, the process is usually not well integrated, and the various design aspects typically require multiple software tools. This increases the cost and duration of the design process. This chapter discusses solutions to the challenges stated above provided by an automated, geographic information system (GIS)-based planning tool. This tool has been developed as a plug-in to a GIS tool and includes optimized and automated network routing algorithms, including all aspects of a district heating network dimensioning as required for a feasibility study. A neighbourhood of Nijmegen was used as a case study to demonstrate the tool, showing the effect of different design parameters such as network pressure level and substation size on total network dimensions, cost, and performance. A variety of future heat demand scenarios were simulated in order to assess their impact on network cost and performance.

2.1 Introduction

District heating (DH) is an effective way to decarbonize future energy systems [36] [37]. It consists of pipe networks connecting the buildings of a city with one or more centralized heating plants [19]. Routing these pipe networks is a complex, time-consuming, and expensive process when performed manually. One way to improve this routing process is to automate it. Routing is very important since the route length determines the trench and pipe length, which in turn impacts the total network capital cost.

A study conducted by a group of leading global energy companies as part of the "Heat Infrastructure Development" project investigated the capital cost breakdown percentage of total heat network trench costs [38]. As per this study (Figure 2.1), trenching cost clearly dominates the total network capital cost. Therefore, automated and optimized routing allows for the creation of less expensive networks. Comsof has been developing in-house automation algorithms to route fiber networks for the past 20 years. These algorithms are scalable for large networks and are proprietary to Comsof. In a project in collaboration with Ghent University, these algorithms were adapted to route pipes for DH networks by embedding traditional methods of DH pipe dimensioning [39] and cost estimation. The geographical features of DH networks make GIS-based models an attractive option [40]. Therefore, the resulting tool (called "Comsof Heat") is developed as a plugin of a GIS tool. Combining routing automation with DH network models enables the simulation of different scenarios fast, precise and with ease. The aim of this chapter is to explain the methods behind this tool and to use it to investigate how different DH network configurations affect the network's dimensions, cost, and performance.

In this chapter, a case study of a 2-layer network (as shown in Figure 2.2) namely, a transport and distribution network using Comsof Heat is presented. The transport network transfers heat from the heat source to the distribution network substations. The distribution network further distributes heat from the distribution cluster substation to the individual building heat interface unit (HIU). Cluster-based design methods are a promising approach to facilitate large-scale modelling and optimization of urban energy systems [41] [42]. They divide the large area into multiple small distribution clusters. Comsof Heat uses cluster-based design models with a clustering algorithm based on network simplification. The distribution cluster (substation) size can be specified to create clusters in terms of maximum heat supply power (e.g. 1 MW, 2 MW). Substation size also affects the network cost since high substation power needs large

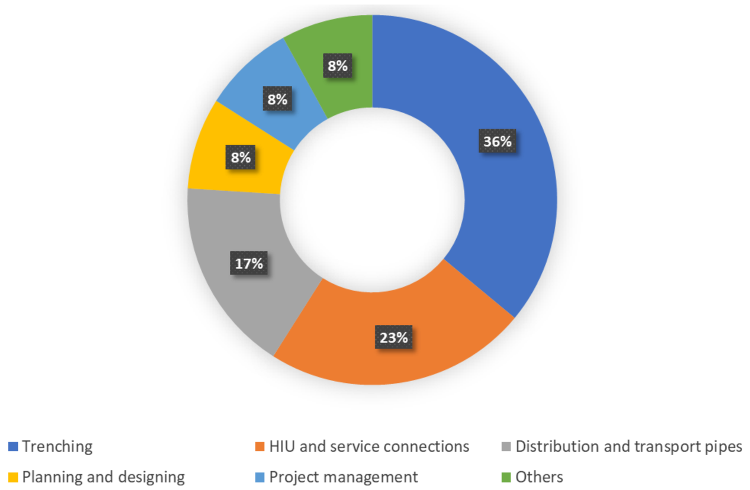

Figure 2.1: Total capital cost composition of a typical heat network [38].

distribution pipe diameters to deliver heat and low substation power results in a large number of substations, which in turn leads to an increase in the transport network pipe length. In this chapter, the impact of substation size on trench length and network cost is studied by defining and comparing several scenarios.

Several studies [43] [44] indicate that low-temperature DH systems operating at 55 °C supply temperature and 25 °C return temperature, can meet building heat demand with extensive control of building HIUs. However, the German regulation for domestic hot water (DHW) suggests a recommended temperature of 60 °C on an individual household level in order to avoid Legionella bacteria growth [44]. Moreover, the suggested return temperature of 25 °C has not been achieved in a number of demonstration projects [43]. Thus, in this study, the supply and return temperatures are chosen as 65 °C and 40 °C for the transport networks and 60 °C and 35 °C for the distribution networks. The DH pipe diameters and insulation material, as well as the network operating temperatures, all have an impact on network heat loss [39]. Therefore, different scenarios are investigated in terms of network heat loss for the

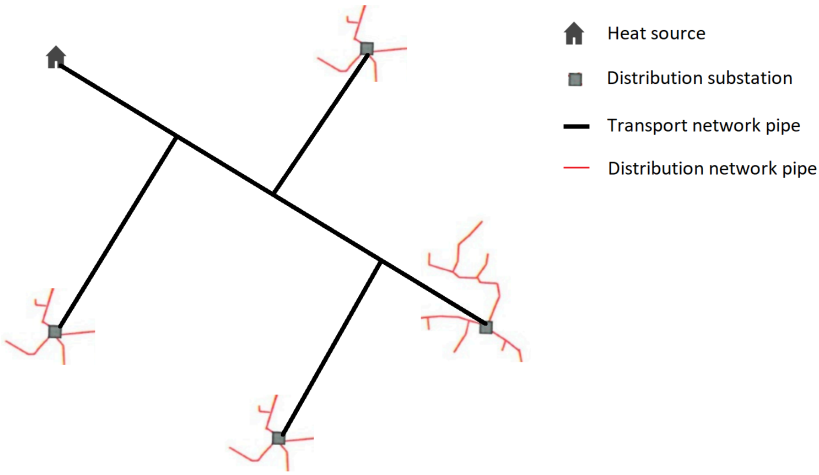

Figure 2.2: Schematic of a typical 2-layer DH network with transport and distribution pipes.

different network configurations and future reduced heat demand cases with and without DHW.

Building peak heat demand is generally used for network pipe dimensioning in order to satisfy demand throughout the year. However, it is unlikely that each building consumes this heat at the peak demand level at the same time. DHW, in particular, is distinguished by extremely high demand in a very short period of time. A typical resident only uses DHW for 15 minutes per day, corresponding to about 1% of a day [26]. Consequently, an over-dimensioned network design is prevented by using simultaneity factors for space heating and DHW demand respectively. While determining the design heat load for every pipe segment in the network, a simultaneity factor is applied based on the number of buildings connected to that segment. Traditional DH pipe dimensioning methods involve selecting the smallest possible pipe diameter to transfer the required heat load while keeping an upper limit for flow velocity and/or pressure gradient in mind [39]. Several scenarios are proposed to evaluate the impact of different network pressure levels and a flow velocity constraint on network dimensions, cost, and performance.

Tol and Svendsen [39] presented a method for a low-temperature DH system design after examining different pipe dimensioning methods, substation types, and network layouts. They used a case study from Roskilde, Denmark to demonstrate their method. Dalla Rosa et al. [45] discussed the opportunities and challenges of implementing DH in Canada, with a focus on network design and operation. Their simulations show that DH can be used to meet current heat demand at medium temperatures and in the future at low temperatures after energy-saving measures such as improved insulation are implemented in buildings. Delangle et al. [46] developed a methodology to find the best DH network expansion strategy under a set of given constraints. Chicherin et al. [40] highlighted the advantages of combining a GIS application with an energy demand forecasting model to create a tool aimed at supporting decision-making. Schweiger et al. [47] presented a framework for dynamic thermo-hydraulic simulation and optimization of district heating and cooling (DHC) systems. Many research papers [39, 46, 47] as well as commercial tools such as NetSim [21, 22] and Termis [48] offer models or frameworks to design DH systems, but these lack automation and an integrated approach.

By merging the already-in-use automated routing algorithm with the newly developed DH network design optimization model/algorithm, the research gap caused by the absence of automated DH network design in the literature is filled. Combining these algorithms is effective since it streamlines the design process and saves a lot of time, effort, and labor. Hence, the developed model is unique, and it leads to easy scenario comparison for different parametric studies. As the detailed algorithms are proprietary to Comsof, this chapter only presents the high-level methodologies behind the automated GIS-based tool. The main objective of this chapter is to develop an automated design framework that is capable of designing the current state-of-the-art network. Moreover, the district heating network model has been created and integrated with Comsof's existing routing algorithm. The developed methods are applied to a case study to analyse the impact on network design, cost, and performance of different network configurations. The network pressure level, distribution cluster size and future low heat demand scenarios for a low-temperature

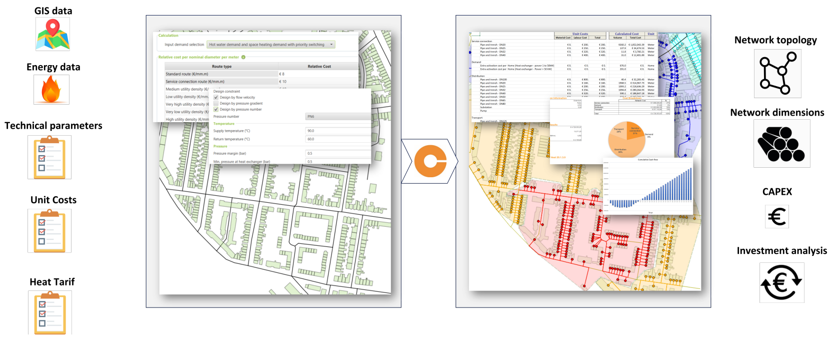

Figure 2.3: Workflow of network model : Inputs, design workflow, and outputs

DH network for a neighbourhood in Nijmegen are investigated in this chapter.

2.2 Methods

In this section, the workflow of network model and the case study neighbourhood is presented first, followed by a high-level overview of the developed models and their usage in Comsof Heat.

2.2.1 Workflow of network model

Figure 2.3 depicts the inputs, design workflow, and outputs of the developed network model. The first prerequisite for setting up the workspace in the network model is the GIS data. Shape files must contain the building polygons, street centerlines, and heat source locations of the design area. After the workspace has been configured, the buildings layer should be provided with the building energy data, such as peak demand and annual energy usage for space heating and domestic hot water. The various street categories can be defined in the layer for street center lines, and the costs for each category can later be configured in the technical/cost configuration section. Then, other area processing procedures are carried out, including the creation of trenches, demand points, and service connection trenches. The network's technical and cost parameters, such as design network supply and return temperatures, design velocity, pipe

Figure 2.4: Case study area: Hengstdal neighbourhood with included / excluded building polygons, demand points, street centerlines, and heat source.

parameters, equipment configuration, and unit costs of pipe and network equipment, should now be configured. Heat tariffs for each building type can be configured if an investment analysis is required. All of the input steps must be completed before the network can be designed.

The network calculation is performed in automated and integrated steps of clustering, routing, network dimensioning, cost estimation, and investment analysis. The network model produces network topology, network dimensions, CAPEX, and investment analysis.

2.2.2 Case study area

This case study takes place in the neighbourhood of Hengstdal (as depicted in Figure 2.4) in the municipality of Nijmegen, Netherlands. Nijmegen was named the 2018 European Green Capital, the most sustainable city in Europe [49]. This area was chosen because a major energy transition is taking place [49]. This neighbourhood's building types are diverse, with several high and low rise buildings, a large shopping centre, and numerous housing corporations. The total number of buildings considered for this study amounts to just over 2300. The total length of a potential DH network was estimated to be about 45 km in a branched network layout, including the service connection pipes to buildings. No future expansion scenarios are considered for this neighbourhood.

The designer starts with the GIS data from the case study area, such as building polygons and street centrelines (as depicted in Figure 2.4) and feeds it into the software. Then, the software can be used to generate demand points in the building polygons at the front edge of the building, which means that the pipes were routed only until the building's front edge. The designer can mark some of the highways and undesirable routes of the street centrelines as excluded in order to avoid these routes during the network calculation. The heat source is located at the top left corner of the chosen area as shown in Figure 2.4. It is assumed that the heat source has enough power to deliver heat to the entire neighbourhood.

2.2.3 Building peak heat demand estimation

The total yearly natural gas consumption of buildings was obtained from the municipality under a confidentiality agreement. These values were estimated by the municipality using open-source street-level data. It was assumed that the yearly natural gas consumption is entirely used to meet the heat demand of the buildings (other usage such as cooking was neglected). The total yearly heat demand was distributed to each month using the monthly heat load factors [45] of similar buildings. The peak monthly heat demand was in January and was estimated to be around 16% of the annual heat demand for residential buildings. The hourly average heat demand was then calculated by evenly distributing the peak monthly heat demand across the hours of January. Finally, for each building type, the most appropriate thermal load factor LF (presented in Table 2.1) [45] was used to estimate the hourly peak heat demand,

$$Q_{peak} = \frac{E_{\text{peak},m}}{t \times LF} \tag{2.1}$$

Table 2.1: Thermal load factors used for different building types [45].

Building type	**Thermal load factor**
Shopping mall	0.36
Residential	0.4
Office	0.47
Hospital	0.5
Multi-family residential buildings	0.51

in kW, where $E_{\text{peak},m}$ is the monthly peak heat demand in kWh and $t = 744$, the total number of hours in the peak month (January). The thermal load factor is defined as the average load divided by the peak load in a specific time period. It was assumed that space heating accounts for 80% of total heat demand, with the remainder attributed to domestic hot water (DHW) [50]. The peak demand of DHW for residential buildings,

$$Q_{peak,DHW} = A \times N + (B \times N^{0.5}) + C, \tag{2.2}$$

in kW was calculated directly with N the cumulative number of homes at each building demand point in the network, and $A = 1.19$, $B = 1.5$, and $C = 0.3$ for a substation with a 120 L buffer tank, or $A = 1.19$, $B = 18$, and $C = 13.1$ for a substation with a heat exchanger only [39]. The simultaneity factor (see section 2.2.4) was integrated into the above equation.

2.2.4 Simultaneity factor

The simultaneity factor is a result of the fact that not all demand points are using their peak power simultaneously. Therefore, if the pipe is dimensioned to satisfy the peak demand of all buildings, the network is significantly over-dimensioned. Several standards (European (EN 806-3:2006) [51], Swedish (SDHA F101) [26] and Danish (DS439) [52]) were developed based on measured heat demand usage profiles and on experience. These standards are different for space heating and DHW since the usage profiles are not similar. Generally, DHW has a high diversity factor due to its very short usage in time every day. The European

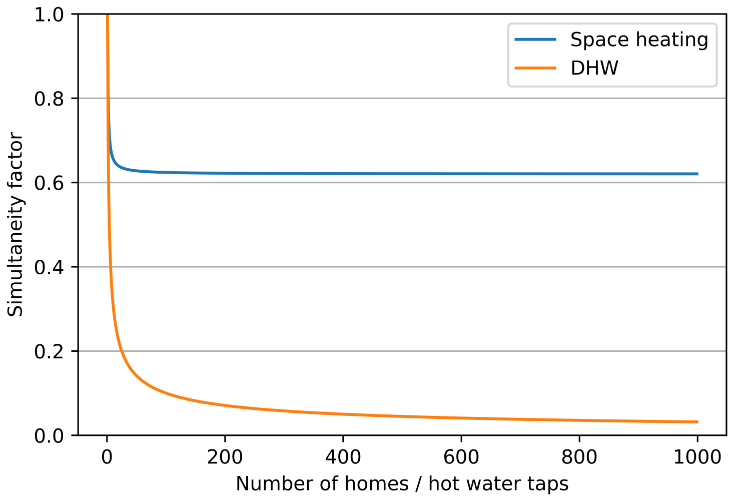

Figure 2.5: Simultaneity factor for space heating and DHW [26].

standard was used in this study because of its wide acceptance.

The space heating simultaneity factor, $SF_{\mathrm{SH},i}$ is calculated based on the total number of homes, N_i connected to the respective pipe node, i:

$$SF_{SH,i} = 0.62 + \left(\frac{0.38}{N_i}\right) \tag{2.3}$$

The simultaneity factor for DHW, $SF_{DHW,i}$ is calculated based on the total number of hot water taps, n_i connected to the respective pipe node, i:

$$SF_{DHW,i} = \frac{1}{\sqrt{n_i}}, \tag{2.4}$$

This is an approximation of the European standard [51] and is used for consumers other than residential houses since the direct peak load [Eq. (2.2)] was used for residential users. The discussed simultaneity factors are represented in Figure 2.5.

The space heating and DHW load for each pipe segment are then calculated with:

$$Q_{SH,i} = SF_{SH,i} \times Q_{CSH,i}, \tag{2.5}$$

$$Q_{DHW,i} = SF_{DHW,i} \times Q_{CDHW,i}, \tag{2.6}$$

where $Q_{CSH,i}$ and $Q_{CDHW,i}$ are the cumulative peak load demands for space heating and domestic hot water at node i, respectively. The cumulative peak load demands are calculated by summing of downstream peak heat demands.

The total heat load after applying simultaneity factors can be calculated for two options, namely cumulative and DHW priority switching strategies. In a cumulative strategy, the total heat load can be obtained by adding both space heating and DHW loads. DHW priority switching means that the power is switched to DHW once the hot water taps are turned on. So, the total heat load for the DHW priority switching strategy can be calculated by taking the maximum of both space heating and DHW loads. The cumulative strategy is used in this study to calculate total heat load:

$$Q_{total,i} = Q_{SH,i} + Q_{DHW,i}. \tag{2.7}$$

2.2.5 District heating network model

In the study reported in this chapter, the network is designed as a branched two-layer network with a transport and distribution layer using Comsof Heat. In addition to the GIS inputs, the network-specific inputs are configured at this stage. The operating temperatures were chosen as 65 °C supply and 40 °C for transport and 60 °C supply and 35 °C return for the distribution network. The ground temperature was chosen as 10 °C at a depth of 1 m. The study area was assumed to be flat, with no height difference between the lowest and highest points to cause an additional pressure drop. Standard commercially available steel pipes in the range between DN20 and DN300, as tabulated in Table 2.2, are configured for the transport of heat. For each pipe size, there are industry-recommended limits for the flow velocities (shown in Table

Table 2.2: Range of standard pipe diameters used in the network model [53] [54].

Nominal diameter	Outside diameter [mm]	Casing outside diameter [mm]	Maximum flow velocity [m/s]
DN20	26.9	110	1
DN25	33.7	110	1
DN32	42.4	125	1.3
DN40	48.3	125	1.5
DN50	60.3	140	1.7
DN65	76.1	160	1.9
DN80	88.9	180	2.2
DN100	114.3	225	2.4
DN125	139.7	250	2.6
DN150	168.3	280	2.8
DN200	219.1	355	3
DN250	273	450	3
DN300	323.9	500	3

2.2), which in turn determine the maximum pressure drops. Allowing a higher maximum pressure drop results in a reduction of pipe sizes but will cause more noise and stress. The pressure drop at the heat interface unit (HIU) of each consumer was set at 0.5 bar. The minimum static pressure required at the end of the return line was set to 2 bar in order to have a safety margin. The extra pressure drop for bends, joints, and valves was assumed as 10% of the total pressure drop in this study. In the remainder of this section, the process of automated network design with Comsof Heat is described.

2.2.5.1 Network clustering

Network clustering groups the building demand points into a set of distribution clusters of a maximum preset size. Every demand point (attributed to the distribution network) in a distribution cluster will be connected to the same substation.

Marquant et al., [41] used parameters such as cluster density, homogene-

Figure 2.6: Output of a simulation indicating the location of distribution clusters, substations and pipe routes.

ity index, and load magnitude for the clustering method. They stated that the clustering methods enable the formulation and solution of large-scale optimization problems for the exploration of the design possibilities of 4DHC networks. Comsof Heat is developed to have input parameters such as the substation size or number of homes and the maximum distance between the substation and a demand point in order to perform the clustering operation. The size of the substation or number of homes will be used to size the cluster, respecting the above-mentioned distance constraint.

There are numerous clustering algorithms in the literature, including k-means [55], hierarchical clustering [56], hierarchical k-means [57], and others. Unternahrer et al., [42] used the K-means algorithm for preliminary clustering and the Integer Linear Programming (ILP) model for main clustering to divide the urban system into spatial clusters (of buildings) with the objective function of minimizing the total distance between the buildings within the same cluster. However, these algorithms are mainly used in statistical data analysis for grouping similar records in a set of data and have limited applications in the context of a network, since not only the location of demand points, but also the topology of the network needs to be considered. For this reason, a problem-specific clustering algorithm based on network simplification was developed. The output of this network clustering algorithm is in the form of shape files (polygons describing the boundary of every cluster), an example of which is visualized for this case study in Figure 2.6.

2.2.5.2 Network routing

The network routing process involves the evaluation of all possible routes that will connect all demand points to the central heat source with pipes according to the specified rules. The streets can be categorized into different types: from low to high densities, from low to high road material costs, and from local streets to highways. The relative cost per meter and per pipe diameter (€/mm/m) can be assigned to each category. Based on the experience of Comsof's industrial partners, the reference costs vary between 6 and 20 €/mm/m in Belgium and the Netherlands. This approach underestimates the cost for small diameter pipes and overestimates the cost for large diameter pipes. However, the effect of this mismatch is negligible on total network costs. Alternatively, the cost factor for each pipe size (€/m) can also be used with detailed cost information (DH pipe, trench fill material, and labour costs). In this study, the network cost is compared between scenarios, so the absolute reference cost will not affect the results. Equipment costs such as for the HIUs, substations, and heat source can also be given as input. Higher costs can be imposed for special cases such as crossing rivers, railways, etc. These cost methods are explained in detail in the network cost estimation section 2.2.5.4.

The discussed cost factors influence the network design, including the pipe routing, the locations where pipes cross a street, the cluster of points to be served from any substation, etc. The choices are made in such a way that the total cost of the designed network is minimal. The complexity lies in the fact that there are many possible combinations, and every decision must also ensure the network satisfies the rules and constraints of the user.

Robledo [58] showed that the problem of optimized fiber network routing (similar to DH routing) belongs to the class of nondeterministic polynomial-time complete (NP-complete) problems. There are no existing methods to solve this type of problem in polynomial time. This means that scalability is a very important challenge, and intelligent heuristics are necessary to find a good solution within a reasonable amount of time. Most of these heuristics are based on graph theory. Comsof Heat makes extensive use of existing graph algorithms from the literature (e.g., breadth-first search and depth-first search [59], the algorithm of Dijkstra [60], the algorithms of Prim [61] and Kruskal [62], etc.). However, the problems in DH network planning are very specific, and almost none of these algorithms could be used immediately. Therefore, many new heuristics and adaptations to existing heuristics were developed, which are often based on meta-heuristics [63] [64]. Within a distribution cluster, every demand point in the distribution layer needs to be connected to a central substation in the cheapest way possible. The Steiner tree problem [65] [66] is another example. Here, the minimum spanning tree over a subset of nodes in the network needs to be found. A modified version of the Steiner tree heuristic was implemented in Comsof Heat. These routing algorithms produce the best possible pipe routes to connect demand points with the heat source while satisfying the imposed rules.

2.2.5.3 Network dimensioning

The network is sized for the peak winter conditions so that it could meet demand throughout the year. Pipe sizing begins with the branch's farthest consumer. The pipe sizing requires taking into account heat flow, pressure loss, and heat loss through the pipes.

Heat flow equation: For a given pipe diameter, the heat flow through the pipe is calculated by:

$$Q = m \times c_p \times \Delta T \tag{2.8}$$

where c_p is the fluid specific heat capacity, ΔT is the temperature difference between the supply and return pipes, and m is the mass flow rate, which is given by:

$$m = A_j \times \rho \times v_j \tag{2.9}$$

with A_j being the internal area of pipe j as determined by:

$$A_j = \frac{\pi}{4} \times {D_i}^2 \tag{2.10}$$

with D_i being the pipe's internal diameter, ρ being the fluid density, and v_j being the fluid velocity of pipe j.

Pressure loss equation: The pressure loss equation is expressed in head loss in terms of the equivalent height of a column of the working fluid:

$$\Delta P = \rho \times g \times \Delta h \tag{2.11}$$

where Δh is the head loss in m and g is the local acceleration due to gravity, $9.81 m/s^2$. The head loss due to friction can be calculated using multiple correlations. These methods of calculating friction head loss are discussed below:

Hazen Williams equation: This equation is an empirical relationship between water flow in a pipe and the pressure loss caused by friction [67]. It is simple, but it has the disadvantage that it is valid only for water. The head loss, h_f is calculated as follows:

$$h_f = \frac{10.67 \times V^{1.852} \times L}{C^{1.852} \times {D_i}^{4.8704}} \tag{2.12}$$

where h_f represents the head loss in meters (water) over the length of the pipe, L represents the pipe length in m, V represents the volumetric flow rate in m^3/s, C represents the pipe roughness coefficient, and D_i represents the internal pipe diameter in m.

Darcy Weisbach equation: This equation [68] relates the head loss by friction to the average velocity of the fluid flow for an incompressible

Table 2.3: Hazen Williams pipe roughness coefficient for some common materials [67].

Material	Hazen Williams Coefficient, C
Aluminium	130 - 150
Cast iron - new unlined	130
Cast iron 10 years old	107 - 113
Cast iron 20 years old	89 - 100
Copper	130 - 140
Metal pipes - smooth	130 - 140
Plastic	130 - 150
Polyethylene, PE, PEH	140
Polyvinyl chloride, PVC, CPVC	150
Steel new unlined	140 - 150
Steel, welded and seamless	100

fluid. It contains a dimensionless friction factor, which can be calculated for different flow conditions.

$$h_f = f \times \frac{L}{D_i} \times \frac{v^2}{2g} \tag{2.13}$$

where f is the Darcy friction factor (also known as flow coefficient), L is the pipe length in m, D_i is the hydraulic diameter of the pipe (for a circular pipe section, this equals the internal pipe diameter) in m, and v is the mean flow velocity in m/s.

Colebrook equation: The Darcy friction factor for rough tubes can be calculated by solving Colebrook's equation [69], which is also drawn in the form of a diagram with a little compromise on accuracy called the Moody diagram. The Colebrook equation [69] and Moody diagram [70] are shown in equation (2.14) and Figure 2.7 respectively.

$$\frac{1}{\sqrt{f}} = -2log_{10}(\frac{\epsilon}{3.7D_h} + \frac{2.51}{Re\sqrt{f}}) \tag{2.14}$$

where f denotes the Darcy-Friction factor, Re refers to the Reynolds number, which is expressed as:

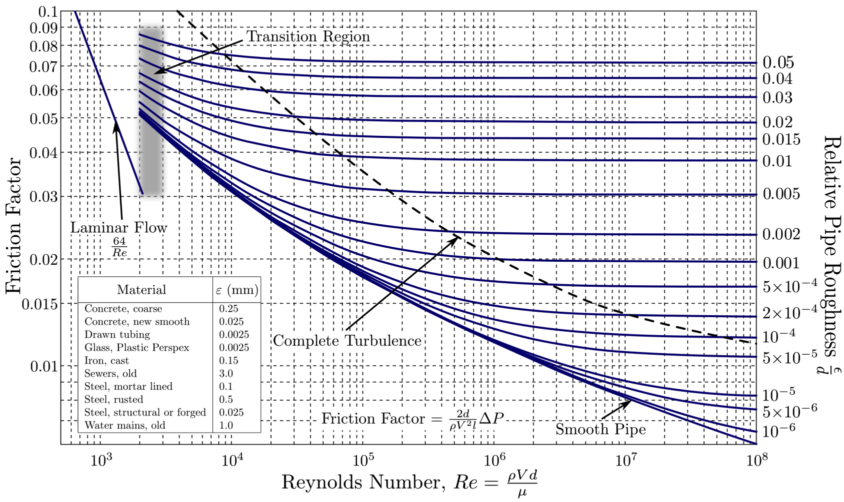

Figure 2.7: Moody diagram showing the Darcy–Weisbach friction factor plotted against Reynolds number for various relative roughness [70].

$$Re = \frac{\rho \times v \times D_i}{\mu} \qquad (2.15)$$

and $\frac{\epsilon}{D_h}$ refers to relative roughness.

The Hazen-Williams equation uses a constant, C to indicate the roughness of a pipe's interior, and its range of applicability is very limited because of its empirical nature. The level of error is very significant if Hazen-Williams' equation is used outside its data ranges [72]. Hence, the Darcy-Weisbach equation is used in this thesis. Literature [73] suggest that the Colebrook equation is the preferred equation to calculate the friction factor in turbulent regimes. In district heating networks, the flow in most pipes at maximum flow rate will be fully turbulent [74]. Therefore, the pressure losses are calculated using the Darcy-Weisbach equation, and the friction factor is calculated using the Colebrook equation in this thesis.

The head loss due to bends, elbows, tees, and valves can be calculated

	Nominal diameter, in								
	Screwed				Flanged				
	$\frac{1}{2}$	1	2	4	1	2	4	8	20
Valves (fully open):									
Globe	14	8.2	6.9	5.7	13	8.5	6.0	5.8	5.5
Gate	0.30	0.24	0.16	0.11	0.80	0.35	0.16	0.07	0.03
Swing check	5.1	2.9	2.1	2.0	2.0	2.0	2.0	2.0	2.0
Angle	9.0	4.7	2.0	1.0	4.5	2.4	2.0	2.0	2.0
Elbows:									
45° regular	0.39	0.32	0.30	0.29					
45° long radius					0.21	0.20	0.19	0.16	0.14
90° regular	2.0	1.5	0.95	0.64	0.50	0.39	0.30	0.26	0.21
90° long radius	1.0	0.72	0.41	0.23	0.40	0.30	0.19	0.15	0.10
180° regular	2.0	1.5	0.95	0.64	0.41	0.35	0.30	0.25	0.20
180° long radius					0.40	0.30	0.21	0.15	0.10
Tees:									
Line flow	0.90	0.90	0.90	0.90	0.24	0.19	0.14	0.10	0.07
Branch flow	2.4	1.8	1.4	1.1	1.0	0.80	0.64	0.58	0.41

Figure 2.8: Loss coefficient for open valves, elbows and tees [71].

as:

$$h_m = \sum k \times \frac{v^2}{2g} \tag{2.16}$$

where h_m is the head loss in m and k is the loss coefficient. Figure 2.8 depicts the loss coefficient for open valves, elbows, and tees. The total pressure loss using the Darcy-Weisbach equation can be calculated by:

$$\Delta P = \rho \times g \times (h_f + h_m) \tag{2.17}$$

$$\Delta P = \rho \times f \times \frac{L}{D_i} \times \frac{v^2}{2} + \rho \times \sum k \times \frac{v^2}{2} \tag{2.18}$$

The temperature difference between the supply and return sides, the pipe roughness, and either the maximum allowed pressure loss or the design flow velocity are input requirements to estimate the heat flow capacity of a pipe. The typical maximum velocity for transmission and distribution pipes is 3.5 m/s and 2.5 m/s, respectively. The design velocity should not exceed the maximum velocity.

Network design constraints: There are three different input network design constraints to the model:

- Design by flow velocity
- Design by pressure gradient
- Design by pressure number

The design by flow velocity constrains mass flow so that a given flow velocity for each pipe is not exceeded. Design by pressure gradient constrains the pipe diameter so that a preset value for the network pressure loss per kilometre is not exceeded. Design by pressure number constrains the pipe diameter so that a given total network pressure loss is not exceeded. The pipes in every segment of the network are then sized based on these constraints and the heat demand. The DH pipe data should be configured, and it will be used to dimension the network and calculate heat losses in the network. There are additional pressure constraints that can be provided as an input to the model.

- Pressure margin
- Minimum pressure difference between supply and return pipe required at the heat exchanger of the building demand point (more relevant for the farthest consumer in the network)
- Minimum pressure required at the end of return pipe (near the heat source/pump)
- Extra pressure loss (as a percentage of friction loss) to take into account the effect of bends and pipe equipment in the network. The above-mentioned method to calculate pressure loss due to bends and pipe equipment is not yet implemented in the tool.

Figure 2.9 shows the pressure diagram of a pressure number design option with 10 bar pressure level. In this example, a pressure margin of 1 bar is used. It is used for safety purposes to not exceed the maximum pressure levels in the system. This leaves 9 bar of maximum allowable operating

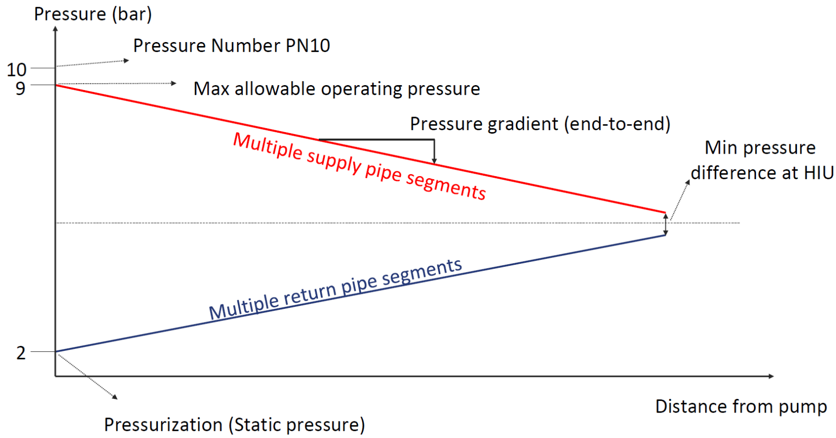

Figure 2.9: The pressure diagram of a pressure number (PN10) design - 10 bar.

pressure. In this example case, the minimum pressure difference between supply and return pipes and the minimum pressure required at the end of the return pipe are defined as 0.5 bar and 2 bar, respectively. Therefore, the available pressure for the supply and return lines is 6.5 bar, and that will be used to dimension the pipes along with other design constraints, if provided. In the case of designing mountain areas or areas with a height difference, the additional input of the height difference between the highest and lowest point is required to take into account the pressure loss due to this height difference. The pressure diagram of a pressure number (PN10) with a height difference of 30 m between the highest and lowest point in the network is shown in Figure 2.10.

Pump power: The pump power can be calculated using the pressure loss (equation (2.18)), volume flow rate, and pump efficiency:

$$P_{pump} = \frac{V \times \Delta p}{\nu} \tag{2.19}$$

For branched networks, the pressure loss should be calculated for each path, and the highest pressure loss of all paths should determine the

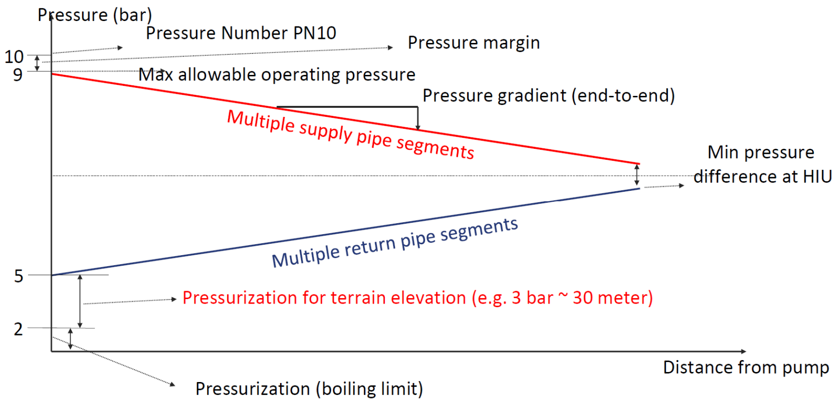

Figure 2.10: The pressure diagram of a pressure number (PN10) design - 10 bar with a height difference of 30 m between highest and lowest point in the network.

network pressure loss.

Heat loss: The costs of operating a DH network are impacted by heat loss. Twin and double pipes have distinct computations for heat loss. The supply and return pipes in twin pipes are encased in a single insulation casing, as opposed to the separate insulation casings for the supply and return pipes in double pipes. Below are the heat loss equations for double pipes.

Heat loss for double pipes: The heat loss for the supply pipe, Q_f, and for the return pipe, Q_r are given by

$$Q_f = U_1(T_f - T_s) - U_2(T_r - T_s), \tag{2.20}$$

$$Q_r = U_1(T_r - T_s) - U_2(T_f - T_s), \tag{2.21}$$

where U_1 refers to the heat loss coefficient from pipe (supply or return) to ground in W/mK, while U_2 refers to the heat loss coefficient from supply pipe to return pipe in W/mK, and T_f, T_r, and T_s are the supply pipe, return pipe, and soil temperatures, respectively. The coefficients

U_1 and U_2 are taken from the European standard (EN 13941) [53]. The overall heat loss is given as:

$$Q_{\text{total}} = Q_f + Q_r = 2(U_1 - U_2)(\frac{T_f + T_r}{2} - T_s). \tag{2.22}$$

$$U_1 = \frac{R_s + R_i}{(R_s + R_i)^2 - R_h^2} \tag{2.23}$$

$$U_2 = \frac{R_h}{(R_s + R_i)^2 - R_h^2} \tag{2.24}$$

where R_s refers to the soil's insulance, R_i refers to the insulating material's insulance, and R_h is the insulance of the heat exchange between the flow and return pipes.

$$R_s = \frac{1}{2\pi\lambda_g} ln \frac{4Z_c}{D_c} \tag{2.25}$$

where Z_c is the corrected depth z value that takes into account the soil surface transition insulance, R_o: $Z_c = Z + R_o * \lambda_s$, where Z is the distance from the surface to the middle of the pipe, λ_g can usually be valued at 1.5–2 W/mK for wet soil, and for dry sand, it will be 1 W/mK, R_o can usually be valued at 0.0685 m^2K/W, and D_c is the outer diameter of the casing pipe.

$$R_i = \frac{1}{2\pi\lambda_i} ln \frac{D_{PUR}}{d_o} \tag{2.26}$$

where D_{PUR} is the diameter of the insulation material, d_o is the outer diameter of the service pipe, and λ_i is the coefficient of thermal conductivity for the PUR insulation.

$$R_h = \frac{1}{4\pi\lambda_g} ln(1 + \frac{2Z_c}{C^i}^2) \tag{2.27}$$

where C^i is the distance between the center lines of the two pipes.

Heat loss for twin pipes: The heat loss for twin pipes [75] can be calculated as follows:

$$Q_{loss} = 4\pi\lambda_i h_s(T_{avg} - T_g) \tag{2.28}$$

where λ_i is the thermal conductivity of the pipe insulation, h_s is the heat loss factor, T_{avg} is the average of the supply and return temperatures, and T_g is the ground temperature.

The heat loss factor is calculated with the equation below:

$$h_s{}^{-1} = \frac{2\lambda_i}{\lambda_g} ln(\frac{2H}{r_o}) + ln(\frac{r_o{}^2}{2DR_i}) + \sigma ln(\frac{r_o{}^4}{r_o{}^4 - D^4}) - \frac{(\frac{r_i}{2D} - \frac{\sigma 2R_i D^3}{r_o{}^4 - D^4})^2}{1 + (\frac{r_i}{2D}{}^2) + \sigma(\frac{2r_i r_o{}^2 D}{r_o{}^4 - D^4})^2} \tag{2.29}$$

where λ_g is the thermal conductivity of the ground, H is the depth between the ground surface and the centre of the pipe, r_o is the outer pipe diameter, D is half the distance between the centres of the pipes, and r_i is the inner pipe diameter.

$$\sigma = \frac{\lambda_i - \lambda_g}{\lambda_i + \lambda_g} \tag{2.30}$$

2.2.5.4 Network cost estimation

The network cost estimation consists of several cost components, such as network pipe and installation cost, equipment costs such as substation (energy centre) cost, HIU cost, and source cost.

Street-level detailed input data is required to better estimate network pipe and installation costs. Therefore, the streets can be categorized into several subtypes, for example, low- to high-density underground utilities, based on road types and traffic, etc. These subtypes can be used to provide input cost data specific to that subtype. Based on the level of detail, network pipe and installation cost calculations are classified into three types. These are:

- Based on reference cost, €/mm/m: Different for each subtype

- Based on price per meter, €/m: Different for each pipe size, as well as a scaling factor for each subtype
- Based on a price per meter, €/m: Different prices for each pipe size and per subtype

Each of these models has its own advantages and disadvantages. The model based on reference cost, €/mm/m is simple, and not a lot of information is required. A reference cost of 20 €/mm/m, for example, will cost 20,000 € for DN100 pipe size with a pipe length of 10 m (20 × 100 × 10). The disadvantage of this model is that the data are based on experiences from past projects, and small pipes are priced low and big pipes are priced high, but errors are averaged out on a larger scale.

The model based on price per meter and scaling factor per subtype has specific costs (€/m) for each pipe size, and the scaling factor is used to multiply the specific costs based on the subtype. This model has better accuracy than the reference cost model since it has a split between material and labour costs. However, the disadvantages are the requirement of more information and the fact that the prices do not always scale linearly for different subtypes, which makes it difficult to represent the prices for different subtypes using scaling factors.

Finally, the third model can have a separate pricing table for each subtype (with different costs for different pipe sizes). This is the most detailed and flexible model, but it requires more detailed price information. The routing is influenced by the subtypes and their respective costs. For the 3 above-mentioned models, a lower reference cost, a lower scaling factor, and a lower average cost per subtype will be a preferred route.

The cost for the substation (energy centre) and HIU can be specified for different power ranges. Those costs will be used in the total network cost estimation. The total source investment cost can be specified, and it will be used in the total network cost estimation.

2.2.6 Scenarios

Several scenarios such as design choice, demand reduction, and repetition have been simulated to study the impact on network dimensions, cost, and performance. Each simulation took about 10-15 minutes to complete using the Intel(R) Core(TM) i7-8750H CPU at 2.20 GHz, 6 Cores, for about 2300 demand points. This section describes different simulated scenarios and their inputs.

2.2.6.1 Design choice scenarios

Four different network configurations are designed, first using the recommended flow velocity constraint (see Table 2.2) and using three pressure number (PN) combinations (PN6 & PN10, PN10 & PN16, and PN16 & PN25 for distribution and transport networks, respectively). For the PN6 and PN10 configurations, substation sizes ranging from 1 MW to 5 MW are simulated to see the impact on cost and trench length.

2.2.6.2 Demand reduction scenarios

Space heating demand is predicted to decrease by 50% over the next 30 years because of the expected prevalence of low-energy buildings with good insulation [36]. In order to see its impact on pipe diameters, network deployment cost, and heat loss, simulations have been performed with space heating demand reduced by 50%. Simulations were done with and without DHW demand since DHW demand is not expected to change.

2.2.6.3 Repetition scenarios

Since the software routing is heuristic, the result can differ between different simulation runs. In these scenarios, this variation is measured by repeating the simulation several times with the same set of inputs and design parameters.

2.3 Results

The total heat demand of the buildings in this case study is 41.5 GWh/yr, based on gas consumption data. The peak demand after applying simultaneity factors was estimated to be 15.6 MW. Several configurations for a DH network were constructed to satisfy this heat demand.

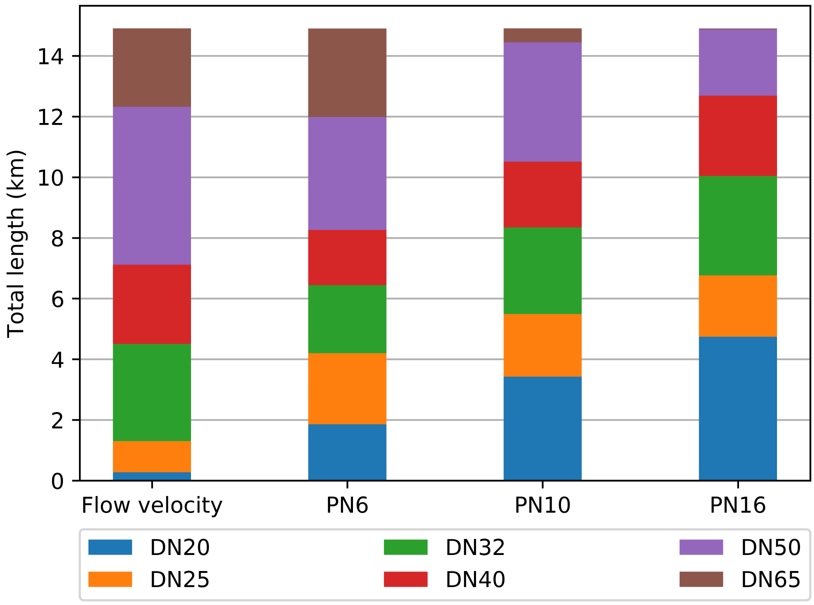

Figure 2.11: Impact of different network pressure levels and flow velocity on DH pipe diameters.

2.3.1 Network pressure levels

The design flow velocity and network pressure levels are the design constraints that have the largest impact on the dimensions of DH pipes. A breakdown of distribution network pipe sizes for the recommended flow velocity constraint and for different network distribution pressure level constraints is presented in Figure 2.11.

Figure 2.12 depicts the total network heat loss and relative network cost as network pressure levels increase. The network deployment cost can be reduced by 18% if the PN16/PN25 configuration is chosen. Furthermore, the heat loss can be reduced by 13% if the highest network pressure level combination (PN16/PN25) is chosen.

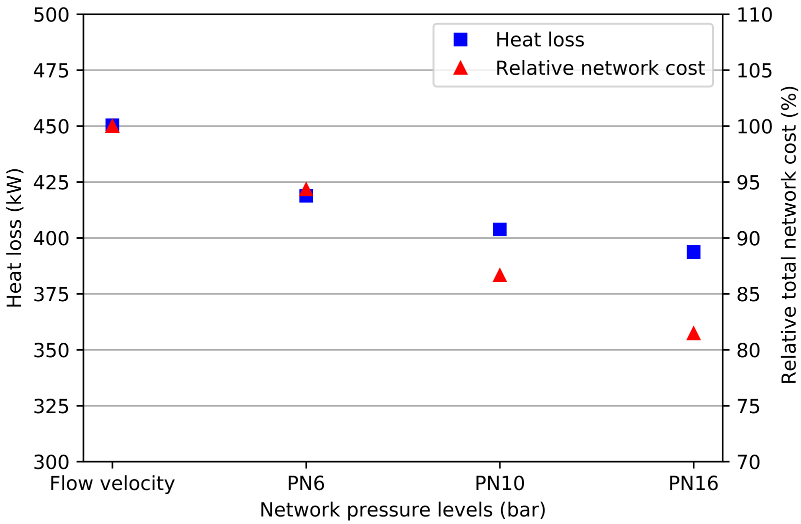

Figure 2.12: Impact of different network pressure levels on heat loss and relative total network cost.

2.3.2 Substation size

The substation size determines the size and number of distribution clusters in the network and influences the distribution pipe size breakdown and network trench length. The total trench length and relative network deployment cost are plotted in Figure 2.13 for substation sizes ranging from 1 MW to 5 MW. Using the cost of a 1 MW substation size case as a baseline, the relative network deployment cost is determined. This implies that if prices increase, the relative cost of network deployment will be greater than 100%. By going from a 1 MW to a 5 MW substation, the overall trench length can be cut by up to 8%. However, the total network deployment cost increases marginally with increasing substation size.

Figure 2.14 shows the trench length and network cost breakdown for both the distribution and transport networks. The length of the distribution network trench is not significantly affected by growing substation sizes. The length of the transport network trench, however, is reduced by

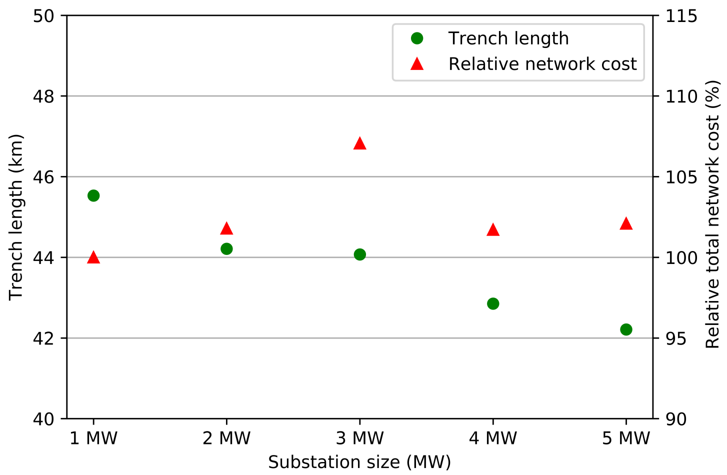

Figure 2.13: Impact of substation sizes on total network: Trench length and relative total network cost.

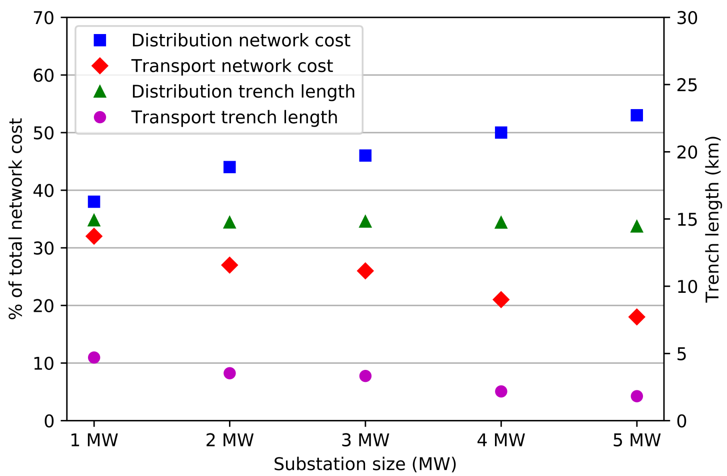

Figure 2.14: Impact of substation sizes on distribution and transport network: Relative cost and trench length.

roughly 60% when the substation size is changed from 1 MW to 5 MW. With larger substation sizes, the distribution network cost percentage

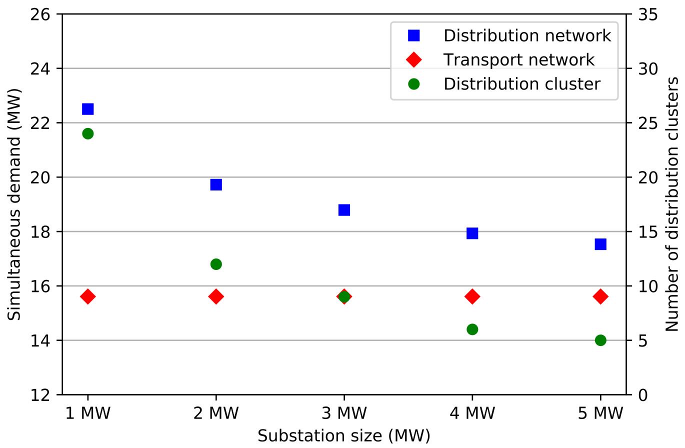

Figure 2.15: Impact of substation sizes on distribution and transport network: Simultaneous demand and number of distribtuion clusters.

rises from 38% to 53%. By converting from a 1 MW to a 5 MW substation size, the transport network cost percentage is reduced from 32% to 18%.

Figure 2.15 depicts the simultaneous demand for both distribution and transport networks as substation size increases. By switching from a 1 MW to a 5 MW substation, the simultaneous demand for the distribution network is reduced by approximately 22%. However, the transport network's simultaneous demand remains unchanged with increasing substation sizes. The number of distribution clusters is also plotted against substation sizes in Figure 2.15. The number of distribution clusters is reduced from 24 to 5 by opting for a 5 MW substation over a 1 MW substation.

2.3.3 Future heat demand cases

The distribution network pipe size breakdown for different heat demand reduction percentages with and without DHW load is compared in Figure 2.16. With DHW loads, the decrease in demand has not resulted in an increase in the proportion of small size distribution pipe lengths.

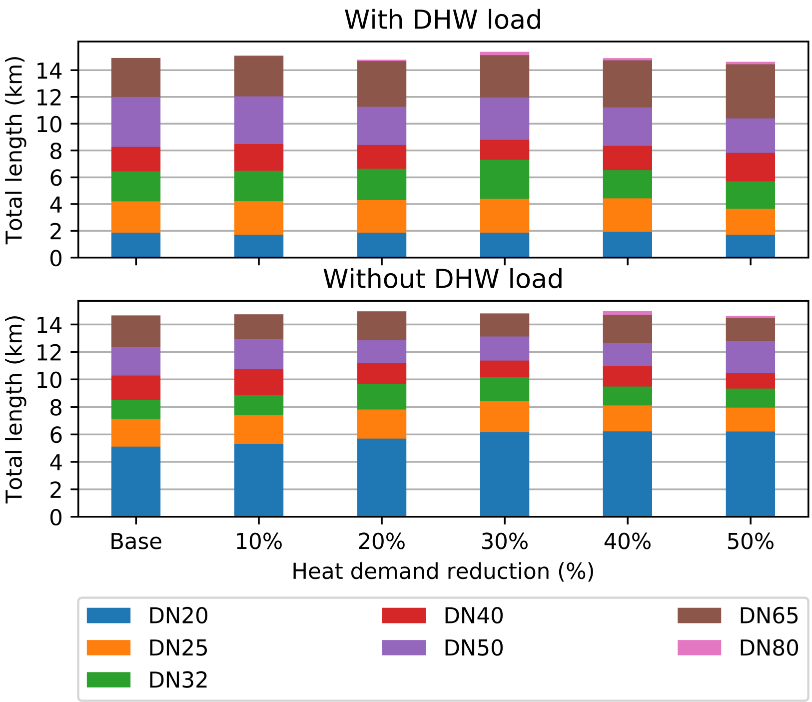

Figure 2.16: Impact of heat demand reduction on pipe diameters with and without DHW.

However, in the absence of DHW load, the proportion of small size distribution pipe lengths increases as demand decreases.

The relative total network cost is plotted with increasing heat demand reduction percentages with and without DHW load in Figure 2.17. The total network cost is reduced only by 9% and 16% for 50% demand reduction case with and without DHW load, respectively. In Figure 2.18, the absolute heat loss and heat loss percentage (% of total heat demand) for the case with and without DHW load are shown. The absolute heat loss remains more or less constant in both cases. However, the relative heat loss increases from 2.7% to 4.8% with DHW load and from 2.9% to 5.7% without DHW load.

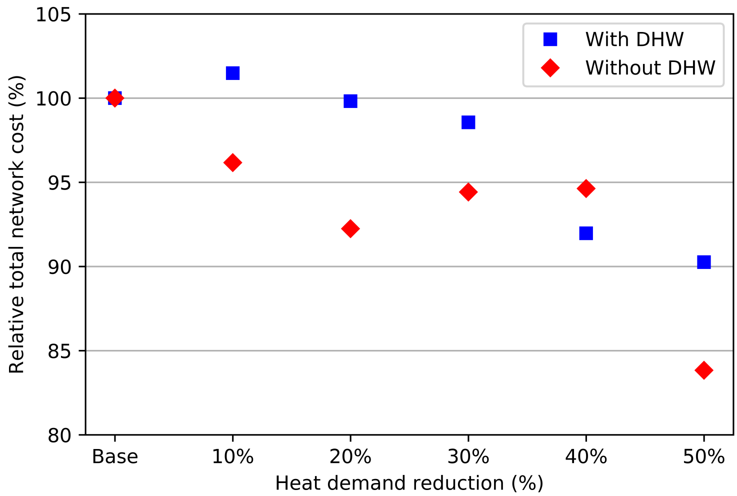

Figure 2.17: Impact of heat demand reduction on relative total network cost with and without DHW.

2.3.4 Results uncertainty

The deviation of the relative network cost for the same input constraints is shown in Figure 2.19. The coefficient of variation is found to be around 0.57%.

2.4 Discussion

In this section, the results are discussed, and they are followed by limitations and future work.

2.4.1 Network pressure levels

The flow velocities recommended by pipe manufacturers are very stringent, necessitating large DH pipe diameters to transfer the necessary power. As illustrated in Figure 2.11, the proportion of small pipe diameters increases with increasing pressure levels. This is due to the fact that smaller pipe sizes can be employed due to the higher network pressure

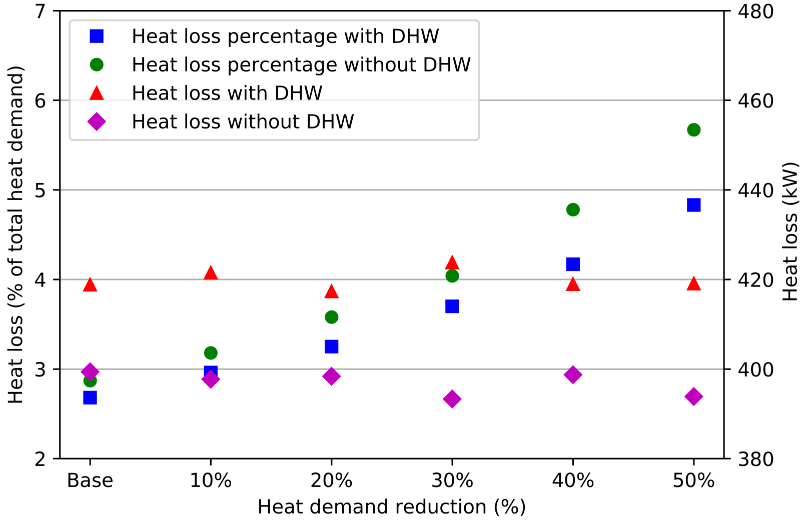

Figure 2.18: Impact of heat demand reduction on heat loss with and without DHW.

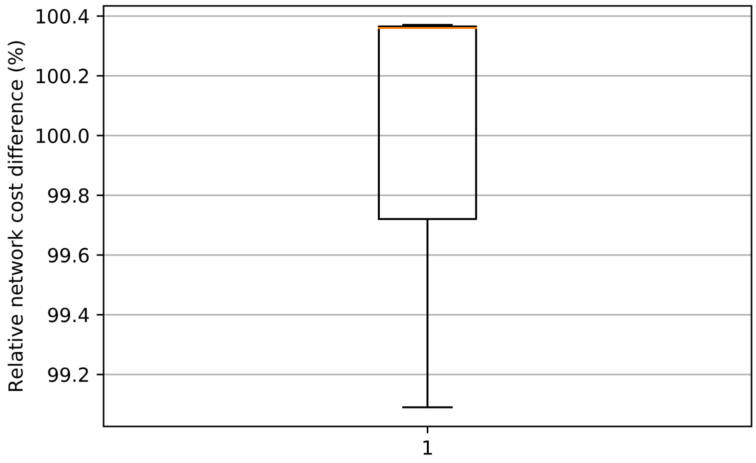

Figure 2.19: Impact of repeating same scenario on total network cost.

levels, allowing for higher pressure losses in the network. Conversely, as network pressure levels rise, the share of large pipe sizes falls. Due to DH pipes' lower cost and smaller diameter, high pressure numbers translate into cheap network capital costs. With higher pressure levels, heat loss is reduced in pipes with smaller diameters because they have less exposed surface area to the environment.

2.4.2 Substation size

A larger substation size results in fewer but larger distribution clusters. This is because a larger substation size leads to more heat being distributed per cluster, which in turn results in larger distribution pipe sizes. Hence, the cost of the distribution network increases with increasing substation sizes. However, the length of the transport network is shortened when there are fewer substations. As a result, the cost of the transport network falls as the size of the substations increases. Additionally, when substation size increases, the overall length of the network trenches gets shorter. Furthermore, as substation size increases, the overall cost of network deployment rises as the cost of the distribution network outweighs the cost of the transport network. The spike in total network cost for 3 MW is because one distribution cluster is created in a location where a longer transport network pipe is needed. As a result, while the cost of the distribution network increased as usual, the overall length of the transport network did not drop as it usually does when a substation is added.

The simultaneous demand of a distribution cluster is higher for smaller substation sizes. This is because a smaller substation size leads to fewer homes per distribution cluster, which results in a higher simultaneous demand per cluster. However, the total number of buildings in the entire network is always constant and hence the transport network simultaneous demand remains constant.

2.4.3 Future demand scenarios

Figure 2.16 illustrates that, unlike when there is no DHW load, a decrease in heat demand does not result in a greater proportion of smaller DH pipes. As a result, we argue that pipe dimensioning is influenced by DHW demand. Costs associated with network deployment do not necessarily decrease when demand declines. The reason for this is that the cost of trenching, rather than the price of smaller pipe diameters, is the most important factor in total network deployment costs. Since heat loss is influenced by operating temperatures, pipe widths, and pipe lengths, the absolute heat loss does not decrease with a drop in heat demand.

2.4.4 Limitations and future work

Only single-source DH networks are taken into consideration in the study provided in this chapter. However, multiple energy sources are gaining traction due to distributed renewable and waste energy sources. Additionally, this study does not take cooling demand into account. In countries with moderate climates like the Netherlands, cooling demand does not now account for a significant portion of energy demand. Climate change, however, has the potential to alter this. Therefore, the goal of the next chapters is to take multi-source distributed district heating and cooling (DHC) systems into account. By including characteristics like multi-source redundant networks, thermal energy storage, combined heating and cooling, energy reciprocity, etc., the current network can be made better. The fourth generation DHC network has a tremendous potential, indicating that more research in this field is necessary.

2.5 Conclusion

In this study, a method for automatically designing DH networks under specified network constraints was described. Utilizing the methodologies discussed here and applied in Comsof Heat, a case study (with more than 2300 buildings) was created to examine the impact of network cost and performance for various network constraints, such as substation sizes and network pressure levels. The network was designed with detailed network attributes such as a two-layer network, service connection pipes to homes, substation location, etc. Automated and optimized routing helped in simulating several scenarios with ease.

The case study demonstrated the effects of several scenarios, including design choices, substation sizes, and demand reduction scenarios, on pipe diameters, network deployment costs, heat loss, and trench length. A smaller substation has a negative impact on the cost of the entire network. One of the findings is that the cost of trenching dominates the overall cost of network deployment. By merging the construction work with that for other services like sewage, gas, roads, etc., this trenching cost can be decreased.

We demonstrated that by reducing the need for space heating by 50%, the cost of network deployment is only lowered by 9% and 16%, respectively, with and without DHW load. This shows that future DH networks' capacity to remain profitable while reducing heat demand would be difficult, and we contend that in order to do so, denser areas will be necessary. Another effect is that *relative* heat loss increases significantly in future demand reduction scenarios. Low-energy buildings are excellent at heating the space at a low temperature. As a result, in the future, the network supply temperature could be further decreased to meet the demand reduction.

Chapter 3

Centralized and Decentralized Storage

Contents

This chapter is largely based on **Jebamalai, J. M.**, Marlein, K., & Laverge, J. (2020). Influence of centralized and distributed thermal energy storage on district heating network design. Energy, 117689, DOI: 10.1016/j.energy.2020.117689.

Future district heating networks have to be flexible enough to absorb the heat load variations and additional heat production variations imposed by increasing intermittent renewable energy sources. Thermal energy storage (TES) is a proven, efficient, and cost-effective technology to provide such flexibility. A centralized hot water storage tank near the source is the most common TES configuration in district heating systems today. Though this configuration provides flexibility and reduces peak load capacity, it doesn't impact the peak transport capacities of the network since the heat still needs to be transported from the source location during peak demand periods. This chapter investigates the benefits of placing thermal storage tanks in the distribution networks to decrease the peak transport capacities of the network and balance the heat loads locally. Building heat demand data is extracted using the open-source street-level gas consumption data, and appropriate heat demand profiles are chosen based on the building type. A case study comparing centralized and distributed storage is carried out using these input data with Comsof Heat, an automated district heating network routing and planning tool. The effect of these storage configurations on total network cost is compared, and several scenarios are explored with different storage sizes. The case study results show that centralized storage can reduce the total network investment cost by 4%, substation-level storage can reduce the total network investment cost by 5% and building-level storage can reduce the total network investment cost by up to 7% for the given inputs.

3.1 Context

The growing importance of waste heat and renewable energy sources is creating a paradigm shift in district heating systems (DHSs) [76, 77, 78]. The problem with utilizing these energy sources is that they are not flexible, and the energy production can't be shifted in time. This energy should be either consumed instantly or wasted. Moreover, the heat demand of buildings is mostly driven by external temperature levels, so the demand profiles are fixed as well [79]. Therefore, TES is becoming an inherent part of DHSs to handle the mismatch between heat supply and demand.

DHSs undergo heat load variations (HLVs) on both daily and seasonal cycles. The daily variations are caused by the occupancy behaviour of buildings, which occurs between and within single days. The seasonal variations are caused by the change in outdoor temperature between summer and winter, which occurs over the year. Generally, daily HLVs are smaller than seasonal HLVs. In Swedish DHSs, daily HLVs account for 3-6% of the annual heat supply [80]. These HLVs lead to increased costs due to increased peak load capacity. Thus, it is important to reduce HLVs and balance the heat output of DHS and the heat load of buildings [19, 81].

TES is an effective solution to reduce HLVs and provide flexibility to DHSs. It also reduces the required genration capacity of the heat source by increasing the full load hours. There are several types of TES systems available based on different physical phenomena, materials or fluids used to store heat, storage duration, etc. Guelpa and Verda [82] reviewed all the possibilities of TES in combination with DHSs. They state that sensible heat TES with water as a storage medium is the most used storage type in combination with DHSs. The reasons behind this selection are low cost, technological simplicity, favourable thermal properties, easy scalability, stratification of water, and the same heat transfer fluid and storage medium [82]. Hence, sensible heat TES with water as a storage medium is used in this study.

In this chapter, a case study of a 2-layer district heating network (shown in [29]) with centralized and distributed storage configurations (shown in Figure 3.1) is investigated. This study designs a new network with a source, network infrastructure, and storage. Hence, the total network cost includes source costs, pipe infrastructure costs, and storage costs.

Centralized storage is the most widely used storage type. This is due to the fact that a large storage volume reduces heat loss because of its

Figure 3.1: A schematic of centralized and distributed thermal energy storage.

good surface-to-volume ratio. Moreover, the larger the storage size, the cheaper the specific storage cost (€/m^3). As stated above, the main function of storage is to reduce load variations, which helps in reducing peak power. Centralized storage reduces the source power in the case study network like any other type of storage. However, since mostly centralized storage is located near the source, the network pipe sizes cannot be designed with smaller diameters. This is because the heat needs to be transported from the same location as the source during network peak demand. The effect of seasonal, daily, and multi-day centralized storage on total network cost is studied in this case study.

The distributed storage is classified into substation-level storage and building-level storage. In substation-level storage, the storage is distributed to all substations in the network. It allows us to distribute the storage within the network. As the storage is located at the substation location, the power doesn't need to be transported from the source to the substation location during network peak demand. Therefore, the transport pipe sizes can be designed with smaller diameters for substation-level storage, but the distribution pipe sizes remain the same. Moreover, the source power can be reduced, similar to centralized storage. However, the disadvantage is that distributed storage is more costly for the same total storage size when compared to centralized storage. The effect of seasonal, daily, and multi-day storage on total network cost is also studied for substation-level storage.

Building-level storage has storage tanks installed in each building, but it is often difficult to locate such storage. Since the storage is located at the building, the heat can be stored and used directly there, so less heat needs to be transported to the building during peak demand. Therefore, both the transport and distribution networks' pipe sizes can be designed with smaller diameters. Furthermore, the source power will also be reduced, similar to other storage types. Though it is not practical to have seasonal storage at building-level, this case is also considered to study the economic impact. Moreover, the daily and multiday storage cases are simulated with the same inputs as centralized and substation-level storage.

Several studies [76, 81, 83, 84] examined the effect of heat storage integration with the district heating network and found benefits such as increased capacity utilization, lower primary energy consumption, lower operating costs, and lower total costs. Manente et al. [76] investigated the integration of a thermal heat storage in the geothermal and waste-to-energy district heating systems of Ferrara to increase energy utilization. A short-term TES with a capacity of 45 MWh is used to decouple the heat production plants from the distribution network. The annual energy stored in the storage tanks from geothermal and waste-to-energy plants is 7000 MWh, which represents almost 4% of the network's annual energy consumption. It results in annual savings of nearly 800,000 cubic meters of natural gas. With these results, they showed that the integration of properly sized heat storage helps to increase the capacity factor of the geothermal plant and the annual conversion efficiency of the waste-to-energy plants.

Turski and Sekret [81] used the buildings and district heating network as TESs to reduce the source power of the district heating system. Their results show that the heat output for central heating can be reduced by

14.8%. Verda and Colella [83] proposed a multi-scale model of storage tanks to analyze the operation of storage systems during the heating season. The analysis is done for the Turin district heating system as a case study. Their findings indicate that primary energy consumption can be reduced by up to 12% while total costs can be reduced by up to 5%. Romanchenko et al. [84] investigated the benefits of applying TES in district heating systems to decrease the heat load variations, comparing centralized storage using a hot water tank and the thermal inertia of buildings. Their results show that the total system's yearly operating cost decreases by 1% when the thermal inertia of buildings is used and by 2% when a hot water tank is added to the district heating system.

The question of centralized or distributed thermal storage or a combination for the cost-effective deployment of district heating networks has not been studied much, but it is relevant because of their high investment costs [85]. However, there are few studies that compare some of their aspects. Nuytten et al. [86] compared the centralized and decentralized storage solutions with CHP and concluded that the storage configuration has an almost linear effect on the overall system flexibility, with the highest flexibility being reached with centralized energy storage. Another study [87] investigated the integration of decentralized thermal storages within a DH network and concluded that they are integrated most efficiently when placed close to the customers in order to obtain high flow velocities for high-temperature thermal media. This helps to reduce the heat losses and achieve better efficiencies in the storage systems and the distribution systems. Marguerite et al. [85] studied the possibilities of integrating centralized and decentralized storages in the DH network of Aarhus, Denmark using two operation strategies. A peak-based strategy has the objective of smoothing the heat demand during peak hours, whereas a price-based strategy has the objective of reducing the operational costs of the DH network. The results show that the system runs at the lowest cost when peak-based strategies are applied to the decentralized storage.

These studies show that thermal storage reduces peak power at the source while increasing cost savings. However, the effect of distributed TES on network design, sizing, and investment costs has not been studied. In this study, different levels of storage (from centralized to distributed) are placed while designing a new DH network, and the total network investment costs are compared to quantify the cost savings. The main objective of this chapter is to perform a parametric study of centralized and distributed storage on the total DH network cost using a case study of a city in Belgium. The cost information used in this analysis is now out of date due to high energy costs and large rates of inflation since it was conducted in 2020.

3.2 Methods

This section summarizes the case study area, the input requirements (for all buildings, source and district heating network model), the storage design, and all the scenarios simulated in this case study. Comsof Heat is used for network routing, pipe dimensioning, and network cost estimation. Storage design and storage cost estimation are done using models developed in Excel. Figure 3.2 depicts the combined work flow of the storage model and Comsof Heat with their key parameters.

3.2.1 Case study area

The case study area is a Belgian city called Kortrijk in the Flemish province of West Flanders, with around 35,000 buildings. Figure 3.3 depicts the process of selecting approximately 2400 buildings from a total of 35000 buildings. At first, the heat map plot of all buildings is plotted to find out the areas with the highest heat density in the city. As expected, the city center has a higher heat density when compared to other areas. The thick dot in the southwest region is due to the single high industrial demand. Then, the city center with around 10,000 buildings is screened for further processing. These areas are then divided into several small clusters to calculate the linear heat density of each cluster. Finally, the clusters with a linear heat density of more than 1 MWh/year/m are selected, and these clusters have around 2,400 buildings. The source is located at the location of a waste incinerator, which is situated around 2 km from the network.

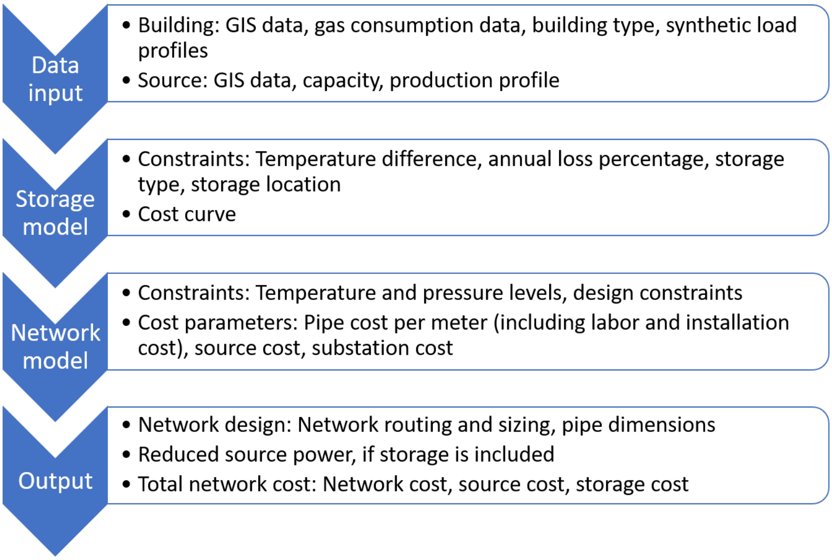

Figure 3.2: Workflow of the storage model and Comsof Heat with their key parameters.

3.2.2 Building and source inputs

The open-source street-level gas consumption data is obtained from the local gas grid operators. Then, the street-level gas consumption data is mapped to building level using the building area ratio for each street. The building polygon area obtained from the open street maps is used in the building area ratio calculation. Now, all the buildings are categorized as one of the following building types: residential, commercial (<0.15 GWh/year) and industrial (>0.15 GWh/year). Figure 3.4 shows the network composition of different building types weighted by their yearly energy consumption. For each of these building types, synthetic load profiles from Belgium for the year 2018 [88] (peak day profile shown in Figure 3.5) are used to estimate the building demand profile. These profiles are generated based on the large data sets and represent a given typical building type in Belgium. The network heat demand is then calculated by aggregating the building heat demand using profiles. The source is assumed to have a constant production profile throughout the year.

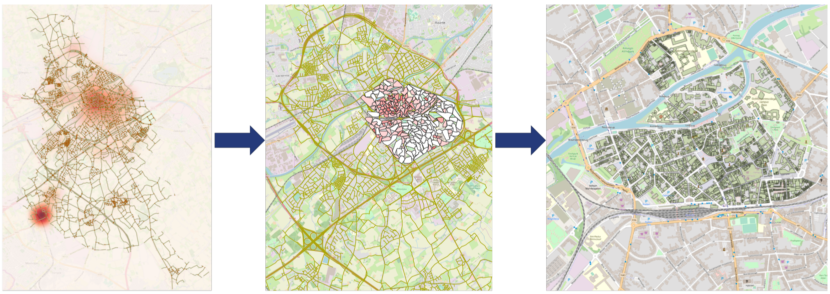

Figure 3.3: Selection of case study area buildings from the total buildings in Kortrijk city.

3.2.3 District heating network configuration

In this case study, a 2-layer network is designed with transport and distribution network temperature levels of 80/50 °C and 70/40 °C respectively. The pressure levels in the transport and distribution networks are designed for PN16 and PN6, respectively. The network constraints are set at 0.5 bar for the minimum pressure at the farthest consumer's heat exchanger and 2 bar for the minimum pressure required to avoid boiling. Table 3.1 displays the standard pipe diameters, maximum flow velocity limits, and costs that are used. The cost reference is obtained from the year 2007 [89] and it is adjusted for inflation in Belgium. The investment cost for the source is considered to be 150,000 €/MW. Comsof Heat (design methodology explained in [29]) creates a new DH network based on these inputs, which include pipe routing, pipe dimensioning, and network cost estimation. The total network investment cost consists of all dimensioned pipe costs, substation costs, source costs, labor costs, and installation costs. Storage costs are calculated and added separately.

3.2.4 Storage design

The TES is designed based on the source production profile and the network demand profile. The surplus or deficit at every time step is calculated using the difference between the production and demand profiles.

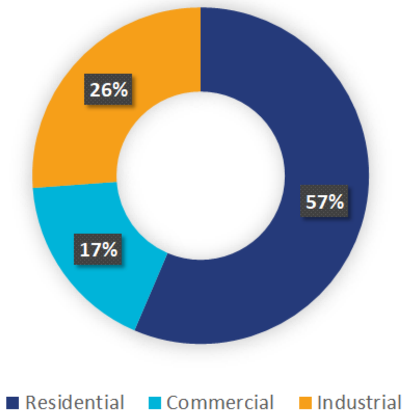

Figure 3.4: Network composition of building types based on yearly energy consumption.

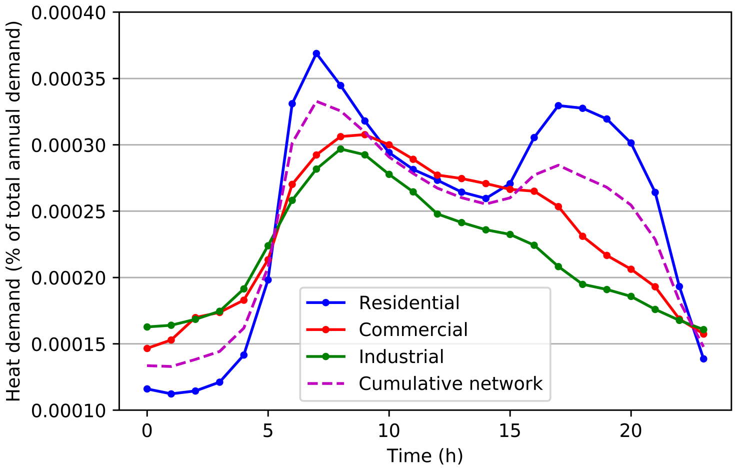

Figure 3.5: Peak daily load profile for building types in Belgium - residential, commercial & industrial and for cumulative network [88].

The storage is charged when there is surplus and available capacity, and it is discharged when there is a deficit and stored energy. Figure 3.6 shows the production profile, demand profile, surplus, and deficit of the

Table 3.1: Range of standard pipe diameters with flow velocity and cost used in Comsof Heat [54, 89].

Nominal diameter	Maximum flow velocity [m/s]	Cost [€/m]
DN20	1	314
DN25	1	377
DN32	1.3	415
DN40	1.5	477
DN50	1.7	503
DN65	1.9	603
DN80	2.2	628
DN100	2.4	691
DN125	2.6	766
DN150	2.8	879
DN200	3	980
DN250	3	1055
DN300	3	1256
DN350	3	1382
DN400	3	1508
DN450	3	1621
DN500	3	1734
DN600	3	1985

storage cycle. Hourly average demand values are used to design the storage.

To model a storage system with a single thermal capacity (one model state), the temperature distribution in the system must be simplified. There are two possible options: one assumes that the temperature throughout the storage tank is constant and that it varies linearly with the amount of thermal energy stored. The second, which is the ideal stratified model, assumes that there is a distinct separation between hot and cold water in the storage tank [74]. Both presumptions are inaccurate in light of the facts. However, the inlet nozzles on the pit and tank storage systems (the ones that are most frequently used in DH networks) are made to minimize the turbulence of the inlet flow in order to preserve the tank stratification [74]. Therefore, the storage model will be based on the assumption of ideal stratification. The thermal energy storage capacity, Q_{TES} can be given by:

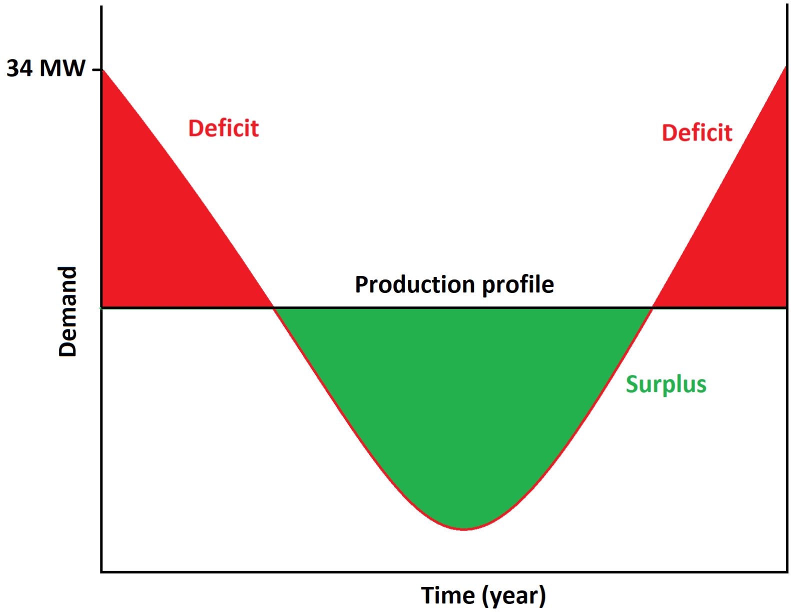

Figure 3.6: Production and demand profile used for the storage calculation.

$$Q_{TES} = V\rho c_p(T_H - T_L) \tag{3.1}$$

where V is the volume of storage, ρ is the density of water, c_p is the specific heat capacity of water, and T_H and T_L are the high and low temperatures of the storage (usually supply and return temperatures of the DH network).

The storage capacity is defined using the maximum storage size for the given production and demand profiles in this study. Maximum storage size is defined as the point where energy produced equals the sum of energy consumed and storage loss. This is calculated by allowing all surplus energy to be stored and all deficit energy to be supplied by storage. The storage cycle should start at the surplus time step (summer time). Then, the source power can be reduced until the storage level goes negative at any certain time step. Now, the maximum storage level is the maximum

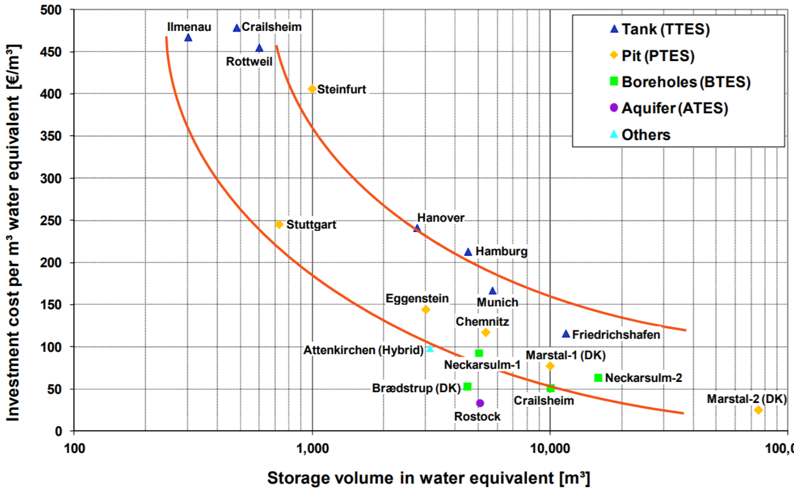

Figure 3.7: Storage cost curve used in the case study [90].

storage capacity for the given production and demand profiles. Then, the storage size can be varied between zero and the maximum storage size to find the optimum for the given inputs. A fixed annual storage loss of 15% is used for the calculation. Figure 3.7 shows the investment cost curve for different storage types used in the case study. The two curves in the figure represent the upper and lower bound costs of all storage types, and the average values are used in this case study.

3.2.4.1 Example storage design calculation

This section explains the storage design calculation using a 12-time step example. The values used in this example are samples and unrelated to the study described in this chapter.

Figure 3.8 illustrates a network generation and consumption profile without storage in 12 time steps, each representing one month. Because there is no storage configured, there is always a surplus and no deficit in every time step. The same example network profile with 100% maximum storage capacity is used in Figure 3.9. Because storage is configured in this case, the generation capacity can be reduced. Reduced generation capacity results in deficits in some time steps and surpluses in others.

Month	Total generation capacity per month (MWh)	Total heating consumption (MWh)	Surplus / Deficit (MWh)
1	6044	5997,57	46,81
2	5459	5417,16	42,28
3	6044	5997,57	46,81
4	5849	5804,1	45,30
5	6044	1190,4	4853,98
6	5849	1152	4697,40
7	6044	1190,4	4853,98
8	6044	1190,4	4853,98
9	5849	5804,1	45,30
10	6044	5997,57	46,81
11	5849	5804,1	45,30
12	6044	5997,57	46,81
Total	71167,7	51542,94	19624,76

Figure 3.8: An example network generation and consumption profile without storage (12 time steps): Each time step representing one month

Start filling the storage

Month	Total generation capacity per month (MWh)	Total heating consumption (MWh)	Surplus / Deficit (MWh)	Storage level_start (MWh)	Storage loss (MWh)	Storage_level_end (MWh)	Generation + Storage	Surplus
1	4462	5997,57	-1535,87	4568,14	57,10	4511,04	10565,71	4568,14
2	4030	5417,16	-1387,24	3123,80	39,05	3084,75	8540,96	3123,80
3	4462	5997,57	-1535,87	1548,89	19,36	1529,52	7546,46	1548,89
4	4318	5804,1	-1486,32	43,20	0,54	42,66	5847,30	43,20
5	4462	1190,4	3271,30	3271,30	40,89	3230,41	4504,36	3313,96
6	4318	1152	3165,78	6396,18	79,95	6316,23	7548,18	6396,18
7	4462	1190,4	3271,30	9587,53	119,84	9467,69	10777,93	9587,53
8	4462	1190,4	3271,30	12738,99	159,24	12579,75	13929,39	12738,99
9	4318	5804,1	-1486,32	11093,43	138,67	10954,76	16897,53	11093,43
10	4462	5997,57	-1535,87	9418,89	117,74	9301,15	15416,46	9418,89
11	4318	5804,1	-1486,32	7814,83	97,69	7717,14	13618,93	7814,83
12	4462	5997,57	-1535,87	6181,28	77,27	6104,01	12178,85	6181,28
Total	52532,93	51542,94	989,99		947,3307385			
	Reduce generated capacity	**Same consumption**	**Creates a deficit In certain months**				**No deficit**	

Figure 3.9: The example network generation and consumption profile with storage (12 time steps): With 100% maximum storage capacity

The overall heating consumption profile remains constant. When there is a surplus, the storage model charges the storage, and when there is a deficit and energy in storage, the storage model discharges the storage. For each time step, the storage loss is computed. Iterative calculations are used to determine the reduced generation capacity so that the sum of generation capacity and storage capacity is always greater than total heating consumption. The required storage capacity in this case is 12739 MWh. If the storage capacity is limited, charging stops when the storage is full. The storage cost is calculated by multiplying the storage unit cost by the storage capacity.

3.2.5 Scenarios

Several scenarios (summarized in Table 3.2) such as storage location scenarios, combined daily and seasonal scenarios, storage on different building types scenarios, demand reduction scenarios, daily profile variation scenarios, and other parameter scenarios are explained in this section. All network calculations are done with the 2 MW substation size unless otherwise stated. In all cases, the storage size is varied from zero to 100 percent of the maximum storage size to study the impact on total network cost. The total network cost includes the source cost, network cost, and storage cost.

3.2.5.1 Storage location scenarios

In these scenarios, the location of the storage varies from centralized to more distributed storage in the network. Four different cases are simulated, namely centralized storage, substation-level storage, building-level storage, and a combination of building-level with centralized and substation-level storage. In all storage location scenarios, three types of storage are considered: seasonal, daily, and multi-day storage. Seasonal storage is designed to buffer all seasonal and daily variations in the profile since hourly demand average values are used. Daily storage is designed to buffer the daily variations of the peak day so that it can handle any other day in the year. Multi-day storage is designed to buffer the daily variations for up to five consecutive days.

Table 3.2: Overview of simulated scenarios with their key input parameters (Storage location: C - Centralized, SS - Substation, B - Building, Storage type: S - Seasonal, D - Daily, MD - Multi-day, Building storage: A - All buildings, R - Residential buildings, CM - Commercial buildings, I - Industrial buildings, Storage ΔT: ΔT - Temperature difference)

Scenarios	**Storage location**	**Storage type**	**Building storage**	**Storage ΔT**	**Source cost [€/MW]**	**Daily profile variation [%]**	**Designed heat demand [%]**	**Substation power [MW]**
Storage locations	C, SS, B, C & B/SS	S, D, MD	A	60	150,000	26	100	2 - 8
Storage in building types	B	D	R, CM, I, CM & I	60	150,000	26	100	-
Heat demand reduction	C, SS, B	MD	A	60	150,000	26	50	4
Daily profile variations	C, SS, B	D	A	60	150,000	6 - 62	100	4
Storage ΔT	C	S	-	50 - 70	150,000	26	100	-
Source costs	C, SS	S	-	60	75,000 - 600,000	26	100	4

In the centralized case, there is one large storage at the source location. In the substation-level case, the storage is distributed to all substation locations. This is studied by simulating the network with 3 different substation sizes: 2 MW, 4 MW, and 8 MW. Consequently, the number of substations (clusters) required for these 3 substation sizes is 7, 10, and 18, respectively. This means that the storage is distributed more when the substation size is reduced. In building-level storage, the storage is distributed to all buildings based on their load fluctuations. Finally, the combined case involves building-level storage to buffer daily variations, and seasonal storage is placed at either the central level or substation level to buffer seasonal variations.

3.2.5.2 Storage on different building type scenarios

Building-level storage is located in various building types, including only residential buildings, commercial buildings, and industrial buildings. Because it is easier to place storage in a few industrial buildings than in all residential buildings, this scenario aids in analysing the cost savings of locating storage in specific building types.

3.2.5.3 Heat demand reduction scenarios

The future heat demand is expected to reduce with increased insulation and energy efficiency [36]. So, the heat demand is reduced by 50% in this scenario. Moreover, multi-day storage is placed at the centralized level, substation level, and building level. The substation-level storage is simulated with a 4 MW substation size, while others are simulated with a 2 MW substation size.

3.2.5.4 Daily profile variation scenarios

The main purpose of storage is to buffer variations, and hence different profile variations lead to different storage sizes and respective cost savings. Seasonal variations are determined by outdoor temperatures and are difficult to modify. However, there can be different daily profiles with different building control strategies since building thermal mass can act as virtual storage.

Generally, daily profile variations mostly depend on the occupancy profile of the occupants. As stated above, it can be adjusted to a certain extent with better control. So, it is possible to shift some of the peaks to other periods. Consequently, different daily profiles exist with different control strategies. In order to study the impact of different daily profile variations on total network cost, three different daily profiles (shown in Figure 3.10) are used to design the network with same input constraints. The relative peak daily profile variations of these profiles are 6%, 26% and 62%. Two of these profiles (6% & 62%) are actual operating profiles of the existing DH network [80, 91] and the other one is generated from the synthetic load profile of buildings in Belgium [88]. These profiles are chosen to study a wide range of daily profile variations.

Henrik and Sven [80] defined an assessment method called relative daily variation, G_d to describe daily variations, which is given below:

$$G_d = \frac{\frac{1}{2}\sum_{h=1}^{24} |P_h - P_d|}{P_a \times 24} \times 100. \tag{3.2}$$

where P_h is the hourly average heat load in W, P_d is the daily average heat load in W and P_a is the annual average heat load in W.

Equation (3.2) is used to calculate the relative daily variation of three peak daily profiles as shown in Figure 3.10. Daily storage is placed at the central, substation, and building locations to study the impact of total network costs and their respective cost savings. 4 MW substation size is used for substation storage, while 2 MW substation is used for centralized and building-level storage.

3.2.5.5 Other parameter scenarios

The other parameters, such as source cost and storage temperature difference, are varied for the centralized storage case to study the impact on total network cost. The source cost is varied from 75,000 €/MW to 600,000 €/MW and the storage temperature difference is varied between 50 °C and 70 °C.

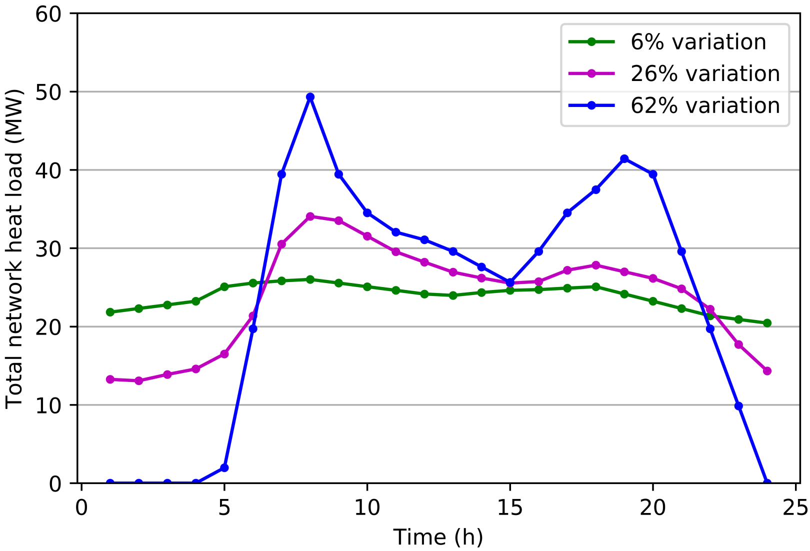

Figure 3.10: 3 different daily profiles of a peak day supplying the same amount of energy.

3.3 Results

The total demand for the case study area in this chapter is calculated to be 95 GWh/year, with a peak load of 34 MW. Several storage configurations, such as centralized, substation, and building level, are analyzed to see their impact on network cost. Figure 3.11 shows the originally designed district heating network using Comsof Heat (explained in [29]).

3.3.1 Centralized storage

Figure 3.12 depicts the impact of storage sizes (seasonal) on source peak power and total network cost. The storage sizes are varied from no storage to 100% of the maximum storage size. The maximum storage size for seasonal storage is calculated to be 450,000 m^3. Between no storage and 1% storage, there is a case called 1 hour storage (for the peak hour in the year), which has a storage size of around 500 m^3. The source peak power can be reduced from 34 MW to around 11 MW with 100% storage

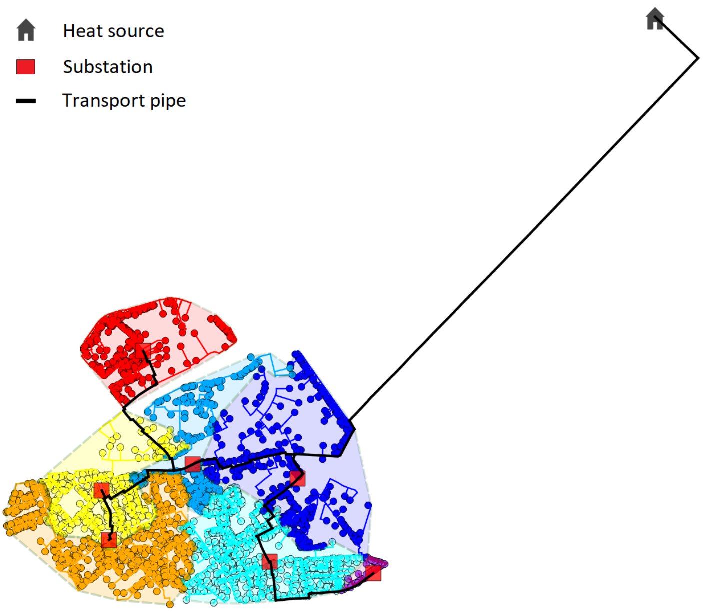

Figure 3.11: Designed district heating network using Comsof Heat.

(450,000 m^3). The total network cost reduces from no storage to 1% storage and then it starts to go up until 100% storage. The minimum total network cost occurs at 1% of the maximum storage size (4500 m^3) for seasonal storage, which is 3.3% cost reduction compared to the case without storage.

The impact of storage sizes (daily) on source peak power and total network cost is shown in Figure 3.13. The maximum storage size for daily storage is around 1000 m^3. The source peak power reduces from 34 MW to around 24 MW with 100% of the maximum daily storage (1000 m^3). The total network cost decreases as the daily storage size increases. The minimum total network cost occurs at 100% maximum storage size (1000 m^3) which is 3.8% cost reduction compared to the case without storage.

The total network cost is plotted against the storage sizes for multi-day storage in Figure 3.14. The minimum total network cost occurs at 2 days

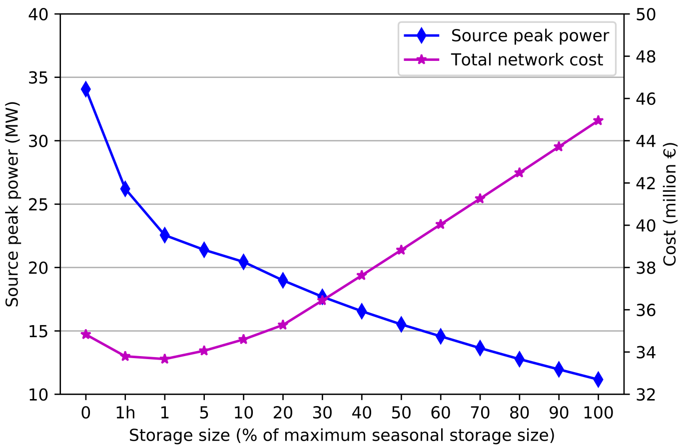

Figure 3.12: Centralized seasonal storage: Impact of storage sizes on source peak power and total network cost with maximum storage size of around 450,000 m^3.

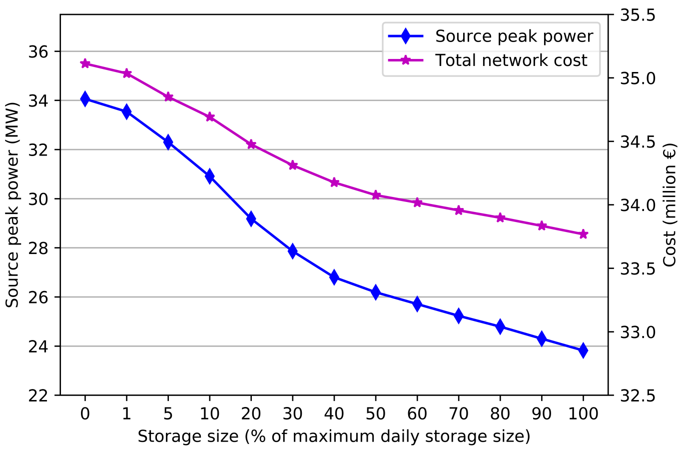

Figure 3.13: Centralized daily storage: Impact of storage sizes on source peak power and total network cost with maximum storage size of around 1000 m^3.

of storage (2000 m^3) which is 3.9% cost reduction compared to the case without storage.

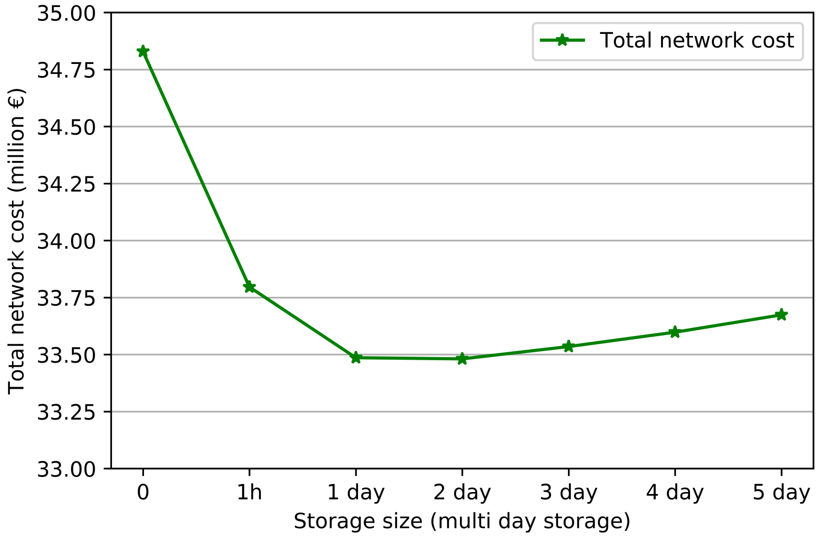

Figure 3.14: Centralized multi-day storage: Impact of storage sizes on total network cost.

3.3.2 Substation level storage

Figure 3.15 shows the effect of substation level seasonal storage on total network cost for various substation sizes. The storage sizes are varied the same way as in the centralized case, and the difference is that they are distributed over all substations. The total network cost drops initially in all three cases, similar to the centralized case. When compared to the other two cases, the total network cost for a 2 MW substation rises sharply after the drop. The 4 MW and 8 MW cases also climb steep initially after the drop, but the cost remains almost the same after a certain storage size. The total minimum cost occurs at 1 hour of storage (500 m^3) for all 3 different substation sizes (2 MW, 4 MW, and 8 MW), and their cost reduction percentages compared to the no storage case are 3.7%, 4.1% and 4% respectively. Furthermore, a 4 MW substation with 1 h of storage (500 m^3) results in the absolute lowest total network cost. The transport cost is plotted against the seasonal storage sizes for different substation sizes, as shown in Figure 3.16. For all substation sizes, the transport network cost decreases as storage size increases.

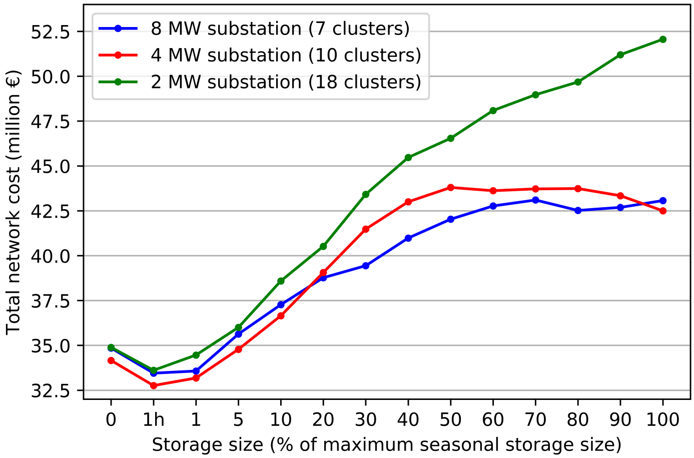

Figure 3.15: Substation level seasonal storage: Impact of storage sizes on total network cost for the substation size of 2 MW, 4 MW and 8 MW.

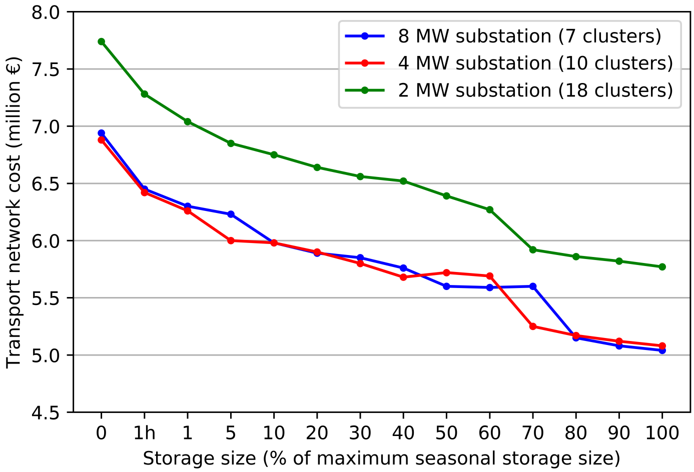

Figure 3.16: Substation-level seasonal storage: Impact of storage sizes on transport network cost for the substation size of 2 MW, 4 MW and 8 MW.

In Figure 3.17, the impact of daily storage sizes on total network cost is shown for 3 different substation sizes. The total network cost occurs

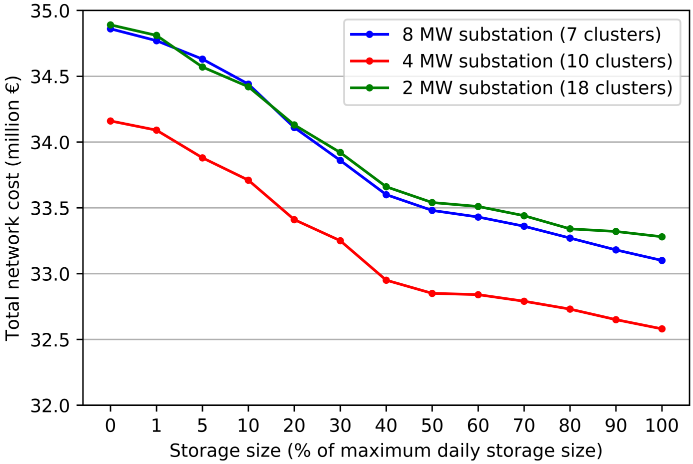

Figure 3.17: Substation-level daily storage: Impact of storage sizes on total network cost for the substation size of 2 MW, 4 MW, and 8 MW.

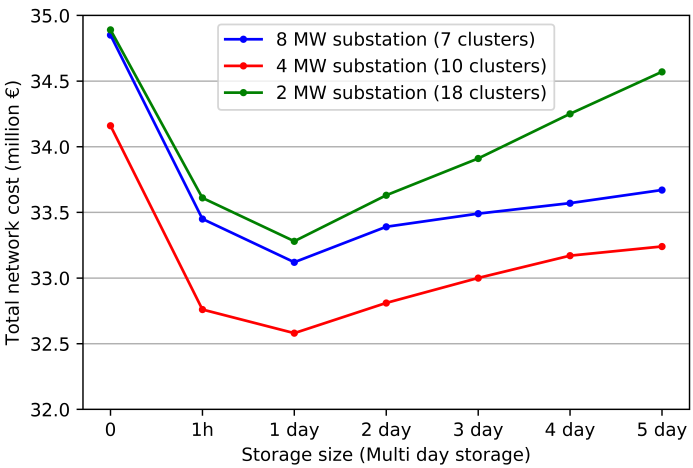

Figure 3.18: Substation-level multi day storage: Impact of storage sizes on total network cost for the substation size of 2 MW, 4 MW and 8 MW.

at 100% maximum daily storage size (1000 m^3) for all 3 cases (2 MW, 4 MW, and 8 MW), and the cost reduction percentages are 4.6%, 4.6% and 5% respectively. The absolute minimum total network cost occurs

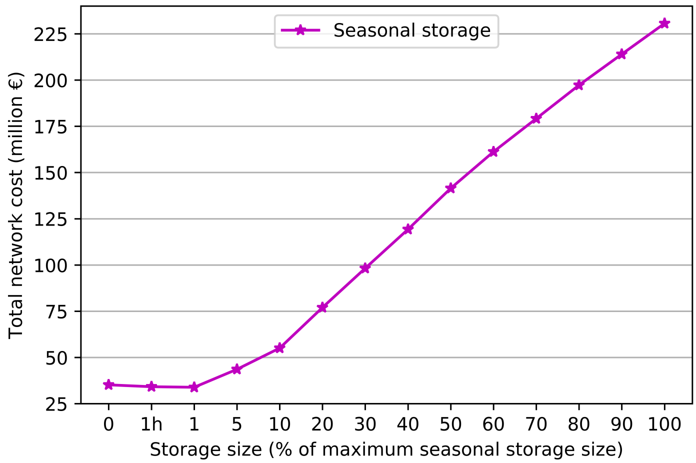

Figure 3.19: Building-level seasonal storage: Impact of storage sizes on total network cost.

with a 4 MW substation size at 100% maximum daily storage size (1000 m^3).

The total network cost for the multi-day storage sizes is plotted in Figure 3.18. The minimum total network cost occurs with a 4 MW substation at 1 day of storage (1000 m^3).

3.3.3 Building level storage

Figure 3.19 shows the impact of building-level seasonal storage on the total network cost. The total network cost drops initially for very small storage sizes and climbs very steeply for large storage sizes. At 1% storage (4500 m^3), the total network cost is reduced by 3.7% compared to the no storage case.

The total network cost is plotted against the building-level daily storage sizes in the Figure 3.20. The total network cost decreases with increasing daily storage size, and the minimum cost occurs at 100% maximum storage size. The cost reduction percentage in this case is 6.6% when compared to no storage case.

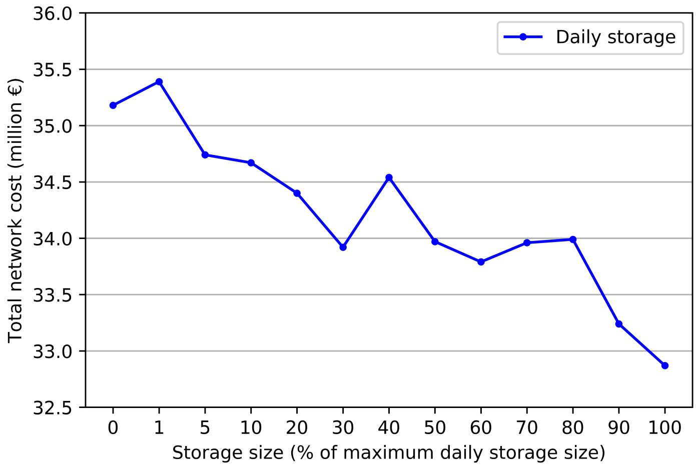

Figure 3.20: Building-level daily storage: Impact of storage sizes on total network cost.

In Figure 3.21, the impact of building-level multi-day storage on total network cost is shown. The 1-day storage case has the lowest total network cost.

3.3.4 Combined daily and seasonal storage

The daily storage is located at building level, and the seasonal storage is located at either a centralized location or a substation location. In all the above cases in this section, daily storage is sized at 100% maximum daily storage size and distributed to all buildings. The seasonal storage is varied from zero to 100% maximum seasonal storage size. Figure 3.22 shows the impact of combined daily and seasonal storage on total network cost. Since there is 100% daily storage in all cases, daily average values are used to calculate the seasonal storage. When there are no daily variations, there are no cost savings from seasonal storage in all four cases. The combination of daily and centralized seasonal storage remains the cheapest when compared with the combination of daily and substation-level storage.

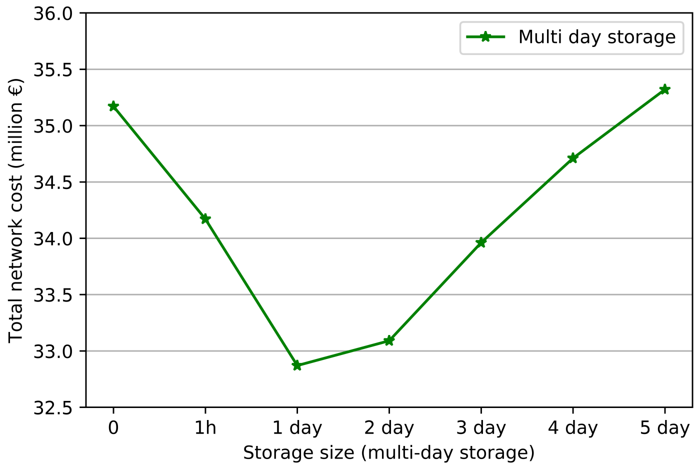

Figure 3.21: Building-level multi-day storage: Impact of storage sizes on total network cost.

3.3.5 Effect of daily storage on different building types

Buildings are classified into three types in this study: residential, commercial, and industrial. This section analyses the impact on total network cost when the daily storage is placed at all buildings, at only residential, only commercial, only industrial, or at a combination of commercial and industrial buildings. Figure 3.23 depicts the total network cost breakdown for all the above cases. The average storage size and total cost reduction of all cases are tabulated in Table 3.3. Daily storage at all buildings has the highest cost reduction (6.6%) compared to the no storage case.

3.3.6 Effect of heat demand reduction

In order to study the effect of heat demand reduction on total network cost, three cases are simulated by reducing 50% of heat demand while keeping the same input constraints. The three cases are multi-day storage at different locations, such as centralized, substation-level (4 MW substation size), and building-level. Figure 3.24 shows the total network

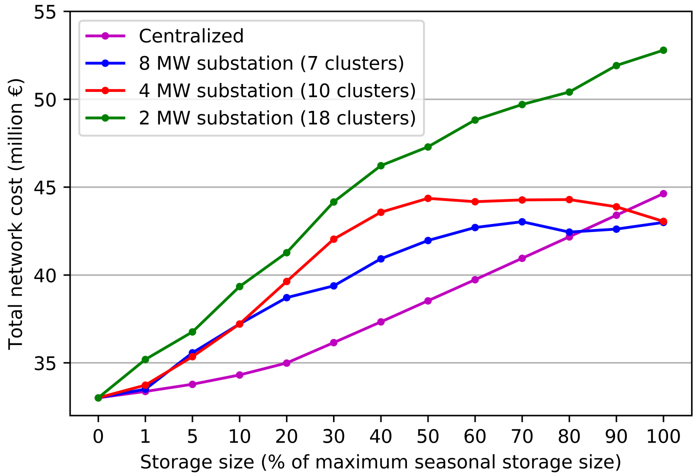

Figure 3.22: Combined daily and seasonal: Impact of storage sizes on total network cost.

Table 3.3: Storage size and total network cost reduction of daily storage at different building types

Building type	**Average storage size** $[m^3]$	**Total storage size** $[m^3]$	**Cost reduction** [%]
All buildings	0.461	1086	6.6
Residential	0.399	699	3
Commercial	0.286	156	0.5
Industrial	3.99	232	0.75
Com and Ind	0.642	388	2.7

cost of different storage sizes for all the above cases. The minimum total cost of centralized, substation-level, and building-level cases occurs at storage sizes of 1 day, 1 day, and 3 days, respectively. Their respective cost reduction percentages are 2.1%, 4% and 8.7% compared to their respective no storage cases. The cost reduction percentages are reduced for centralized and substation-level storage and increased for building-level storage when compared with their respective no demand reduction cases. Furthermore, the total minimum network cost reduces only by

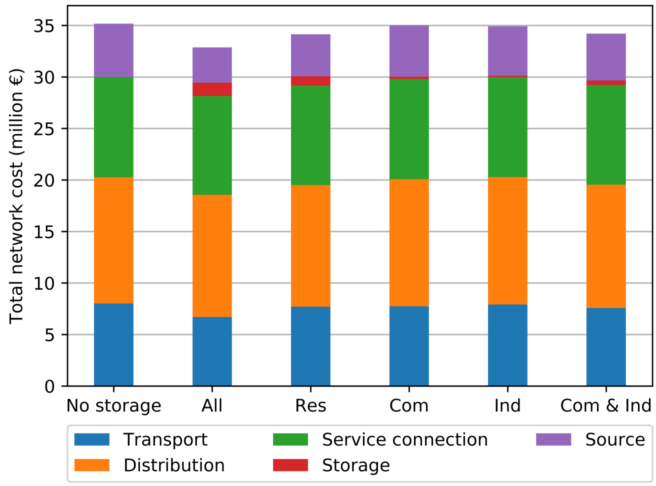

Figure 3.23: Building-level storage: Impact of daily storage at different building types on total network cost.

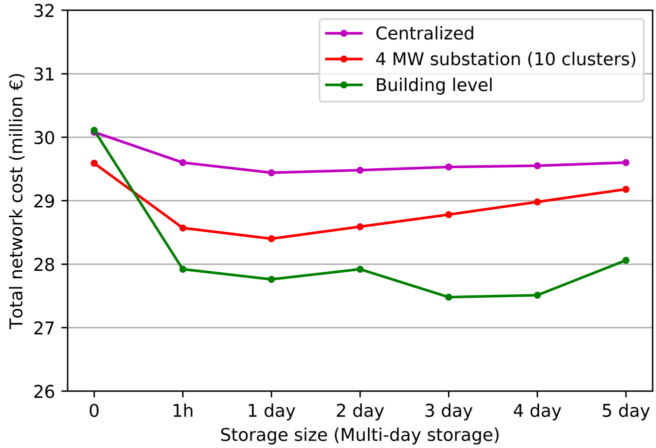

Figure 3.24: Multi-day storage: Effect of 50% reduced heat demand on total network cost.

12%, 12.8% and 16.4% for centralized, substation-level, and building-level cases when the heat demand is reduced by 50%.

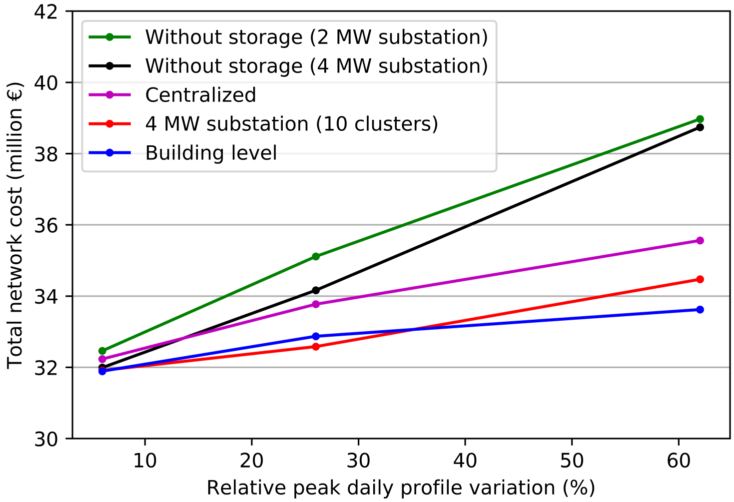

Figure 3.25: Maximum daily storage: Total network cost for different relative daily profile variations.

3.3.7 Effect of daily profile variations

Figure 3.25 shows the total network cost using these daily profiles for centralized storage, substation-level storage (4 MW substation size), building-level storage, and without storage (2 MW & 4 MW substation size) cases. Moreover, the storage size required to buffer the daily variations and the source peak power are tabulated in Table 3.4. Furthermore, the total cost reduction percentage of 100% maximum daily storage size compared to no storage case for centralized, substation-level (4 MW substation) and building-level storage are illustrated in the Figure 3.26.

The larger the relative peak daily variations, the higher the source peak power, storage size, and total network cost in all cases. The total network cost reduction percentages are higher for larger relative peak daily variations. However, the absolute total network costs are cheaper with the lower relative peak daily profile variation. Building-level storage offers the cheapest cost for the maximum daily storage size in all cases.

Table 3.4: Daily maximum storage size and network peak power required for different daily profiles

Peak daily variation [%]	Storage size [m^3]	Source peak power [MW]
6	244	26.1
26	1086	34.06
62	2336	49.31

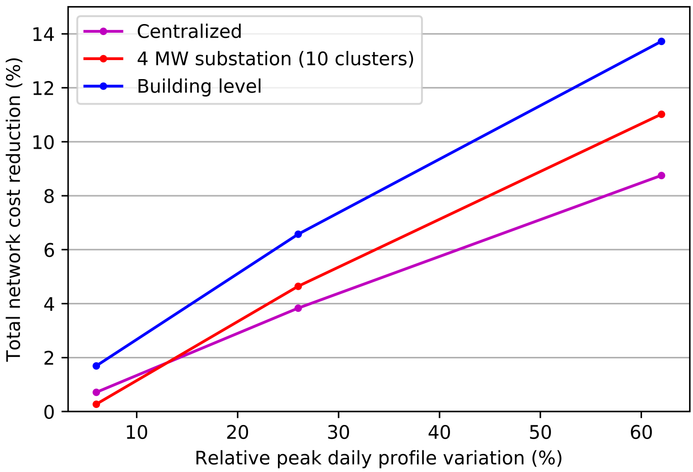

Figure 3.26: Maximum daily storage: Total network cost reduction percentage for different relative daily profile variations.

3.3.8 Effect of source cost

Currently, heat sources such as waste incinerators, CHP plants, heat pumps, waste heat, solar thermal, etc. are available to power district heating networks. The investment cost required for each source varies widely. In order to study the effect of these cost variations, five different source costs are used to design the network with the same input constraints. Figure 3.27 shows the effect of different source costs with centralized seasonal storage on total network cost. The absolute total network cost increases with increasing source costs, but the savings due to storage also increase. The total network cost reduction compared to

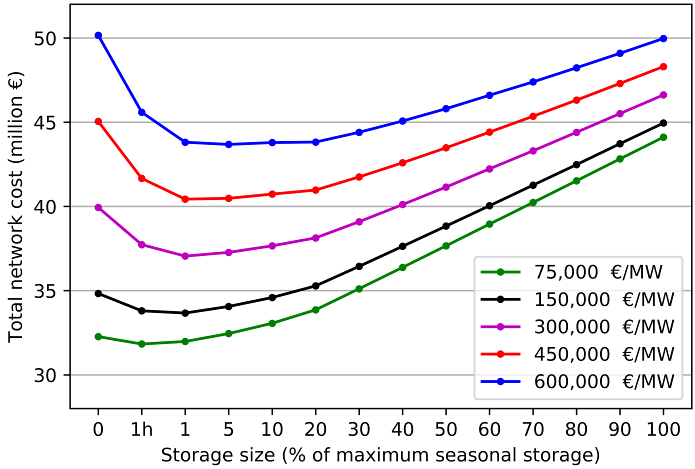

Figure 3.27: Centralized seasonal storage: Total network cost for different source costs.

no storage case increases to 12.9% (600,000 €/MW) from 3.3% (base case: 150,000 €/MW) for centralized seasonal storage. The minimum total network cost shifts toward higher storage sizes when the source costs are higher.

In Figure 3.28, the above cases are repeated with substation-level storage (4 MW substation size) and the total network costs are plotted against the storage size. Similar phenomena is observed in substation-level storage as in the centralized one. The total network cost reduction compared to no storage case increases to 12.4% (600,000 €/MW) from 4.1% (base case: 150,000 €/MW) for substation-level seasonal storage, and the minimum cost occurs at larger storage. Therefore, storage becomes increasingly important to reduce peak power, especially when the source costs are higher.

3.3.9 Effect of storage temperature difference

The storage temperature difference determines the storage size. Figure 3.29 shows the total cost of the network designed with different storage temperature difference for centralized seasonal storage.

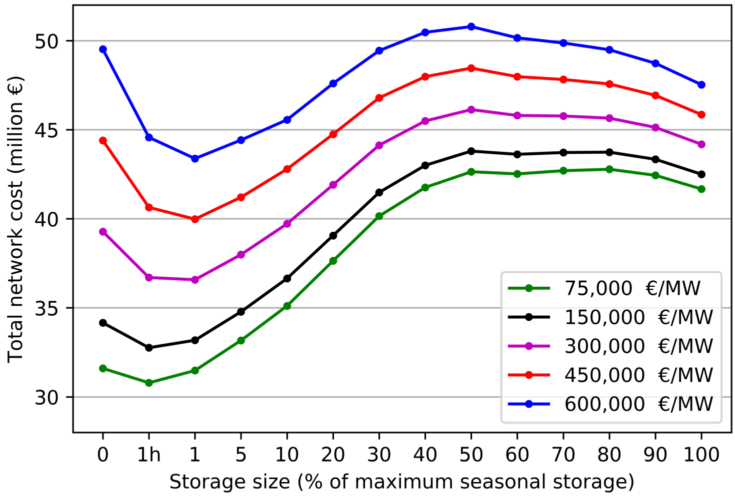

Figure 3.28: Substation-level seasonal storage (4 MW substation size): Total network cost for different source costs.

3.4 Discussion

3.4.1 Storage location scenarios

Table 3.5 provides an overview of optimal scenarios with various levels of storage and their associated network cost reduction. For the given cost parameters and profiles, the optimum storage size for the centralized storage lies between 500 m^3 and 22,500 m^3. High demand profile variation and high peaks for a few hours can be easily reduced with a comparatively smaller storage size. It can be seen in Figure 3.12 that the source peak power decreases drastically at first and then gradually afterwards. Because network costs are constant in centralized storage, source cost reduction contributes to total cost reduction.

For substation-level storage, the optimum storage size lies between 0 m^3 and 4500 m^3. Though substation-level storage contributes to lower transport network costs, the optimum shifts to the left with smaller storage sizes when compared to centralized storage. The minimum total network cost shifts from 2000 m^3 (centralized case) to 1000 m^3 (4 MW substation case). This is due to the fact that large storage sizes have a lower specific

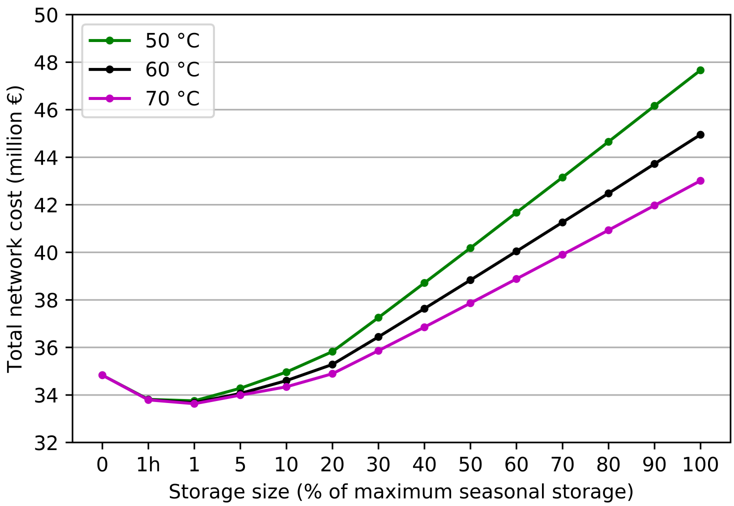

Figure 3.29: Centralized seasonal storage : Total network cost for different storage temperature difference.

storage cost than small storage sizes. Since the storage is distributed at the substation level, the same total storage size is way more expensive compared with centralized storage. However, the cost reduction percentage is slightly higher for 4 MW substation-level storage when compared with centralized storage. Furthermore, there is an optimal point for distributing the storage. It can be seen in the total minimum network cost reduction percentages of seasonal storage (3.7%, 4.1%, 4%) that the cost reduction increases when distributed to 7 and 10 clusters but drops for 18 clusters. Furthermore, the higher storage cost for distributed storage can be observed in Figure 3.15 at 2 MW substation size (18 clusters). In that figure, the total network cost of 18 cluster case goes up drastically with the larger storage size. However, the total network cost of 7 and 10 cluster cases stabilizes at around 40% of the storage size due to the fact that the reduction in transport network costs outweighs the increase in storage costs. There are some unusual curve points in the simulation of substation-level and building-level storage scenarios. This is because these scenarios require network design change and hence reclustering of buildings are done. Since Comsof Heat is heuristic-based software, clus-

Table 3.5: Overview of optimal scenarios with storage at different levels and its corresponding network cost reduction.

Storage location	**No. of storage tanks**	**Storage type**	**Storage size [m^3]**	**Maximum network cost reduction [%]**
Centralized	1	multi-day (2 day)	2000	3.87
Substation-level (8 MW substation size)	7	daily (1 day)	1000	5.06
Substation-level (4 MW substation size)	10	daily (1 day)	1000	4.64
Substation-level (2 MW substation size)	18	daily (1 day)	1000	4.63
Building-level	2328	daily (1 day)	1000	6.57

ters are different every time, and these cause some unusual curve points in the results.

The optimum storage size of building-level storage also lies between 0 m^3 and 4500 m^3. Even though building-level storage has cost reductions due to the source, transport network, and distribution network, the optimum didn't shift to the right because storage at the building level is way more expensive than centralized storage. It is almost impossible or impractical to place large storage units at building level. However, small storage to buffer daily variations is best placed at building level so that the network cost can be reduced as well. Daily storage at the building level can result in the highest cost savings of 6.6% for the cost parameters and profiles specified.

Based on these results, building-level storage is best for daily storage, and centralized or substation-level storage is best for seasonal storage. This leads to a study of the effects of these combinations. The results show that the combination of daily storage at building level and seasonal storage at central level remains the cheapest for the given cost parameters and input profiles. These results are subject to change with parameters such as daily profile variations, source costs, and storage temperature differences.

3.4.2 Effect of daily profile variations

High load variations result in a much higher total network cost when there is no storage. Moreover, the higher the relative peak daily profile variation, the greater the total network cost reduction for daily storage. When compared to substation-level storage, centralized storage offers a better cost reduction for the small daily profile variation. Substation-level storage, on the other hand, provides greater cost savings for higher daily profile variations. This is due to higher variations having higher network peak power and, as a result, larger pipe sizes and costs. So, distributed storage benefits from the reduction in transport network costs for large daily variations and offers higher cost reduction benefits. For daily storage, building-level storage always offers a higher cost reduction, irrespective of the daily variations.

3.4.3 Effect of source cost

The increase in source cost results in a high total network cost. However, high source costs result in a higher total network cost reduction. Moreover, the high source costs shift the optimum storage size towards the right, meaning the optimum storage size is increasing with increasing source costs. This is obvious because source costs are also part of the total network cost. A similar pattern is observed for substation-level storage as well. But the respective optimum storage size of substation-level storage is smaller than centralized storage, as expected.

3.4.4 Limitations and future work

Only three building types are categorized, and the same synthetic load profile is used for all buildings in the same category. However, this is not the case in reality since not all buildings in the same category have exactly the same profile. Currently, the storage calculations are done using Excel, and simulations with storage require a lot of manual effort, but in the future, this will be automated and integrated with Comsof Heat. The automation allows for the use of different profile types for different buildings with ease. Moreover, the location of storage is not optimized and is placed at the same location as the substation. One future task would be to find out whether an optimal storage location exists or not.

3.5 Conclusion

This study analysed the effect of centralized and distributed storage on the total network cost of a district heating network under the given input constraints. The best 2,400 buildings out of approximately 35,000 are chosen for the case study. Then, the district heating network is designed to supply heat to these buildings using Comsof Heat, and Excel is used for storage calculations.

The case study results show that the maximum network cost reduction using centralized storage compared to no storage is 3.9% with a 2-day storage capacity (2000 m^3). For the substation level storage (4MW substation size), the maximum network cost reduction inch upto 5.1% with 1 day of storage (1000 m^3). The building level storage further provides the higher maximum network cost reduction of 6.6% with 1 day of storage (1000 m^3). This shows that an optimal storage size exists for all cases and that it differs with storage distribution. Moreover, the maximum network cost reduction increases when the storage is distributed to 7 and 10, but then drops while distributing further. This proves that there is an optimal point for distributing the storage. Beyond that point, it is no longer profitable to distribute further. In this case study, the optimum storage distribution is between seven and ten clusters. Furthermore, building-level storage remains the cheapest for small storage sizes. When analyzing the combination of daily and seasonal storage, the combination of building level daily storage and centralized seasonal storage remains the cheapest network. In a nutshell, building-level storage is more suitable for daily storage, and centralized to substation-level storage is more suitable for seasonal storage.

For the scenario with 50% heat demand reduction, the maximum network cost reduction will only be around 16.4% with building level storage. Hence, the demand reduction does not correspond with the respective total network cost reduction.

Three different daily profile variations are quantified using an assessment method from the literature using the relative peak daily profile variation. It is shown that the higher the relative peak daily profile variation, the greater the maximum network cost reduction. Moreover, centralized storage offers the best cost savings for smaller peak daily profile variations. Substation level storage is favourable for high peak daily profile variations. Building-level storage remains the cheapest, irrespective of the relative peak daily profile variations. Furthermore, high source costs result in high cost savings and shift the optimal storage size towards larger storage sizes.

The results and conclusions are based on the input network design and cost assumptions, which are specific to the network design and location. As a result, different input assumptions and cost data will produce different outcomes. By examining various demand profile variations, source costs, and storage temperature differences in this study, we attempted to generalize the findings. Furthermore, the costs at the time of this study (2020) are outdated but the conclusions are largely unaffected because costs for both heat sources and storage may have increased. When using the most recent cost data, minor changes are possible.

Chapter 4

Multi-Source Network Design - Branched Topology

Contents

This chapter is largely based on **Jebamalai, Joseph Maria**, Kurt Marlein, and Jelle Laverge. “A method for automated routing and designing of multi-source district heating networks” 15th conference on sustainable development of energy, water and environment systems, September 2020.

District heating systems are getting decentralized because of the increasing necessity to integrate distributed waste heat and renewable energy sources. Multiple sources are becoming an integral part of district heating systems. However, efficient routing of the district heating network is challenging with multiple sources. Therefore, optimization is necessary to choose the most cost-efficient route and source allocation for the building demand points. The goal of this chapter is to present a method for automated routing and design of multi-source district heating networks that uses a combination of assignment and routing algorithms. The developed method is implemented as a proof of concept in Comsof Heat, a GIS-based district heating network planning and dimensioning tool. This can help in calculating different scenarios quickly, and the tool can provide a network deployment cost estimation and return on investment calculation as well. A municipality from Belgium is used as a case study to demonstrate the developed method using Comsof Heat. Several scenarios with different possible source options and building demand points will be studied, and their impacts on network costs will be compared. The tool is used to select the best possible energy sources out of the several given possibilities based on the following parameters: source investment cost, energy production cost, carbon cost, or combinations of the above. Then, the network routing is done to connect the building demand points and the selected energy sources. Finally, all the simulated cases are compared to study the effect of design choices on costs and CO2 emissions.

4.1 Relevant literature

Integrating renewable energy sources into the district heating network has a lot of potential. These renewable energy sources, such as solar thermal energy and industrial waste heat, are decentralized. The integration of these distributed sources with district heating systems will result in the concept of next-generation district heating systems that are more energy-efficient and environmentally friendly. However, the complexity of network topology will increase if renewables are integrated with district heating systems. Therefore, automated design methods are imperative, especially for large-scale, complex topology networks with multiple heat sources.

Bordin et al. [92] emphasized the importance of developing DH models with mesh networks and multiple heat sources. They presented preliminary results showing the potential to solve realistically sized networks. Mertz et al. [93] developed a mixed-integer non-linear formulation for structure and technology optimization involved in district heating network design, minimizing the total costs over multiple reference periods.

Vesterlund and Dahl [94] proposed a method for modelling complex district heating systems with multiple source meshed DH networks. They explained the method to analyse how loops and bottlenecks affect the behaviour of the network and its thermal energy distribution path. Using the proposed method, the authors simulated a complex meshed DH network for the town of Kiruna.

Morvaj et al. [95] used a mixed-integer linear approach to the multi-objective optimization of the topology, design, and operation of a distributed energy system, including heating networks. They investigated different scenarios about the available technologies, layout limitations, and operating constraints. Fang and Risto [96] developed a genetic algorithm-based method for optimizing the heat production simultaneously at multiple heat sources at different district heating network locations to minimize the combined production and distribution costs. Wang et al. [97] proposed a mathematical description of the hydraulic characteristics of large-scale DH networks with a mesh topology and multiple sources. They introduced the general reduced gradient algorithm to optimize the hydraulic performance of the network.

Aberg and Widen [98] presented a study on the cost optimization of heat generation in DH systems considering different types of fuels (fossil and renewable). But, in their method, the DH network is described as a black box with an overall heat demand of the users. Sartor et al. [99] studied the operation of combined heat and power plants connected to district heating networks, but they focused more on the plant side than on the network side of the simulated system. Pirouti et al. [100] aim at minimizing capital costs and energy consumption in a district heating network by varying the flow rates and supply temperatures. However, their study consists of a simple tree structure with one heat source and seven user clusters.

Kuriyan and Shah [101] described a combined spatial and technological model for planning district heating systems. They used a mixed integer linear program to select the optimal mix of technology types, sizes, and fuels for local energy generation, combined with energy imports and exports. This model can also be used to select the energy source locations, the distribution route, and optionally the heat loads that will be connected to a district heating system. This optimisation model combines a map-based spatial framework with a flexible resource technology network representation that incorporates multiple heat sources.

This chapter describes the method for automated routing and designing of the multiple-source district heating networks using a combination of assignment and routing algorithms. Using the developed multiple source design method, a case study with 2,400 buildings in the Belgian city of Kortrijk will be developed. Six potential heat sources will be given as an input to supply these 2400 buildings using a multiple-source district heating network. Several different scenarios are simulated using different orders of substations and different source selection KPIs such as optimizing for investment cost, optimizing for energy production cost, optimizing for carbon cost, and optimizing for combinations of the above and different carbon costs. These simulated cases are compared to study the effect of design choices on costs and CO2 emissions. Due to high energy prices and significant rates of inflation from the time this study was conducted in 2020, the cost data used in it are now out of date.

4.2 Methodology

This section summarizes the case study area, the input requirements (for buildings, sources, and the district heating network), the multiple source design method, and all the scenarios simulated in this case study. The developed design method for multiple sources is implemented in Comsof Heat as a POC. Network routing, pipe dimensioning, and network cost estimation are done using Comsof Heat.

4.2.1 Case study description

Kortrijk, a Belgian city in the Flemish province of West Flanders, is chosen as a case study area. It has around 35,000 buildings, including residential, commercial, and industrial buildings. Among them, 2400 buildings are selected based on the linear heat density. The case study area is divided into several small clusters, and clusters with a linear heat density greater than 1 MWh/year/m are selected (as explained in section 3.2.1).

Figure 4.1 shows the selected buildings (in green) that are included in this case study. Figure 4.2 shows the six potential sources that are considered in this case study. The main baseload source is a waste incinerator, located around 2 km from the network. There are 3 water source heat pumps placed close to the river. Moreover, there is a combined heat and power (CHP) plant located in the Howest University campus. Furthermore, a gas boiler is placed at the newly developed area with swimming pool.

4.2.2 Building and source inputs

The buildings' energy consumption is estimated using open-source street-level gas consumption data obtained from the local gas grid operators. Then, the building's peak heat demand is estimated using the equation 2.1 explained in the section 2.2.3. For the source, the main input is the capacity of the source. The other inputs are source type, percentage of annual network energy consumption delivered by the source, investment cost per MW, energy production cost per MWh, CO2 emissions per MWh, CO2 cost per tonne CO2, and reference CO2 emissions per MWh

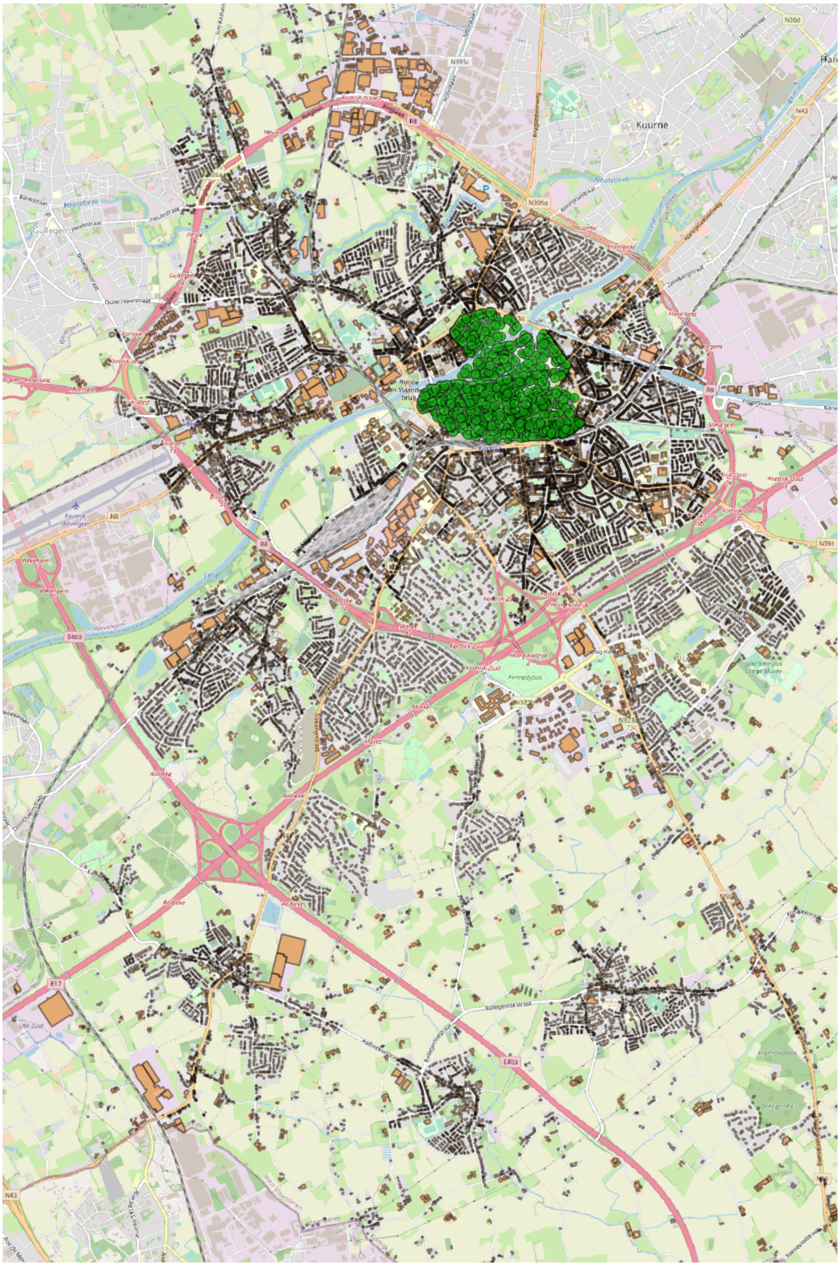

Figure 4.1: Selected buildings (in green) out of 35000 buildings.

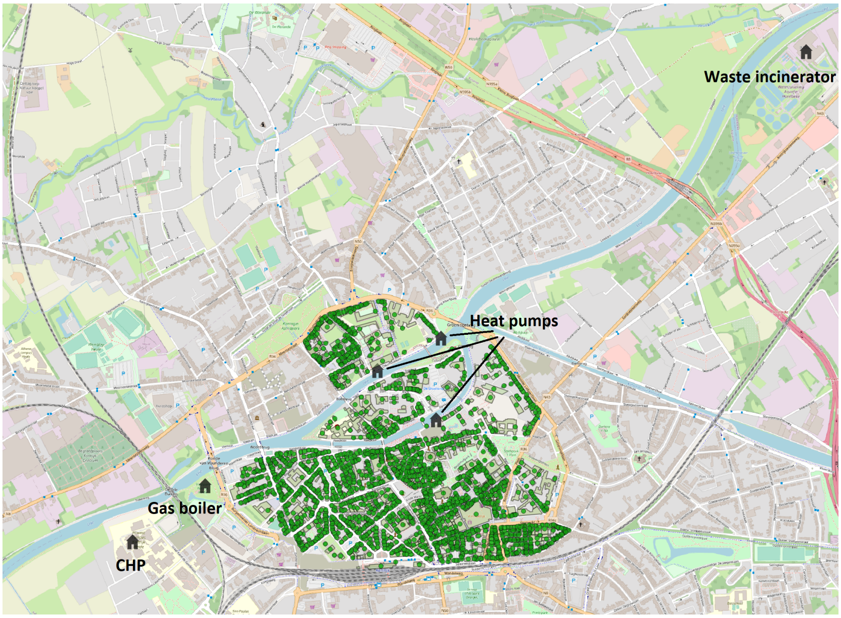

Figure 4.2: Selected buildings (in green) with the potential heat sources.

to calculate CO2 savings. These inputs are defined per scenario, so they will be mentioned under the scenarios section.

4.2.3 District heating network inputs

In this case study, a 2-layer network configuration is chosen with transport and distribution network temperature levels of 80/50 °C and 70/40 °C, respectively. The pressure level of PN16 is used for the transport network, and PN6 is used for the distribution network. The network constraints are set at 0.5 bar for the minimum pressure at the farthest consumer's heat exchanger and 2 bar for the minimum pressure required to avoid boiling. The pipe costs data are used from this paper [102].

4.2.4 Multiple source design method

In this method, the assignment (substation with heat source) and routing algorithms are combined to design the network automatically. Some of the assumptions for this method are as follows:

- All sources are assumed to have the same supply temperatures. In cases of low temperature sources, an extra heat pump can be used to increase the temperature. In cases of high temperature sources, an extra heat exchanger is required to decrease the temperature. This would incur additional costs.
- Simultaneity factor is set to 1 in the transport layer. Generally, a high simultaneity factor (0.9 or close to 1) is used in the transport network to ensure heat delivery at all times. As a result, this limitation will have little impact on design flexibility.
- Multi-source design method is used only in the transport network. Comsof Heat's existing method is used for the distribution network calculation [103].

4.2.4.1 Distribution network calculation

The demand points (selected buildings) are clustered to form the distribution network with a substation. The size of the cluster will be determined by the user inputs, such as power in MW or the number of homes. After the cluster creation, we have several distribution networks with substation on each cluster (shown in Figure 4.3). These substations and sources are the inputs for this multiple source design method. The methodology for the clustering and distribution network calculation is explained in the chapter 2.

4.2.4.2 Transport network calculation

The results of the distribution network calculation are the inputs for the transport network calculation. The main inputs are clusters with substation locations, simultaneous demand of each substation, source locations, and source capacity.

There are two possible approaches to connect the substations with the sources: a bottom-up approach and a top-down approach. Bottom-up means starting with a substation and looking for the best (cheaper) source, while top-down means starting with a source and looking for

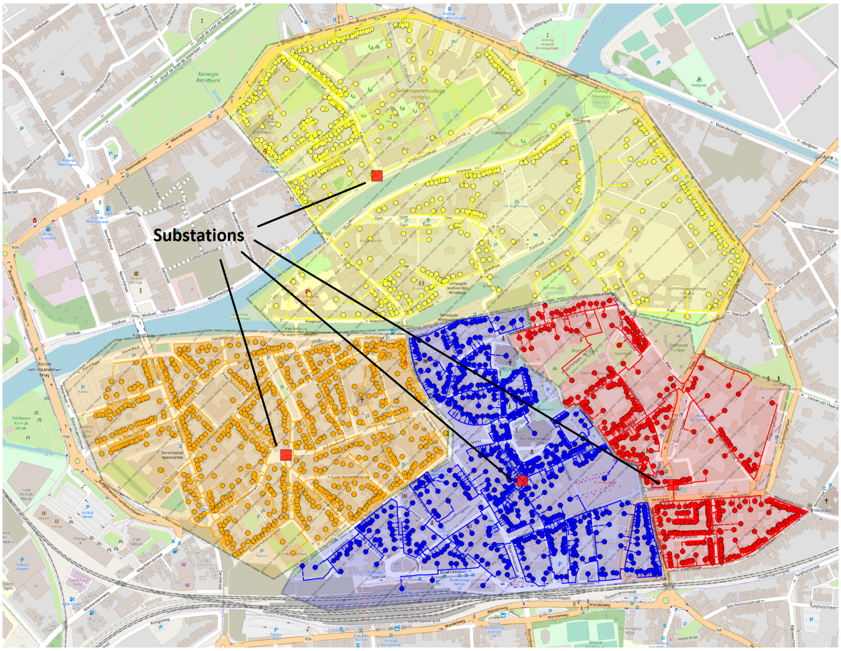

Figure 4.3: Clusters (distribution networks) with substations.

the best (high linear heat density) substation. A bottom-up approach is used in this method to be consistent with the existing Comsof Heat methodology.

4.2.4.3 Routing and capacity allocation - Bottom up approach

- Initially, a substation needs to be picked to start with the calculation. The order of substations is important because different substation orders will provide different network designs, which in turn will lead to different network costs. For example, the substations can be sorted based on linear heat density. However, the solution will not be the optimal one. Therefore, all the combinations need to be checked to find the optimum network design with the lowest network investment cost.

- Once the substation order is fixed, the routing costs between the

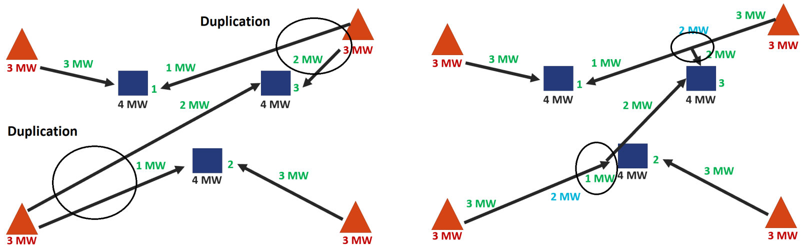

Figure 4.4: Duplication of pipes – With and without remaining source capacity made available along the connection.

first substation and all the available sources will be calculated using the algorithm of Dijkstra [104] and the user-provided scaling factor, which is a street attribute indicating the relative pipe deployment cost in the respective street.

- Then, the lowest-cost source will be connected to the selected substation along the cheapest possible route. Now, the remaining demand of the substation and the remaining capacity of the source will be calculated using the demand of the substation after applying diversity in the particular cluster to which the substation belongs.
- If the substation demand is not completely met, the second lowest cost source will be connected along the cheapest possible route. This process continues until the substation's power needs are completely met.
- After the substation demand is met and there is remaining source capacity, this remaining capacity will be made available on all nodes along the connection between the connected substation and the source. This is to avoid duplication of pipes to that source again (shown in Figure 4.4).
- Once a connection is made between a substation and a source along the path in a direction, the algorithm restricts the future connection of that path in the opposite direction.
- Now, the second substation will be picked, and the routing costs between that substation and all the available sources and all the

nodes that have remaining source capacity will be calculated using the same procedure as mentioned before. This process is repeated until all the sources are utilized or all the substations are connected.

- It is not allowed to have partially connected substations. Therefore, if the last substation demand is not completely met due to a lack of source capacity, the connection between that substation and any other source will be removed, and it will remain unconnected.

4.2.4.4 Pipe dimensioning

The power that needs to be transported through each pipe is calculated using the above-mentioned approach. In Comsof Heat, users can define the network constraints using 3 design options: design by flow velocity, design by pressure gradient, and design by pressure number. Combinations of these constraints are also possible to configure, but the most stringent constraint applies to the network. The detailed explanation of this pipe dimensioning methodology can be found in the chapter 2. Using these network constraints (design velocity and allowed pressure drop) and the power that needs to be transported, pipe sizes can be calculated.

4.2.4.5 Pressure and heat loss calculation

The pressure loss is calculated using the Darcy-Weisbach equation [105] and the friction factor is calculated using the Colebrook equation [106]. The heat loss equations are used from the chapter 2. The pressure losses have to be calculated for each source because it will be required to calculate pump power for each source. In the multiple source design method, one substation can be supplied with more than one source. However, the pump always need to overcome the overall pressure loss since the pumps are connected in parallel. Other attributes such as mass flow, heat loss, water volume, etc. from the route to that substation must be split between the connected sources. This is done using the percentage of a substation's peak power supplied by each source. The usage of peak power is because the design is done for the peak situation and is valid only for the peak situation (full load).

Table 4.1: Attributes of each source type

Source type	Capacity [MW]	Investment cost [€/MW]	Energy production cost [€/MWh]	CO2 released [t per MWh]
Waste incineration	13	-	6	0.6
Heat pump	6	600,000	50	0.075
CHP	2	-	14	0.42
Gas boiler	4	150,000	42	0.5

4.2.5 Scenarios

Several scenarios, such as substation order scenarios, source selection scenarios, and substation selection scenarios, are simulated using the multiple source design method. In this section, these scenarios are explained with their associated parameters.

4.2.5.1 Substation order scenarios

As mentioned in the above section, different orderings of substations result in different network designs. As a result, it is critical to test all substation order combinations to determine whether an optimal result exists. In these scenarios, all 24 possible combinations of substation order are simulated to see the effect on network cost and length. Table 4.1 shows the source attributes such as source capacity, investment cost, energy production cost, and CO2 released per MWh for each source type. The standard Logstor Series 2 steel pipe catalogue is used in this case study. The pipe costs are used from this paper [102]. The cost of the substation is set as 15,000 €/MW. The cluster size (substation power) is limited to a maximum of 6 MW. All the distribution clusters are locked to avoid changes between one simulation and another since the multiple source design method is applied only to the transport network. For the source selection, three possible key performance indicators (KPIs) can be selected: select by investment cost, select by energy production cost, select by carbon cost, and combinations of the above. In these scenarios, the total cost KPI is chosen (which is a combination of all three KPIs) to select the sources. The carbon cost is set at 30 € per tonne of CO_2.

4.2.5.2 Source selection scenarios

There are more potential sources provided than required to select the best ones. The total peak demand of the network is 18.15 MW. However, the provided total source capacity is around 37 MW. In these scenarios, different KPIs are used to select the best possible sources. First, the sources are selected based on investment cost, energy production cost, and carbon cost individually. Then, the combinations, such as investment and energy production costs, energy production and carbon costs, investment and carbon costs, and investment, energy production, and carbon costs, are used as KPIs to select the best possible sources. Then, the selected sources are connected with substations using the multiple source design method. The network lifetime is set at 35 years.

4.2.5.3 Carbon cost scenarios

In these scenarios, the carbon cost varies from 10 € per tonne of CO_2 to 60 € per tonne of CO_2. The source selection KPIs are chosen as the total cost KPI (a combination of all three KPIs: investment cost, energy production cost, and carbon cost). Using different carbon costs, the network is simulated to see the effect on source selection, network cost, and CO_2 emissions.

4.2.5.4 Substation selection scenarios

In these scenarios, limited source capacity is provided as input, and the best substations will be selected to match the available source power. It will be selected based on linear heat density. Three scenarios are simulated with the limited source capacities of 15 MW, 10 MW, and 6 MW.

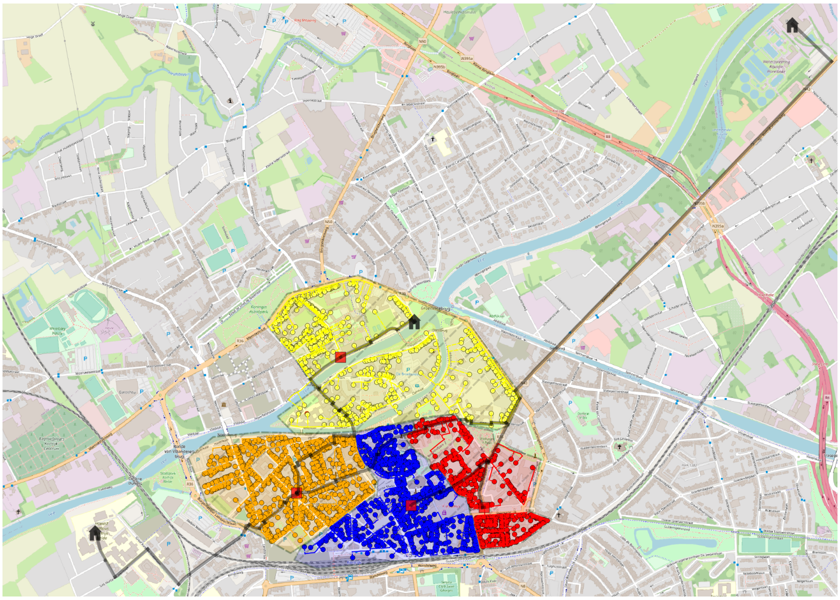

Figure 4.5: Designed multi-source DH network connecting substations and sources.

4.3 Results

The buildings in this case study are calculated to have a total energy consumption of 95.4 GWh/year. The peak heat demand of the DH network after applying simultaneity factors in the distribution network is estimated to be 18.2 MW. Figure 4.5 shows the designed multiple source district heating network using Comsof Heat. The results of different scenarios are presented in this section.

4.3.1 Substation order

Figure 4.6 shows the total and transport network investment costs for each simulated scenario of different substation order combinations. The lowest total network investment cost is about 40.7 million € whereas the highest total network investment cost is about 43.1 million €. The lowest transport network investment cost is about 9.8 million € whereas the highest transport network investment cost is about 12.2 million €.

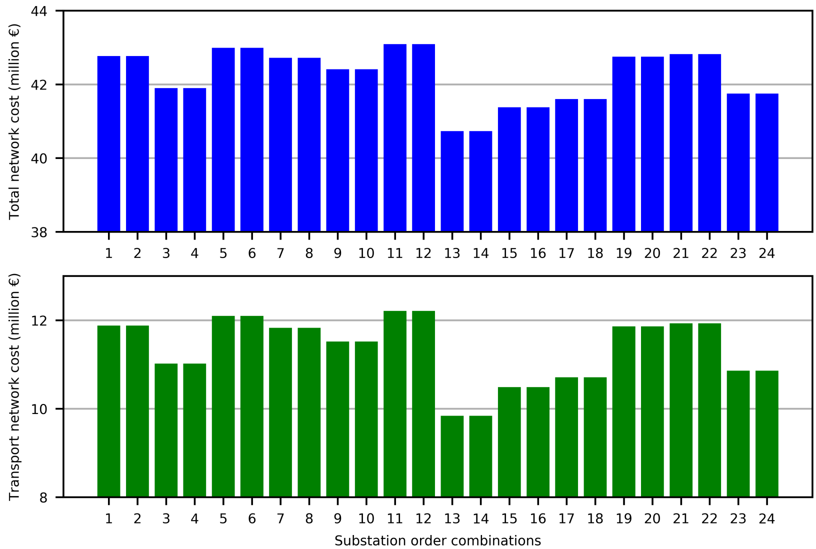

Figure 4.6: Total and transport network investment cost for different substation order combinations.

The lowest and highest points for transport and total network investment costs occur at the same substation order. The total and transport network pipe lengths for each simulated scenario of different substation order combinations are presented in Figure 4.7. The shortest and longest total network pipe lengths are about 60.9 km and 63.5 km, respectively. Within that, the shortest and longest transport network pipe lengths are about 7.1 km and 9.7 km, respectively.

Figure 4.8 shows the deviation from optimum total network and transport network investment cost for all substation order combinations. The maximum deviation of total network investment cost from the optimum is about 5.8% whereas the maximum deviation of transport network investment cost from the optimum is about 24.1%.

The deviation from optimum total network and transport network pipe length for different substation order combinations is shown in the Figure 4.9. The maximum deviation of total and transport network pipe lengths from the optimum is about 4.2% and 35.8% respectively.

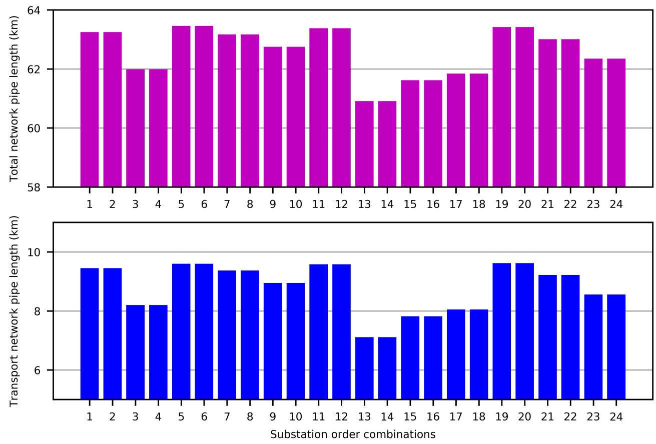

Figure 4.7: Total and transport network pipe length for different substation order combinations.

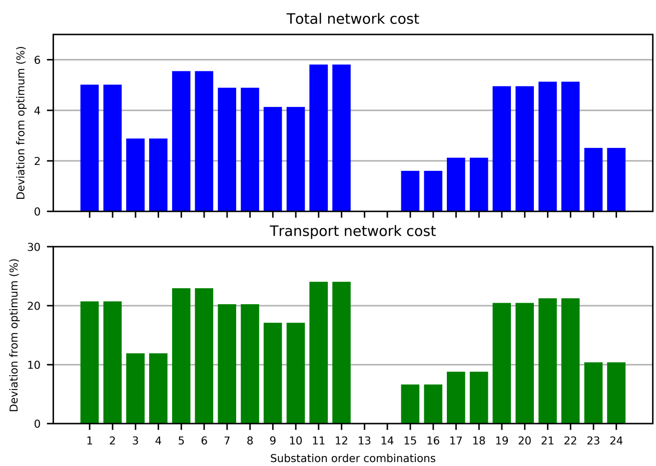

Figure 4.8: Deviation from optimum total and transport network investment cost for different substation order combinations.

4.3.2 Source selection

The energy production and CO2 cost for different source selection KPIs are shown in Figure 4.10. The carbon cost source selection KPI has the highest energy production cost of about 4.98 million € per year. On the

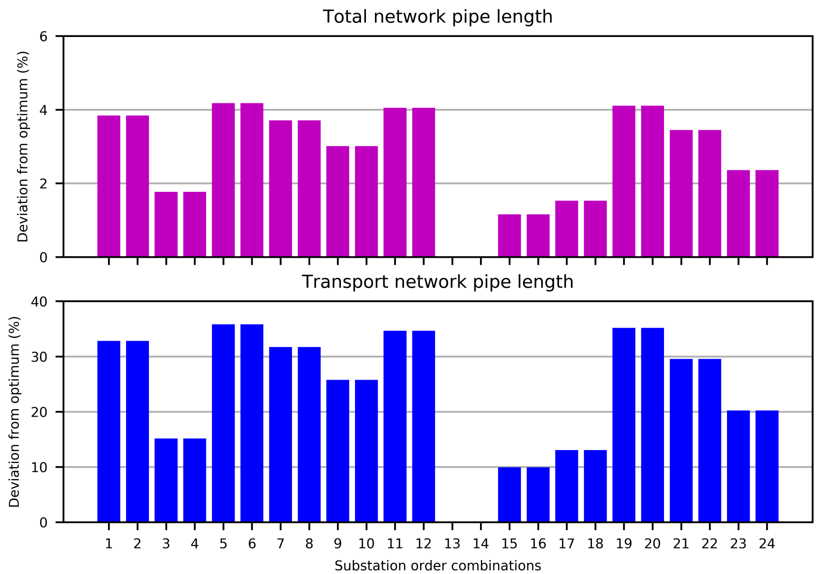

Figure 4.9: Deviation from optimum total and transport network pipe length for different substation order combinations.

other hand, it has the lowest CO2 cost of about 0.23 million € per year. The investment cost and energy production cost source selection KPI has the lowest energy production cost of about 1.49 million € per year. On contrary, it has the highest CO2 cost about 1.7 million € per year. The combination of investment, energy production and carbon cost KPI has the energy production cost of 2.15 million € per year. The CO2 cost of this combination is moderate at about 1.22 million € per year. The total network investment cost and total cost over network lifetime for different source selection KPIs are shown in Figure 4.11. The carbon cost KPI has the highest total network investment cost and total cost over the network lifetime of about 45.68 million € and 228.16 million €, respectively. The investment cost and energy production cost KPI has the lowest total network investment cost and total cost over the network lifetime of about 38.7 million € and 150.5 million €, respectively. The combination of investment, energy production, and carbon cost KPI has a total investment cost of about 42.77 million €. The total cost over the

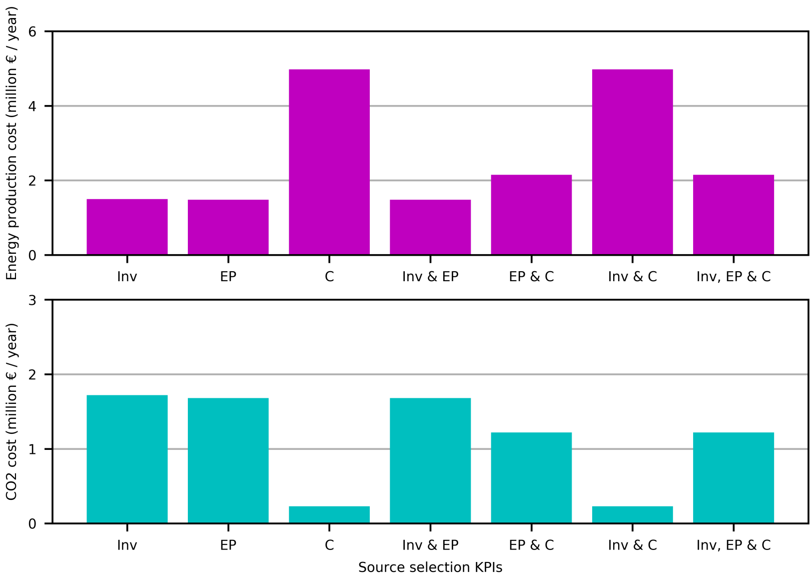

Figure 4.10: Energy production and CO2 cost for different source selection KPIs (Inv – Investment cost, EP – Energy production cost and C- Carbon cost).

network lifetime of this combination is about 160.69 million €. Figure 4.12 shows the CO2 emissions and CO2 saved for different source selection KPIs compared to the reference of gas boiler emissions. The investment cost KPI has the highest CO2 emissions of about 57,443 tonnes per year, whereas the carbon cost KPI has the lowest CO2 emissions of about 7,808 tonnes per year. The combination of investment, energy production, and carbon cost KPI results in CO2 emissions of about 40,748 tonnes per year. By comparing with the gas boiler reference, the carbon cost KPI has the highest CO2 savings of 42,292 tonnes per year. The investment cost and energy production cost KPI has higher CO2 emissions than the gas boiler reference. The combination of investment, energy production, and carbon cost KPI has CO2 savings of about 9,353 tonnes per year.

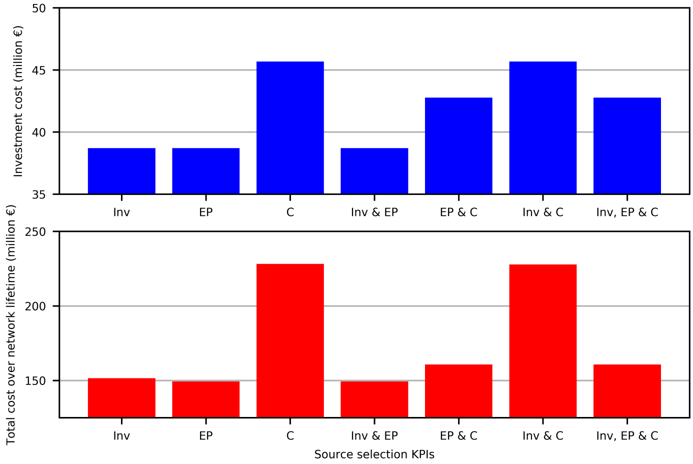

Figure 4.11: Total network investment cost and total cost over network lifetime (including energy production and carbon cost) for different source selection KPIs.

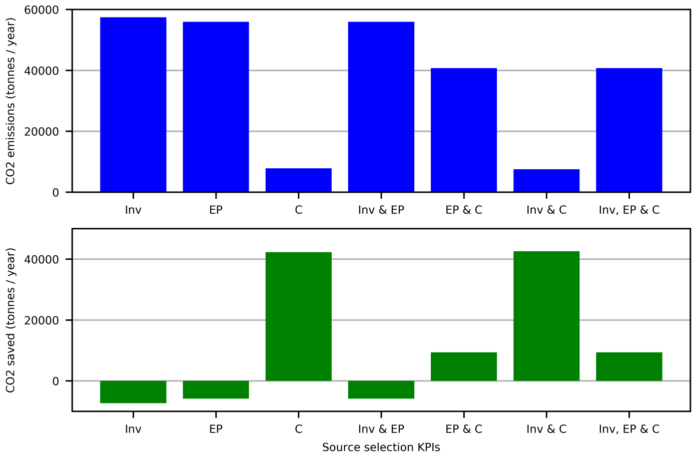

Figure 4.12: CO_2 emissions and CO_2 saved for different source selection KPIs.

4.3.3 Effect of different carbon cost

The energy production and CO2 cost for different carbon costs are shown in Figure 4.13. The energy production and CO2 cost increases when the carbon cost is increased. Figure 4.14 shows the total investment cost and total cost over the network lifetime for different carbon costs. Both parameters increase when the carbon cost increases. Figure 4.15 shows

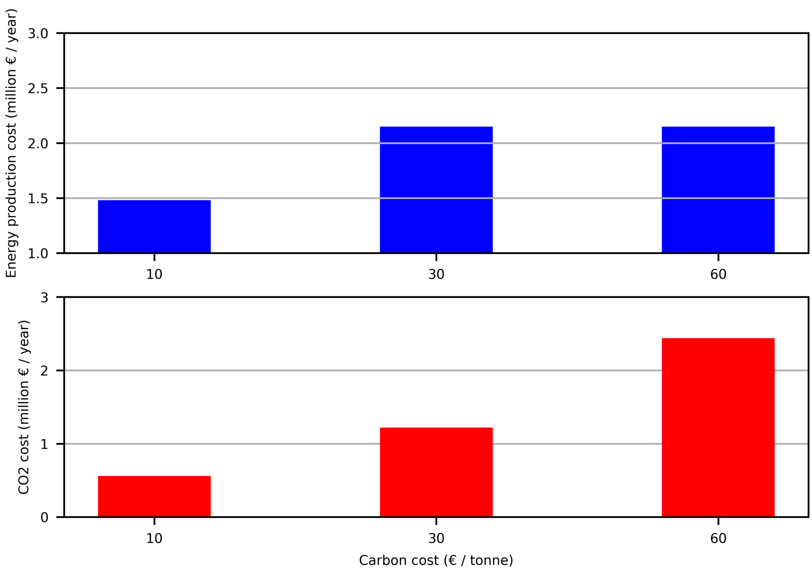

Figure 4.13: Energy production and CO2 cost for different carbon costs.

the CO2 emissions and CO2 saved for different carbon costs. The CO2 emissions are decreasing, and CO2 saved is increasing when carbon cost is increased.

4.3.4 Limited source power - Substation selection

Figure 4.16 shows the distribution clusters with their linear heat density. In the case of a source capacity with 15 MW, clusters 1 and 2 are connected. Only cluster 1 is connected to the transport network for the 10 MW and 6 MW scenarios. These designs are shown in Figure 4.17.

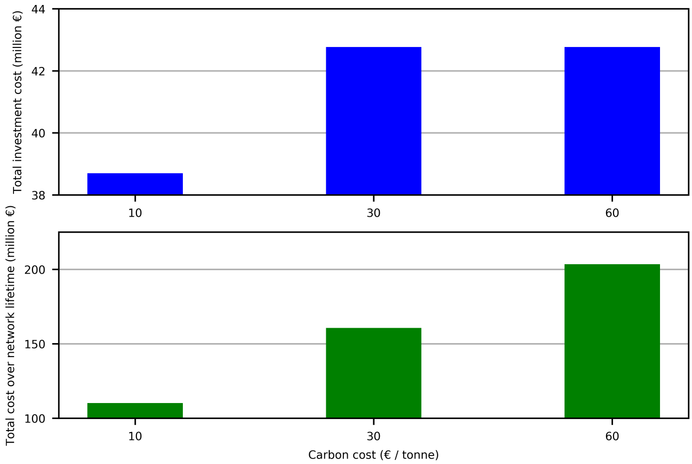

Figure 4.14: Total investment cost and total cost over network lifetime for different carbon costs.

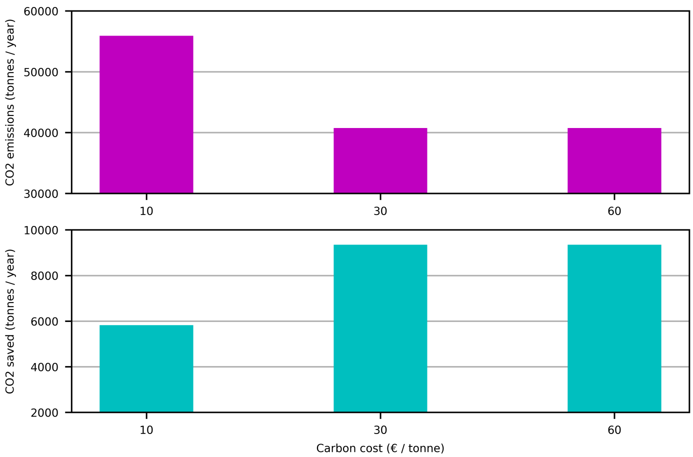

Figure 4.15: CO2 emissions and CO2 saved for different carbon costs.

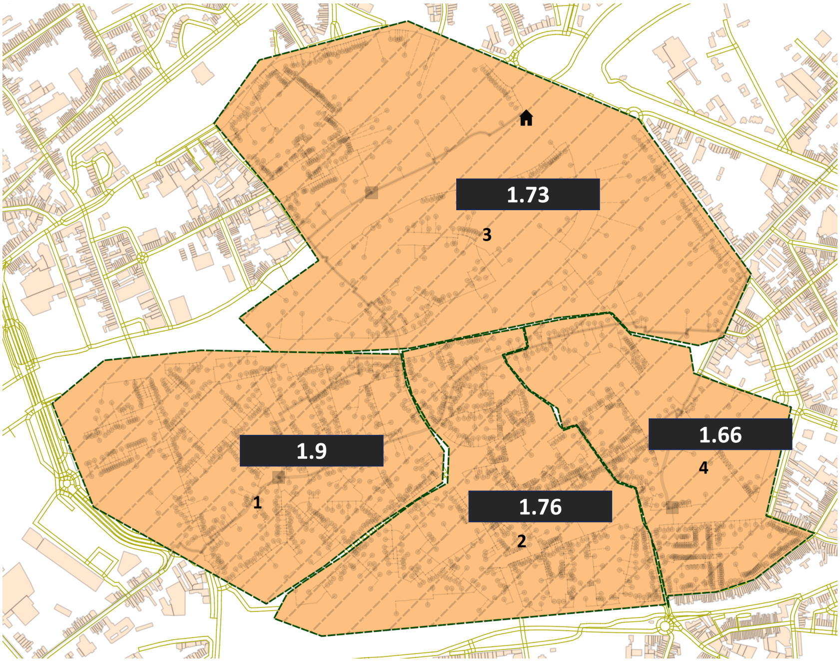

Figure 4.16: Distribution clusters with linear heat density.

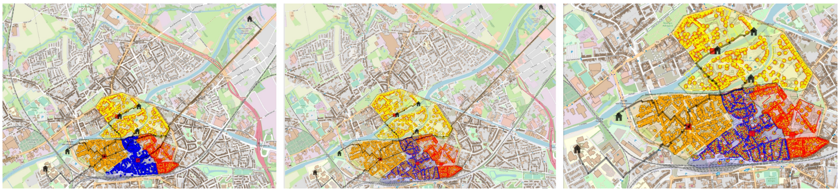

Figure 4.17: Designed network with 15 MW, 10 MW and 6 MW input source capacity.

4.4 Discussion

4.4.1 Substation order

The optimum total network cost exists with the different substation order simulations. Since the first picked substation takes precedence to connect with the low-cost source, different substation order results in different network design. As it is shown from the results, there is a deviation of 5.8% in the total network cost. This is because of the decreasing total network length between different substation orders. The reduction in total network length happens because of the reduction in transport network length. The transport network length deviation is much higher compared to the total network length. Therefore, it is important to consider all possible combinations of substations in order to find the optimum network cost using this multiple source design method.

4.4.2 Source selection

The selected sources for investment and energy production cost KPI are waste incinerator, CHP plant, and gas boiler with a capacity breakdown of 12.6 MW, 2 MW, and 4 MW, respectively. The energy production and investment costs are lower because the energy production cost of a waste incinerator is much lower, and the investment cost is lower because it is already existing. However, the carbon emissions per MWh of waste incinerator are higher than those from other sources. It leads to high CO2 emissions and CO2 cost, which in turn provides less CO2 savings in this scenario.

For the case of carbon cost KPI, the selected sources are heat pumps and CHP plant. The energy production cost of heat pumps is very high (50 €/MWh) compared to waste incinerator (6 €/MWh) or other sources. Moreover, the investment cost of heat pumps stands at 600,000 €/MW much higher when compared to other sources. So, the energy production and investment cost are much higher for the carbon cost KPI. However, heat pumps have a very low CO2 footprint compared with other sources. This leads to reduced CO2 emissions and increased CO2 savings.

The selected sources for the combination of investment, energy production, and carbon cost KPI are heat pump, waste incinerator, and CHP plant with capacity breakdowns of 6 MW, 10.15 MW, and 2 MW, respectively. Since there is a combination of heat pump and waste incinerator, it leads to moderate energy production and investment costs. Also, it has moderate CO2 emissions and CO2 savings.

The energy production and carbon cost combination KPI selected waste incinerator, heat pump, and CHP as potential sources. The investment and carbon cost combination KPI selected heat pumps and CHP as potential sources. This is due to the fact that the carbon costs over the network's lifetime are higher than the investment cost. In this scenario, the carbon cost has thus been the deciding factor. As a result, it leads to higher costs and lower emissions.

4.4.3 Effect of different carbon cost

For the case of a carbon cost with 10 €/tonne, the selected sources are waste incinerator, a CHP plant, and a gas boiler, with a capacity breakdown of 12.15 MW, 2 MW, and 4 MW, respectively. When the cost is increased to 30 €/tonne, gas boiler is replaced with a heat pump. The selected sources for the cases of 30 €/tonne and 60 €/tonne are a waste incinerator, a CHP plant, and a heat pump, with a capacity breakdown of 10.15 MW, 2 MW, and 6 MW, respectively. A higher carbon cost favours the introduction of low-carbon sources for the combination of investment, energy production, and carbon cost scenarios. This leads to higher costs and lower emissions when the carbon cost is increased.

4.4.4 Limited source power - Substation selection

For the case of 15 MW source capacity, two clusters with higher linear heat density are connected via the transport network. The 3rd cluster cannot be fully connected to the transport network for the given input power, and that is the reason for that cluster to be left unconnected. In the same way, only the demand of cluster 1 can be completely met with 6 MW and 10 MW source capacity. Hence, only cluster 1 is connected in the case of 6 MW and 10 MW source capacity.

4.4.5 Limitation and future work

One of the limitations of this approach is that if the number of substations is increased, it will take a lot of computation time to check for all possible combinations. The optimum results can be achieved only by checking all the combinations. Another limitation is that the transport network's simultaneity is assumed to be 1. Therefore, it is not easy to extend this approach to the distribution network as well. The future work will be to improve the connection algorithms by switching from assignment and routing algorithms to flow algorithms.

4.5 Conclusion

This study demonstrated a method for automatically designing a multiple-source district heating network for the given network constraints and design options. The case study is developed using Comsof Heat to design multiple-source district heating networks for different KPIs and design choices. The effect of these design choices on investment cost, energy production cost, carbon cost, and emissions is studied.

The result of the case studies with different substation order combinations shows that checking all possible combinations is required to find the optimum network cost since there is a 6% deviation in the network cost. The source selection with different KPI scenarios shows that low-carbon sources have higher investment and energy production costs. With the chosen carbon cost of 30 €/tonne), optimizing for costs does not favor low-carbon sources such as heat pumps. When total costs (investment, energy production, and carbon cost) are optimized, the different carbon cost scenarios show that an increasing carbon cost favors low-carbon sources. In order to compete with the other available sources in this case study, the carbon cost has to be increased to 80 €/tonne. Although prices have risen since the study's completion in 2020, and the projected cost of carbon has not been updated, the overall findings remain valid, though minor changes are possible.

The developed method will also be used to select the best possible substation for the provided source capacity. This automated multiple-source design method will enable quick simulation of different multi source scenarios with ease.

Chapter 5

Multi-Source Network Design - Ring Topology

Contents

This chapter is largely based on **Jebamalai, Joseph Maria**, Kurt Marlein, and Jelle Laverge. "Design and Cost Comparison of District Heating and Cooling (DHC) Network Configurations using Ring Topology – A Case Study." Energy (2022)., DOI: 10.1016/j.energy.2022.124777.

District heating systems have evolved from steam systems (1st generation) to low-temperature water-based systems (4th generation) and pilot projects are coming out on ultra-low-temperature systems along with building-side heat pumps (5th generation). Some of the notable features of future (4th and 5th generation) district heating and cooling (DHC) networks are the integration of distributed low-temperature sources, combined DHC systems, integrated heat and cold storage, and the usage of heat pumps at the building side. The design of large-scale DHC networks with all these features poses many challenges. In this chapter, a method to design 3-pipe DHC networks and ultra-low temperature DHC networks using a ring network configuration will be described, and their network costs will be compared. The developed method is implemented as a proof of concept in the DHC design tool, Comsof Heat, and a case study is developed to design and compare these two configurations and study the effect on the network cost. According to the case study findings, the network deployment cost of ultra-low temperature DHC ring networks is approximately 23% higher than that of 3rd generation ring networks. Furthermore, ultra-low temperature (5th generation) networks are only economically attractive if a free low-temperature waste heat source is available.

5.1 Introduction

District heating and cooling (DHC) systems are a long-proven technology to decarbonize energy systems, especially in the building sector. There are approximately 80,000 DHC networks worldwide, covering 3% of total energy consumption, 4500 of which are located in Europe and cover between 11 and 12% of their heating requirements [107]. These systems are widely used in Scandinavia, Eastern European countries, and Russia [108]. For example, 90% of buildings in Iceland are heated via

DHC systems using geothermal energy [109]. Even though the technology is proven in Northern Europe, many countries such as the UK, the Netherlands, and Belgium are still lagging behind. In recent years, DHC networks have become part of the national strategy in the UK and the Netherlands [110]. For instance, DHC networks currently provide only about 2% of the overall heat demand in the UK, despite research showing that it could be increased to 43% by 2050 [109]. So, these countries have the advantage of learning from the experiences of early adopters and can build the latest generation of networks that are suitable for their climatic conditions.

The most recent technological advancement in DHC networks is fifth-generation district heating and cooling (5GDHC) networks (otherwise known as ultra-low temperature DHC networks). This concept meets both heating and cooling demand simultaneously using ultra-low temperature distribution networks along with heat pumps at each building. These heat pumps can increase (or decrease) temperatures according to the user's requirements. Gagné-Boisvert et al. [111] analyzed two-pipe and single-pipe configurations for 5GDHC networks. Though a two-pipe configuration is common, there are systems with a single-pipe configuration for 5GDHC networks. In a two-pipe configuration, each connected building has two pipe (hot and cold) connections to draw from and discharge into the network. This configuration results in less heat loss and exergy destruction. However, in a single pipe configuration, each connected building draws from and discharges into the same distribution pipe of the network, resulting in different inlet temperatures for the buildings. The single-pipe 5GDHC configuration has half the total pipe length when compared with the two-pipe 5GDHC configuration. It is highlighted that single-pipe 5GDHC systems have 5% higher total electricity consumption compared to two-pipe configurations [111]. Moreover, the two-pipe 5GDHC configuration provides more flexibility to the network. In this study, a two-pipe 5GDHC network design is used as one of the configurations to compare the network cost.

The two-pipe 5GDHC network configuration consists of one hot and one cold ring circulating hot water and cold water, respectively. The building-side heat pump uses water from the hot or cold ring, depending on whether heating or cooling is required, and returns the heated or cooled water to the hot or cold ring. This allows the network to utilize the waste heating or cooling of one user to match the cooling or heating demand of other users. Because of the energy transfer between different buildings, this system is much more efficient and can make use of low-temperature waste energy. This configuration is suitable for areas that have complementary building types (having simultaneous heating and cooling demand), such as supermarkets that require cooling and residential buildings that require heating. The role of a building substation (with heat pump) is more critical in 5GDHC systems, as each connected substation can act as both a consumer and a producer (known as a prosumer) of thermal energy.

Heat pumps can provide a meaningful contribution towards a sustainable and low-carbon future by converting electric power into more efficient heating/cooling [112, 113, 114]. The integration of heat pumps into DHC systems will result in significant environmental and performance improvements, along with sector coupling benefits. Heat pumps have high market potential, and this can result in several socio-economic benefits. However, heat pumps are still not a prevalent technology in European district heating systems. There are several challenges such as technological (electrical grid limitations), economic (high investment cost), and regulatory uncertainties to overcome in order to achieve wider adoption [113].

In spite of these advantages with a fair share of challenges, only a small number of 5GDHC networks are currently in operation, and most of them are demonstration projects. In Europe, Germany has more than 30% of active 5GDHC pilot projects [115]. Buffa et al. [115] investigated 40 5GDHC thermal networks that are in operation in Europe, and it was highlighted that the knowledge of 5GDHC technology is limited and not yet widespread. Moreover, the temperature difference in 5GDHC networks is smaller than previous generation networks, so a higher circulating flow is required. As a result, distribution pipes will be larger in diameter, and hydraulic pumping costs will rise. On the other hand, the building substation is more expensive for 5GDHC systems because

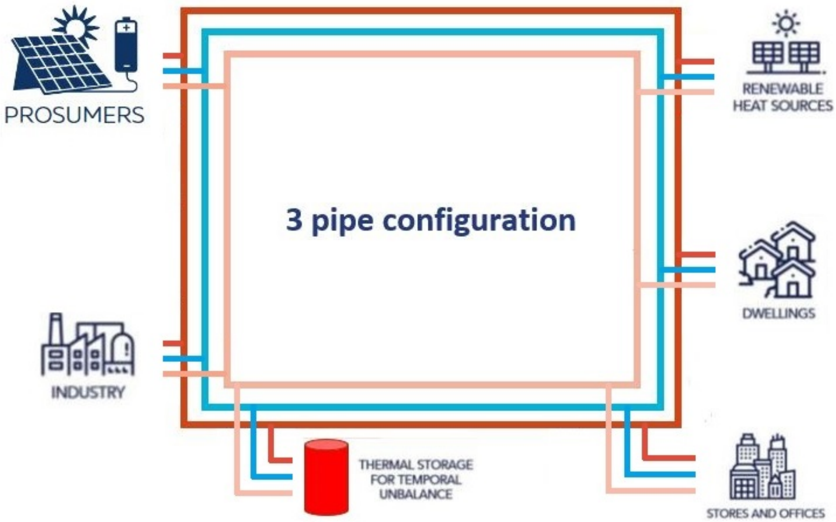

Figure 5.1: 3rd generation 3-pipe DHC network configuration with ring topology.

of the heat pump inclusion. However, the investment cost of the energy generation plant can be reduced because of the very low temperature requirement. In some cases, free waste energy can be utilized based on its availability.

The current state of the art in DHC networks is third-generation DHC networks, which operate at a high temperature and can supply energy to older buildings. These can be transformed into 4th generation DHC networks by reducing the network temperatures when the buildings are better insulated. The 3rd generation DHC networks can have two possible network configurations, namely 3-pipe and 4-pipe configurations. The 3-pipe configuration has three pipes present in the network: one hot supply pipe that provides hot water to heat homes, one cold supply pipe that supplies cold water to cool homes, and one return pipe that is used to return the hot and cold water back to the sink. The 4-pipe configuration has an additional pipe to separate the return line for heating and cooling. The core idea of this concept is to have the potential to cover both heating and cooling demand simultaneously using the same infrastructure.

Therefore, this configuration is suitable only if there is a simultaneous requirement for heating and cooling. If simultaneous heating and cooling are not required, a 2-pipe configuration can meet both demands by heating in the winter and cooling in the summer. In this chapter, 3$^{\text{rd}}$ generation 3-pipe DHC network configuration (shown in Figure 5.1) is used as one of the configurations to compare the network cost.

The possible topologies of DHC networks are branch/tree, ring, and mesh networks. Depending on the network's function and purpose, each of these topologies has advantages and disadvantages. The typical branched topology is simple but operates centrally due to its distribution flow in one direction. The ring topology provides increased network reliability and good integration of distributed energy sources but has higher investment costs than a branched network topology. The integration of distributed energy sources helps transition the network to supply with renewable and local excess sources for heating and cooling. The other key advantages of ring topology over branched topology are redundancy, flexibility, and prosumer integration. The mesh network topology ensures high reliability in the energy supply but has higher investment costs compared to the ring topology. The ring network topology is used in this study for third-generation (3-pipe) and fifth-generation (2-pipe with building-side heat pump) DHC networks, and network costs are compared to those of traditional branched networks.

Tol et al. [116, 117] developed an optimization method to improve the DH network pipes based on the simultaneity factor of energy demand in Denmark. They compared the use of booster pumps and increasing the supply temperature during peaks for tree and loop networks, and their conclusion was that they lead to reduced pipe dimensions. Bunning et al. [118] developed the concept for 5GDHC network control and optimization based on temperature set point optimization. This operation optimization leads to electricity use reductions of 13% and 41% when compared to networks with free-floating temperature control. Lund et al. [119] discussed the possibility of installing micro heat pumps for DHW temperature boosting in each building and concluded that this will be challenging due to high investment costs. Ostergaard and Svendsen [120] proposed that by lowering the supply temperature to match the building temperature requirement (possible in 5th generation networks due to building side heat pumps), the distribution heat losses can be reduced by 30% when compared with the third generation district heating systems. Zeng et al. [121] developed a mathematical model based on a genetic optimization algorithm to optimize pipe diameter in DHC networks, including investment cost, operation cost, and maintenance cost for the hydraulic loop. Their study shows that a fluctuating electricity price has a marginal impact on pipe diameter, but the variation in nominal flow rate impacts the optimal pipe diameter significantly. Tunzi et al. [122] investigated a double loop network operated with ultra-low supply/return temperatures of 45/25 °C and compared the proposed concept with a typical tree network and an individual heat pump solution. They proposed a pump-driven system that has separate circulations for supply and return flow to increase the flexibility of the system. Their study concluded that this concept was cost-competitive when considering the required capital and operating costs.

Several studies[116, 117, 118, 121] studied various aspects such as pipe optimization, network control, and optimization of 3rd and 5th generation DHC networks. Some literature [120] compared the network heat loss of both 3rd and 5th generation DHC networks. However, the detailed network design and cost comparison of both 3rd and 5th generation networks considering different network topologies are not studied. Despite the fact that Lund et al. [119] compared the total network costs of fourth and fifth generation networks, a detailed network design comparison taking into account different network topologies is lacking. The key objective of this chapter is to design a combined heating and cooling network using ring topology and study the impact of different design options on total network cost. The cost of network investment (deployment), operational cost, and total cost (investment and operational) of third and fifth generation DHC networks are compared in this study.

Table 5.1: Input cost parameters of consumer substation for 3rd and 5th generation systems [123, 124, 125].

Power [kW]	3rd gen cost [€]	5th gen cost [€]
1 to 50	3000	10,000
50 to 100	10,000	20,000
100 to 400	25,000	80,000
400 to 1000	100,000	200,000
1000 to ∞	150,000	300,000

5.2 Methodology

This section summarizes the case study area, the demand and supply input requirements, district heating and cooling network design constraints, ring topology design, and all the scenarios simulated in this study. Comsof Heat is used for network routing, pipe dimensioning, and network deployment cost estimation. The cost of the ring is estimated using Excel models in combination with Comsof Heat.

5.2.1 Case study area

A Belgian city called Kortrijk is used as a case study area in this chapter as well. The city center of Kortrijk with about 2400 buildings and the potential sources are shown in Figure 4.2.

5.2.2 Building and source inputs

The building's peak heat demand is estimated using the annual energy consumption and demand profile of the building. The building and source inputs are explained in 3.2.2. Figure 3.4 shows the network composition of different building types weighted by their yearly energy consumption. Synthetic load profiles of Belgium (peak day profile shown in Figure 3.5) are used to estimate the building demand profile for each of these building types. These load curves show that the buildings have high peak loads in the morning and in the evening. The peak load could be reduced significantly if a better building control strategy is used. However, this is outside the scope of this study. The aggregated network heat demand

Table 5.2: Range of standard pipe diameters with flow velocity and cost used in Comsof Heat [54, 89].

Nominal diameter	Maximum flow velocity [m/s]	Cost [€/m]
DN25	1	500
DN32	1.3	550
DN40	1.5	600
DN50	1.7	650
DN65	1.9	700
DN80	2.2	750
DN100	2.4	800
DN125	2.6	850
DN150	2.8	900
DN200	3	1000
DN250	3	1100
DN300	3	1200
DN350	3	1250
DN400	3	1350
DN450	3	1450
DN500	3	1500
DN600	3	1600
DN700	3	1700
DN800	3	1800
DN900	3	1900
DN1000	3	2000

is calculated using these profiles and building energy consumption. Figure 5.2 shows the aggregated network heat demand over the year. The building cooling demand data has been estimated using cooling demand density and gross floor area density (which are extracted from the open-source EU project HOTMAPS) of the case study area.

5.2.3 District heating and cooling (DHC) network configuration

In this chapter, a 2-layer network is designed with transport and distribution network temperature levels of 90/50 °C and 5/15 °C for heating and cooling, respectively. Different pipe configurations, such as the tra-

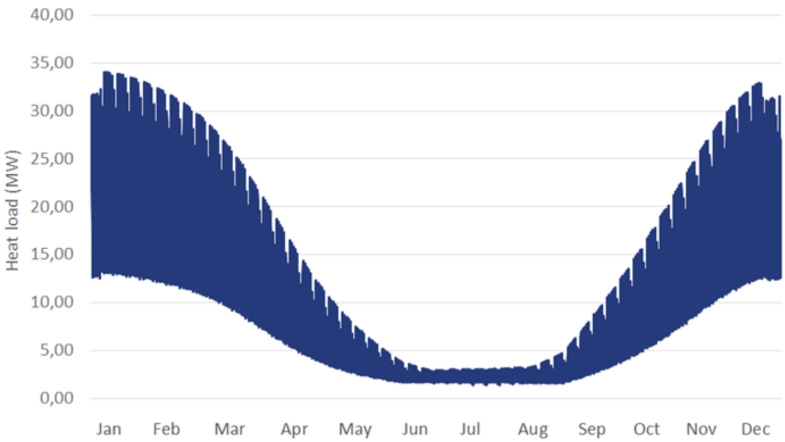

Figure 5.2: Aggregated network heat demand over the year.

ditional branched network, the 3-pipe ring network configuration, and the ultra-low temperature ring network configuration, are used for the transport layer. The pressure levels of the transport and distribution networks are designed for PN16 and PN6, respectively. The network constraints are set at 0.5 bar for the minimum pressure at the farthest consumer's heat exchanger and 2 bar for the minimum pressure required to avoid boiling. Table 5.1 shows the consumer substation input cost parameters for both 3rd generation and 5th generation DHC networks. The 3rd generation consumer substation costs are based on values from industry experts (which are in line with the costs used by Gudmundsson et al. [125] in their study), whereas the 5th generation consumer substation (with heat pump) costs are based on the specific cost assumption of 300 to 400 €/kW [123, 124]. The average power ranges are used to calculate substation costs for the power ranges specified in Table 5.1. Table 5.2 shows the range of standard pipe diameters, maximum flow velocities limit, and costs that are used. The cost assumption is a slight modification of the cost reference obtained from the year 2007 [89] (adjusted for inflation of Belgium). Comsof Heat (design methodology explained in [29]) uses these inputs to design a new network that involves pipe routing, pipe dimensioning, and network investment (deployment) cost

Table 5.3: Description of parametric information of 3rd generation 3-pipe network and 5th generation 2-pipe network configuration.

Description	3rd gen 3-pipe network	5th gen 2-pipe network
Network temperature	90/50	15/5
Ring topology	Yes	Yes
Heat pumps at buildings	No	Yes

estimation. The total network investment cost can include pipe costs, substation costs, source costs, labor costs, installation costs, and storage costs. The storage design method of Comsof Heat is explained in the chapter 3 [126].

5.2.4 Ring routing and dimensioning method

The ring routing method is based on the drawn-ring strategy available in the Comsof Heat POC. The drawn ring strategy requires the user to select the sources and energy centers or substations that need to be placed in a ring. Once these source and substation points are selected, the algorithms in the Comsof Heat POC create a ring that connects these points in a cost-optimal way. The ring dimensioning is based on the total demand of the connected substations. The total demand is calculated as the sum of all the demands of the connected substations. This demand is then used to dimension the ring.

5.2.5 Scenarios

This section describes several network configurations such as 3rd generation 3-pipe ring network configuration, 5th generation 2-pipe ring network configuration, traditional branched network configuration, and other scenarios. Table 5.3 describes the parametric information of 3rd generation 3-pipe network and 5th generation 2-pipe network configuration. The total network deployment cost includes source cost, substation cost, and network cost.

5.2.5.1 Effect of different design configurations on total network deployment cost

In these scenarios, different design configurations such as 3rd generation and 5th generation networks are designed. In the 3rd generation ring network configuration, the transport network is designed using a ring topology, while the distribution network is designed using a branched network topology. In the 3rd generation branched configuration, all layers are branched / tree structured starting from the energy plant towards the buildings. In the 5th generation ring network configuration, 2 different Coefficient of Performance (COP) values (2.5 and 3.5) of building heat pumps are used to design the networks. These COP values mainly depend on the temperature requirements of the buildings. Older buildings require higher temperatures, whereas newer buildings require lower temperatures due to better insulation.

5.2.5.2 Storage location scenarios

In these scenarios, two different cases, such as centralized and substation-level storage, are simulated. In both of these cases, two types of storage are considered: seasonal and multi-day storage. Seasonal storage is designed to buffer all seasonal and daily variations in the profile since hourly demand average values are used. Daily storage is designed to buffer the daily variations of the peak day so that it can handle any other day in the year. Multi-day storage is designed to buffer the daily variations for up to five continuous days. In the centralized case, there is one large storage at the source location. In the substation-level case, the storage is distributed to all substation locations. This case is simulated using a 4 MW substation size, resulting in 10 clusters, and so storage is distributed to 10 substation locations in the network. All of these scenarios are simulated for networks with third-generation branched and ring topologies. The heat storage option is not used in the case of 5th generation networks.

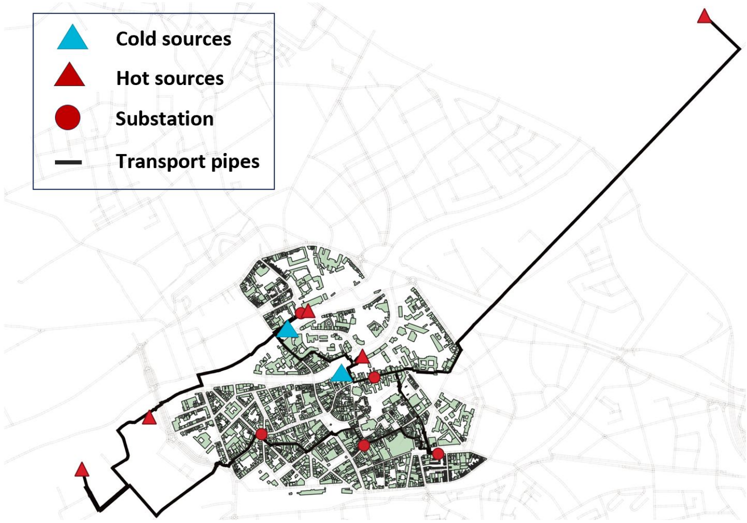

Figure 5.3: Designed district heating and cooling network using Comsof Heat POC.

5.2.5.3 Free low temperature waste heat source scenarios

In these scenarios, two different cases, such as with and without free low-temperature waste heat source, are simulated. For both the cases, the total and operating cost of the network are calculated for 3rd generation branched, ring, and 5th generation networks. The average cost of heat used for the calculation is 70 €/MWh, and the cost of electricity used in the calculation is 220 €/MWh. 35 years of network lifetime are used for the calculation.

5.3 Results and Discussion

The case study area in this chapter is estimated to have a total energy consumption of 95 GWh/year with a peak load of 34 MW. Several network configurations, such as 3rd generation 3-pipe ring network configuration, 5th generation 2-pipe ring network configuration, and the traditional branched network configuration, are designed to compare the network costs. Figure 5.3 shows the designed district heating and cooling

Table 5.4: Largest supply pipe diameter and network temperature levels for 3rd and 5th generation systems.

Description	3rd gen branched	3rd gen ring	5th gen (COP 2.5)	5th gen (COP 3.5)
Largest selected heat supply pipe diameter	DN200	DN400	DN500	DN600
Network temperature level	90/50	90/50	15/5	15/5

network with ring topology using Comsof Heat POC. Table 5.4 shows the largest selected heat supply pipe diameter of 3rd generation branched, ring configuration, and 5th generation networks with COP of 2.5 and 3.5.

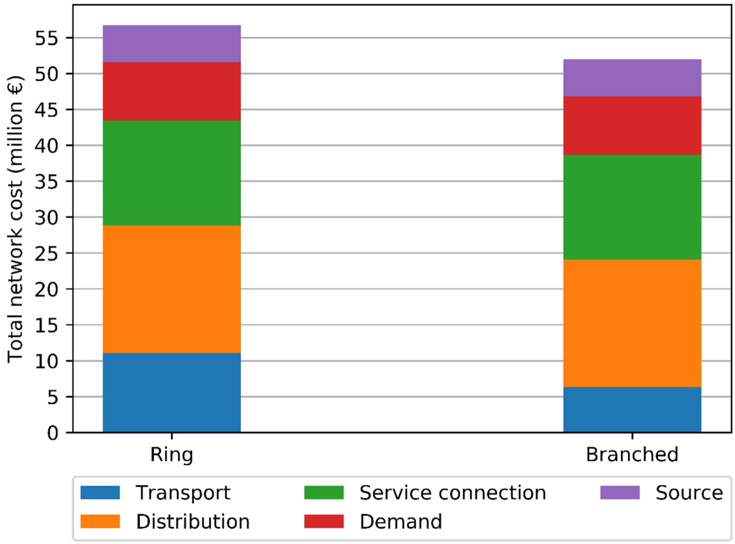

Figure 5.4: Comparison of total network deployment cost of 3rd generation 3-pipe ring network configuration and branched network configuration.

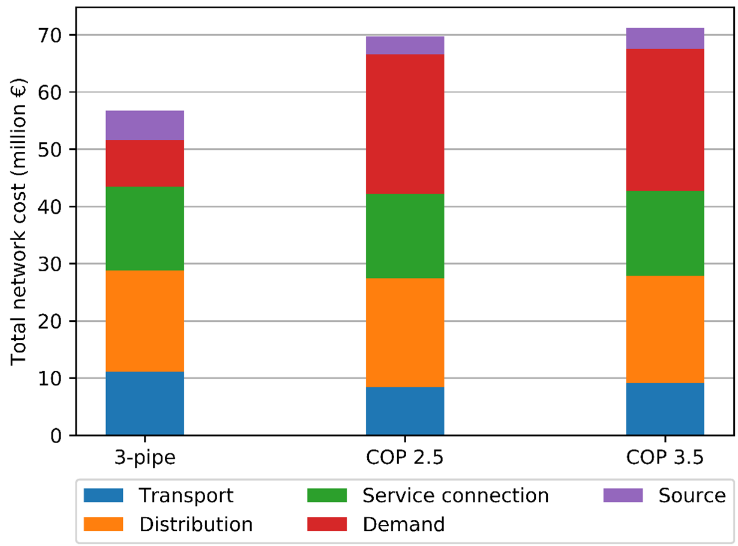

Figure 5.5: Comparison of total network deployment cost of 5th generation 2-pipe ring network configuration and 3rd generation ring network configuration

5.3.1 Effect of different design configurations on total network deployment cost

Figure 5.4 compares the total network deployment cost of the third generation 3-pipe ring network configuration versus the branched network configuration. The total network investment costs for the ring and branched topologies are around 57 million € and 52 million € respectively. The ring topology is 8.8% more expensive than the branched topology. However, if we compare the transport layer cost, it is 75% more expensive than the branched topology since the ring is created only in the transport layer. This is due to the fact that a ring connection requires a longer pipe length to connect the sources with substations than a branched connection. Moreover, the ring configuration has the same bigger size diameter entirely whereas the branched configuration is dimensioned for the exact peak power that flows through the pipe. These increased pipe lengths and larger pipe diameters in the transport network resulted in a higher cost for the transport layer.

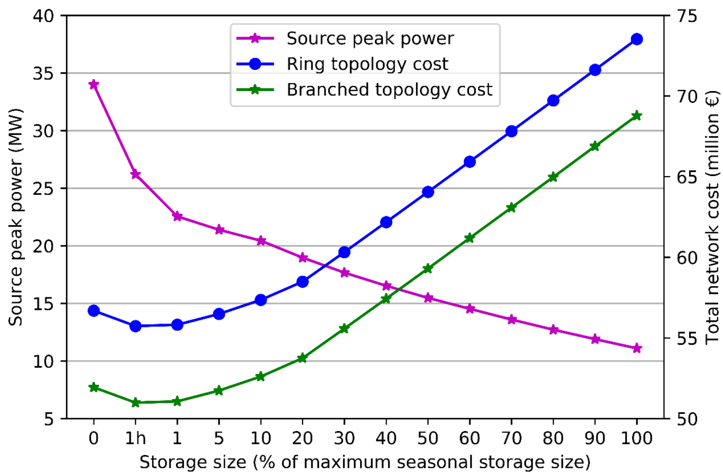

Figure 5.6: Centralized seasonal storage: Impact of storage sizes on source peak power and total network deployment cost for 3rd generation ring and branched network topology.

Figure 5.5 compares the total network deployment of 5th generation 2-pipe ring network configuration and 3rd generation ring network configuration. Table 5.3 provides the parametric information of these configurations. The total network investment cost of the 5th generation 2-pipe ring network configuration with COP 2.5 and 3.5 and the 3rd generation 3-pipe ring network configuration are around 70 million € and 57 million € respectively. The cost of a fifth-generation network with a building-side heat pump configuration is 22.8% higher than that of a third-generation network. This is mainly because of the very high building substation costs due to the decentralized heat pump inclusion.

5.3.2 Effect of storage on total network deployment cost

Figure 5.6 shows the impact of storage sizes (centralized seasonal) on source peak power and total network deployment cost for 3rd generation ring and branched network topology. The storage sizes are varied from no storage to 100% of the maximum seasonal storage size. The source peak

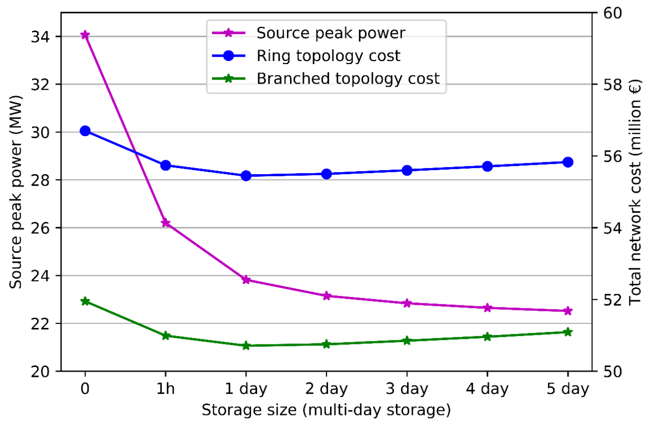

Figure 5.7: Centralized daily storage: Impact of storage sizes on source peak power and total network deployment cost for 3rd generation ring and branched network topology.

power can be reduced from around 34 MW to 11 MW for the 100% maximum storage size (explained in [126]) scenario. In both cases, branched and ring topologies, the total network deployment cost decreases initially but then increases when storage size is increased further. For the ring case, the minimum total network deployment cost occurs around 1000 m^3 of storage, and the total network deployment cost can be reduced by 1.7%. For the branched topology, the total minimum network cost is 1.8% lower when compared to the no storage scenario. The decrease in total network deployment costs for centralized storage is primarily due to a decrease in source costs. This is obvious because as storage size increases, the source peak power decreases. However, the steep rise in total network deployment costs in the later stage is due to high storage costs.

Figure 5.7 shows the impact of storage sizes (multi-day storage) on source peak power and total network deployment cost for the 3rd generation ring and branched network topology. In the case of multi-day storage, the source power can be reduced to around 22 MW. For the ring topology, the minimum total network deployment cost occurs at 1 day of storage (around 1500 m^3) with a 2.2% cost reduction compared to the case without storage. For the branched topology, the total minimum network cost is 2.4% lower when compared to the no storage scenario. The reason for the network cost reduction is mainly because of the peak power reduction at the source, which in turn reduces the source cost. Figure 5.8

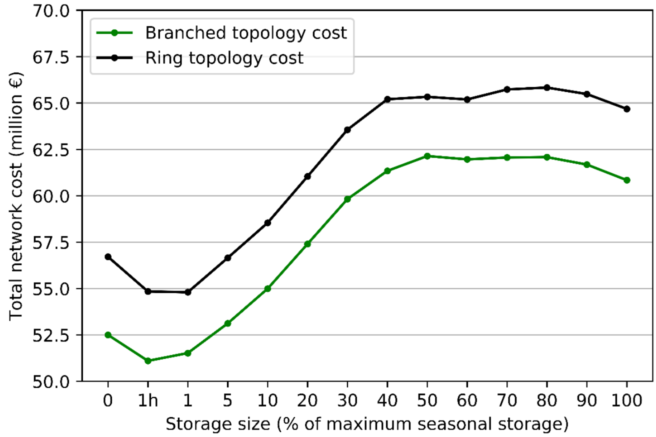

Figure 5.8: Substation level seasonal storage: Impact of storage sizes on total network deployment cost for 3rd generation ring and branched network topology.

shows the effect of substation level storage on total network deployment cost for both 3rd generation ring and branched topology. The storage sizes are varied the same way as in the centralized case, but the storage is distributed among 10 different locations. For the ring topology, the minimum network cost occurs around 4500 m^3 and the cost can be reduced by 3.3% when compared to the no storage case. For the branched topology, the total minimum network cost is 2.7% lower when compared to the no storage scenario. In the substation-level storage scenario, the network cost reduction is not only due to source cost reduction but also a reduction in transport network costs. The cost reduction is greater in the case of ring topology compared to branched topology. This is because the ring has the same larger diameter, and when that is reduced, it results in a higher reduction when compared to a branched topology.

In Figure 5.9, the impact of multi-day substation level storage on total network deployment cost is shown for both 3rd generation ring and

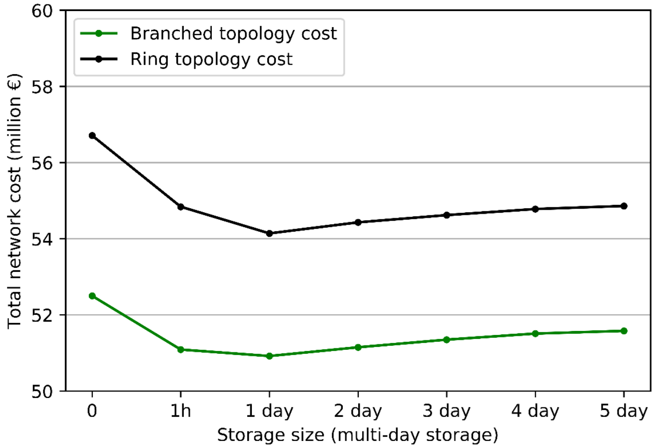

Figure 5.9: Substation level multi-day storage: Impact of storage sizes on total network deployment cost for 3rd generation ring and branched network topology.

branched topology. For the ring topology, the minimum total network deployment cost occurs around 1 day of storage, and the cost is 4.5% less compared to the no storage scenario. The total minimum network cost occurs at 1 day of storage for branched networks as well. However, the cost can be reduced only by around 3% when compared with the no storage scenario. Similar behaviour (more cost reduction for ring topology) is observed in the daily case scenario as in the seasonal case.

The centralized heat storage might not be attractive for 5th generation networks because of the ultra-low temperature heat source. However, this varies depending on the source temperature and availability over the year. The distributed storage is better suited for 5th generation systems since there are distributed building-side heat pumps. However, this is not studied within the scope of this chapter and it can be studied in future work.

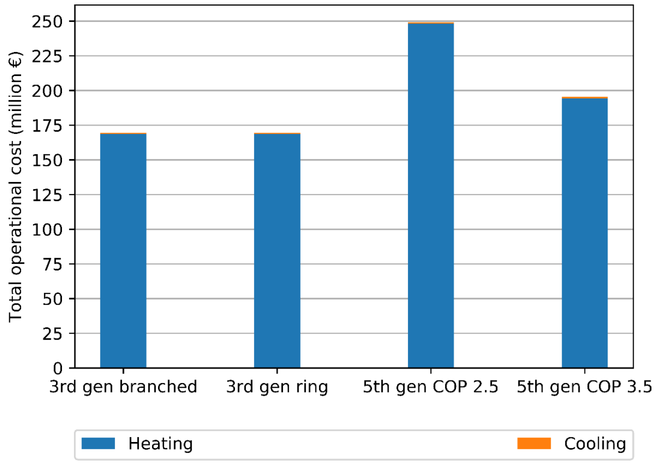

Figure 5.10: Total operation cost for 3rd generation branched, ring and 5th generation networks without free waste heat source availability.

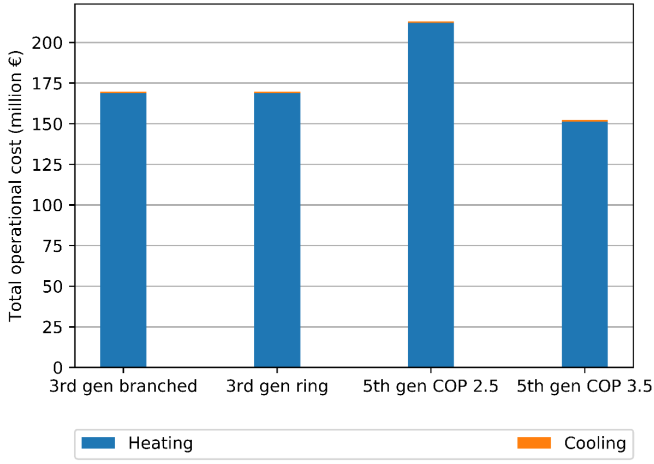

Figure 5.11: Total operation cost for 3rd generation branched, ring and 5th generation networks with free waste heat source availability.

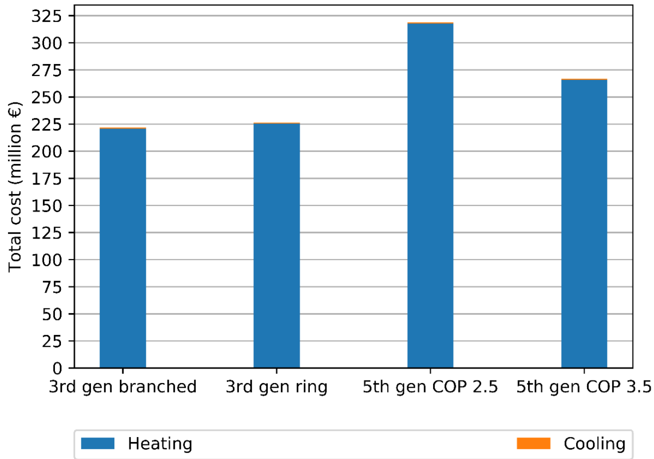

Figure 5.12: Total cost (investment and operational) for 3rd generation branched, ring and 5th generation networks without free waste heat source availability.

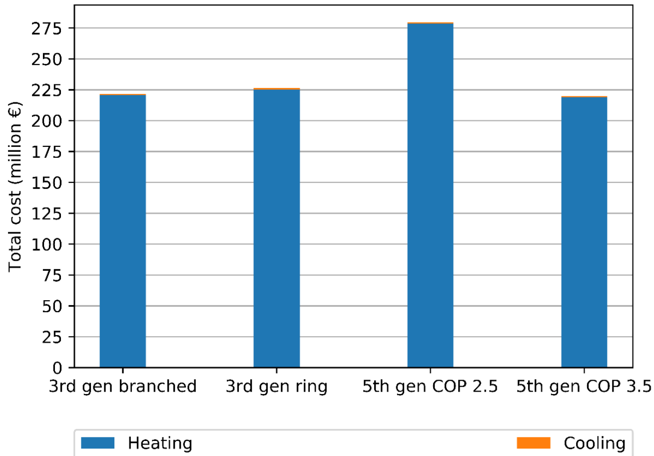

Figure 5.13: Total cost (investment and operational) for 3rd generation branched, ring and 5th generation networks with free waste heat source availability.

5.3.3 Effect of free low temperature waste heat source on operating and total cost

Figure 5.10 shows the total operating cost of heating and cooling for 3rd generation branched, ring, and 5th generation networks. The total operating cost for third-generation networks is around 170 million €, and for fifth-generation networks with COPs of 2.5 and 3.5, it is around 250 million € and 195 million €, respectively. Higher electricity prices are primarily to blame for the higher operating costs of fifth-generation networks. In this scenario, the fifth-generation network has higher operating costs than the third-generation network, and competing with high electricity prices and a relatively low heating cost is difficult. However, Figure 5.11 shows that the operating costs of 5th generation networks can get lower if there is a free low temperature waste heat source available. The total cost of cooling is insignificant because cooling demand is nearly 1/40th of heating demand.

Figure 5.12 shows the total cost (investment and operational) of 3rd generation branched, ring, and 5th generation networks. The total cost of 5th generation networks is significantly higher than that of the 3rd generation networks. This is due to high investment and operating costs. The operational cost plays a larger role in the total cost over the network lifetime of 35 years. The operational cost of 5th generation systems is higher due to high electricity costs (220 €/MWh) in Belgium, whereas the cost of heat (70 €/MWh) is much cheaper. Therefore, 5th generation systems are economically unattractive with this current scenario in Belgium unless a free low-temperature waste heat source is available. This can be different for other countries with low electricity prices and a relatively high cost of heat for alternatives. The results of this study are purely based on these cost parameters, and hence the conclusions might be different for other cost parameters. It is to be noted that the current prices of electricity and heat have fluctuated a lot since this study was made. Figure 5.13 shows that the total cost of 5th generation network with the COP of 3.5 is lower when compared to the 3rd generation networks if there is free low temperature waste heat source is available.

5.4 Conclusion

A combined district heating and cooling network is designed with a ring topology to supply heat and cold to the buildings using Comsof heat. The network configuration of 3rd generation is used, and both branched and ring topology are compared. This chapter studied the effect of the ring topology on total network deployment costs and compared it against the branched topology. The total network deployment cost of the 3^{rd} generation ring topology is 8.8% costlier than the 3^{rd} generation branched network. However, the ring configuration provides redundancy, flexibility, and possible prosumer integration. When the transport layer is compared (where the ring is present), the total network deployment cost of the ring topology is 75% costlier than the branched network. In addition to the 3^{rd} generation network design, the 5^{th} generation network configuration is also designed. The total network deployment cost of 5^{th} generation networks (ultra-low temperature district heating and cooling with building side heat pump) are 22.8% costlier than the 3^{rd} generation ring networks. This is consistent with the findings of Lund et al. [119], who found that the investment costs of fifth-generation networks are significantly higher than those of fourth-generation networks.

The study also analysed the effect of centralized and distributed storage on total network deployment costs for the 3^{rd} generation ring and branched networks. In the centralized seasonal case, the minimum total network deployment cost can be reduced by 1.7% for the ring topology, whereas it can be reduced by 1.8% for branched topology compared to the no storage scenario. In the centralized multi-day storage case, the minimum total network deployment cost can be reduced by 2.2% and 2.4% for the ring and branched topologies, respectively. In the substation-level seasonal case, the minimum network deployment cost can be reduced by 3.3% and 2.7% for the ring and the branched topologies, respectively. In the substation level multi-day storage, the total minimum network deployment cost can be reduced by 4.5% and 3% for the ring and branched network topology respectively. In substation-level storage, the cost reduction is greater in the ring topology when compared to the branched topology.

The operational and total costs are studied for 3^{rd} generation and 5^{th} generation networks with and without free low temperature waste heat source. The results show that the 5^{th} generation networks are economically attractive only if there is a free low-temperature waste heat source.

Moreover, ring topology is expensive, but it has its fair share of advantages and is economically feasible with a free low-temperature waste heat source.

Chapter 6

5th Generation District Heating Network Design

Contents

6. 5TH GENERATION DISTRICT HEATING NETWORK DESIGN

This chapter is largely based on **Jebamalai, Joseph Maria**, Kurt Marlein, and Jelle Laverge. "Design and Cost Comparison between Ultra Low Temperature Networks with Distributed Heat Pumps and Traditional District Heating Networks" 17th International Symposium on District Heating and Cooling (DHC), Nottingham, UK, September 2021.

District heating and cooling (DHC) networks play an important role in the decarbonization of the heating and cooling sector. One of the main advantages of DHC networks is that they provide supply-side flexibility to adapt and evolve over time. As the energy efficiency of the buildings improves, more and more low-grade energy sources can be utilized. Heat pumps are widely used along with low-grade energy sources to boost the heat to suit the energy demand of the buildings. Recently, district heating networks have been combined with building-side distributed heat pumps, and this configuration provides better energy efficiency of the network. This configuration allows for the supply of both heat and cold using a two-pipe network configuration. The energy demand for space cooling has grown significantly since the 1990s, as evidenced by the fact that the number of central and room air conditioners installed increased by more than 50 times from 1990 to 2010 in the European Union. Moreover, heating degree days have decreased and cooling degree days have increased in the last 15 years in Europe. This emphasizes that space cooling is becoming more important. This chapter studies the configuration of circulating low-temperature water in the network and having a building-side heat pump to lift or drop the temperature to the desired level and compares it with traditional district heating networks. While it is good for the environment to have a sustainable solution and better energy efficiency, it is also important to study the associated costs and primary energy usage. Therefore, the above-said configuration is designed using Comsof Heat and the costs of the network will be calculated. A case study area is used to compare the design and cost of this configuration with traditional district heating networks. The effect of different design parameters is investigated, and several scenarios, such as different costs of electricity and coefficient of performance (COP) are explored. The total cost of the 5^{th} *generation district heating (5GDH) network over the network's lifetime*

of 35 years is lower by 16% when compared with the traditional network design if there is an available low temperature waste heat source.

6.1 Introduction

Traditional district heating networks supply heat to the buildings from the centralized heat source at high network temperatures. As technology matures, the district heating (DH) networks evolved from steam systems to pressurized hot water systems and then to low temperature networks. On the building side, the building energy efficiency measures are given higher importance recently especially in European Union. The increased building energy efficiency paves the way to utilize more low grade and waste heat energy sources.

In order to effectively utilize these low-grade energy sources, heat pumps are widely used, and they could be an alternative source for future DH production. Many authors [127, 128] mentioned that heat pumps would be prevalent in the future energy system. Mathiesen and Lund [127] concluded that large-scale heat pumps are promising as they effectively reduce the excess electricity production. Connolly and Mathiesen [128] mentioned that the introduction of small and large-scale heat pumps is the second stage of the transition to renewable energy supply after district heating. Lund and Persson [129] pointed that sea water most likely will have to play a substantial role as a heat source in the future energy systems in Denmark, but heat pumps are required to tap these sources. Moreover, heat pumps can provide sector coupling between the thermal and electricity grids to handle the intermittent renewable energy sources in the future electricity grid.

5GDH networks distribute heat at very low network temperatures (15 to 25 °C), and there will be additional equipment at the building side to boost the temperature to the desired levels. Mostly, that equipment on the building side would be a heat pump. Because of the low network temperature levels in this configuration, the distribution network's heat loss will be reduced. There are many projects already operating with this configuration. For example, a new building area in Brig (Switzerland), where the heat source is an artificial canal of the Rhone River, and in

Wustenrot (Germany), where the central heat source is a near-surface geothermal field and PV panels produce more electricity than required by the heat pumps over the year. In the above cases, the heat pumps are supplied by cold water around 10 to 16 °C, and there is a possibility of supplying both heat and cold with this network design [130].

Many studies have studied the performance of this configuration and compared it to that of low- and medium-temperature DH networks. Ostergaard and Andersen [131] showed that the booster heat pumps at the building side enable the district heating system to operate at lower temperatures and improve the COP of central heat pumps while simultaneously reducing the district heating network's heat losses significantly. They also stated that the performance of a district heating heat pump with a booster combination outperforms that of individual heating or heat pump solutions. Ommen et al. [132] compared the 5GDH network with booster heat pumps to the performance of low-temperature district heating (LTDH). The results have shown that the 5GDH systems have a lower coefficient of system performance when compared with LTDH when the network is supplied with an extraction combined heat and power plant. However, the 5GDH systems have high performance when the network is fed by a central heat pump supplied by water at 20/10 °C. Vivian et al. [130] investigated the performance of booster heat pumps assuming network supply temperatures in the range of 15 °C and 45 °C. Their economic analysis shows that the system is already competitive with individual gas boilers, provided that a local low-temperature heat source can be recovered with minor marginal costs. Meesenburg et al. [133] studied the economic feasibility of three 5GDH concepts and compared them to the LTDH system. They found that in most cases LTDH was economically preferred and 5GDH could be feasible if the linear heat demand density was high, if the cost of decentralized units could be lowered, or if the investment cost of the central heating unit was significantly lower compared to LTDH. Yang and Svendsen [134] analyzed the impact of the system combination of a centralized heat pump and a local booster configuration. Their results show that the LTDH system without supplementary heating has the highest energy and exergy efficiency. The 5GDH system has better performance compared to medium-temperature district heating due to substantial savings from the distribution heat loss.

While most of these studies focus on energy efficiency and system performance, it is also important to study the costs associated with the 5GDH network design. However, none of these studies designed a large-scale network with detailed network cost calculations and compared it with the detailed traditional network design. In this chapter, a case study of a single-layer network with an 5GDH network with a distributed heat pump configuration and a traditional DH network configuration is investigated. The main objective of this chapter is to perform a detailed network design of both an 5GDH network with distributed heat pumps and a traditional network and compare their associated costs using a case study for a Scottish city.

6.2 Methodology

This section summarizes the case study area, the input requirements and network configuration of both traditional district heating networks and 5GDH networks with distributed heat pumps, and all the simulated scenarios in this case study. Comsof Heat is used for pipe routing, network dimensioning, and network cost estimation.

6.2.1 Case study area

A Scottish city, Glasgow, in the United Kingdom, is the selected area of this study. The case study area in the Glasgow city center has over 1300 buildings (mainly commercial and residential). It has an estimated population of about 17,000 permanent residents. The annual heat demand for this area is approximately 140 GWh. This heat requirement will be met with the energy extracted from the River Clyde using heat pumps. The Clyde River is a rich source of energy, capable of producing more than 250 MW_{th} at peak or 2000 GWh annually. The case study area is divided into 4 clusters (as shown in the Figure 6.1) and the energy for these clusters will be extracted from the river flowing just below these

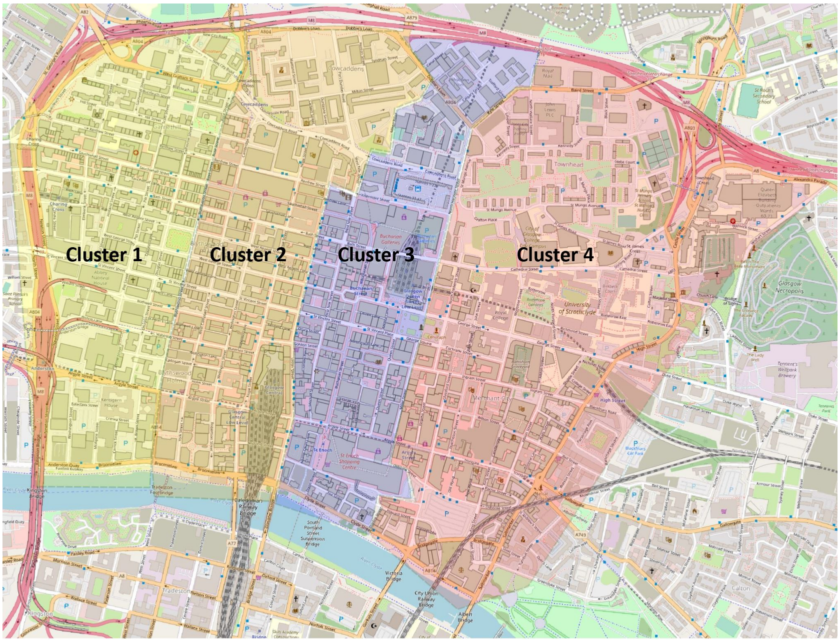

Figure 6.1: Case study area (Glasgow city center) divided into 4 clusters.

areas. This case study area is used to design two types of networks: traditional centralized district heating networks and 5GDH networks with distributed heat pumps.

6.2.2 Heat demand data

The building energy consumption data is estimated using Hotmaps, the open-source mapping and planning tool for heating and cooling. Hotmaps provides heat demand density (kWh/ha-y) and gross floor area density (m^2/ha) data for the selected area (shown in Figure 6.2). These data are mapped to all the buildings (shown in Figure 6.3)). For each building, the heat demand density per square meter of gross floor area (kWh/m^2-y) is calculated by dividing the heat demand density by the gross floor area density. The yearly heat consumption of each building is then calculated by multiplying the building's gross floor area by the heat demand density per square meter of gross floor area. The peak

Figure 6.2: Hotmaps data for Glasgow city center .

heat demand is calculated using the full load hours of 2000. These calculated heat demand data are used for both design cases mentioned in the previous section.

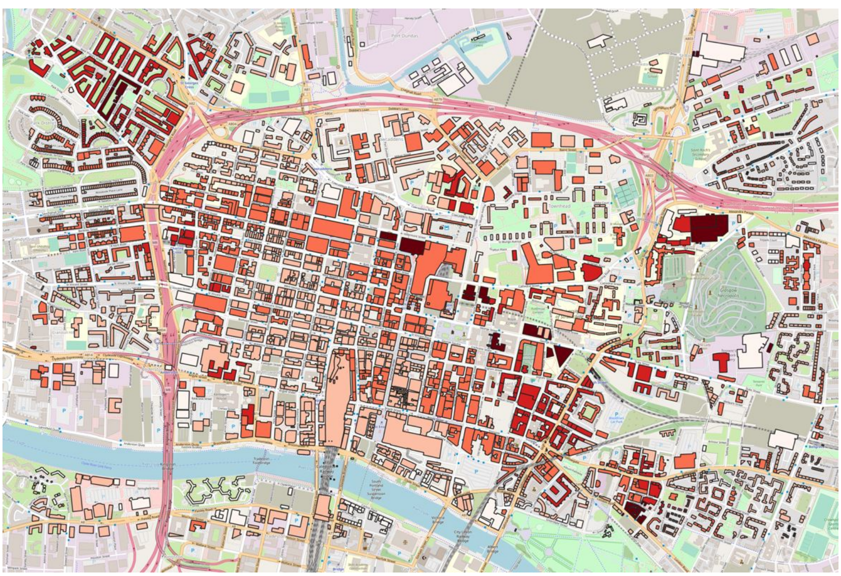

Figure 6.3: Mapped input data to the buildings.

Table 6.1: Network cost used in 5GDH and traditional network configuration

Nominal diameter	Traditional cost [£/m]	Investment cost [£/m]
DN20 to DN65	750	500
DN80 to DN150	1000	750
DN200 to DN350	1500	1000
DN400 to DN800	2000	1500

6.2.3 Traditional district heating network

The traditional district heating network supplies heat to all the buildings from centralized sources. In this design, four centralized heat pumps are used to supply heat to the buildings in the four clusters (shown in Figure 6.4)). A single-layer network configuration (where the heat pump in one cluster will be directly connected to the buildings in that cluster) is chosen with network temperature levels of 80/50 °C. The pressure level of the network is designed for PN10. The network constraints are set at 0.5 bar for the minimum pressure at the farthest consumer's heat exchanger and 2 bar for the minimum pressure required to avoid boiling. Steel pipes are used in this network design. Table 6.1 shows the standard pipe definitions with their specific costs, which are used for both traditional and 5GDH network configurations. The cost per meter of pipe includes the excavation costs, pipe costs, welding and installation costs, refill and repair costs of the top layer, and also project management overhead. The investment cost of the source (the heat pump) is considered to be 1 million pounds. This cost includes the heat pump, ancillary equipment, energy center, and electricity infrastructure. The circulating pump cost is considered to be 50,000 £/ MW. Table 6.2 shows the heat delivery unit cost for different power ranges which are used in this network configuration. Using these data inputs, Comsof Heat designs the traditional district heating network, which involves pipe routing, network dimensioning, and network cost estimation.

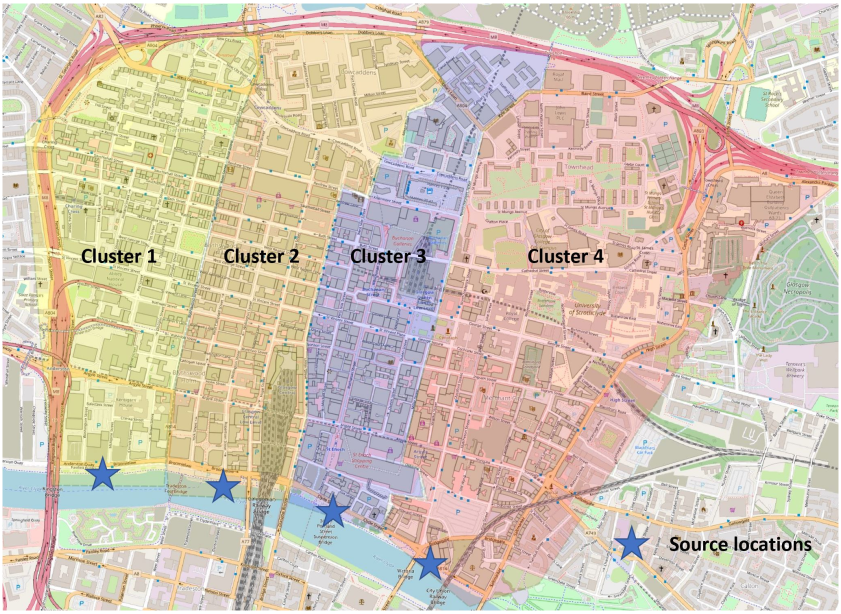

Figure 6.4: Four centralized heat pumps supply heat to four clusters.

6.2.4 5GDH networks with distributed heat pumps

This configuration includes 5GDH networks that provide low-temperature water to all buildings, where the temperature is raised using heat pumps. In this design, heat pumps are installed in all the buildings. A single-layer network configuration is chosen with a network temperature level of 15/5 °C. A drawback of extracting energy directly from the river is that the supply temperature of 15 °C cannot be obtained without additional energy supply. Therefore, a centralized heat pump is used to increase the temperature to 15 °C. Since the temperature increase that the centralized heat pump has to deliver is small, the COP of this centralized heat pump will be very high (a COP of 8 is used in this study). The pressure level of the network is designed for PN6. Other network constraints are used same as the previous configuration. Plastic pipes are used in this design configuration. The network temperature levels (15/5 °C) are lower compared to the traditional network, and so

Table 6.2: Heat delivery unit specific cost used in this network configuration

Power [kW]	Cost [£]
1 to 50	3,000
50 to 100	10,000
100 to 400	25,000
400 to 1000	100,000
1000 to ∞	150,000

the DH pipe insulation is not required for this configuration. Therefore, the network costs of this configuration are lower when compared to the traditional network configuration. Table 6.1 shows the specific cost of standard pipe diameter ranges in this configuration. The investment cost of the centralized heat pump is considered to be 1 million pounds. The specific investment cost of the distributed heat pumps is considered to be 400 £/kW. The circulating pump cost is considered to be 50,000 £/MW. Since the heat pumps are installed at the building side, heat delivery units are not required in this design configuration. Comsof Heat designs the 5GDH networks with distributed heat pump configurations using the above design data. The calculation and methodology of this configuration, which Comsof Heat uses, are explained in the below subsections.

6.2.4.1 COP calculation

Figure 6.5 shows the heat pump representation on the building side and the energy flows on the building and network sides at the consumer building. The building's peak heat demand is denoted as Q_{heat}, and the heat required from the low temperature network is denoted as Q_{heat}, n. The electricity required for the heat pump is represented as Q_{el}. The COP calculation on the building side is presented using the following equations:

$$COP = \frac{Q_{\text{heat}}}{Q_{\text{el}}} \tag{6.1}$$

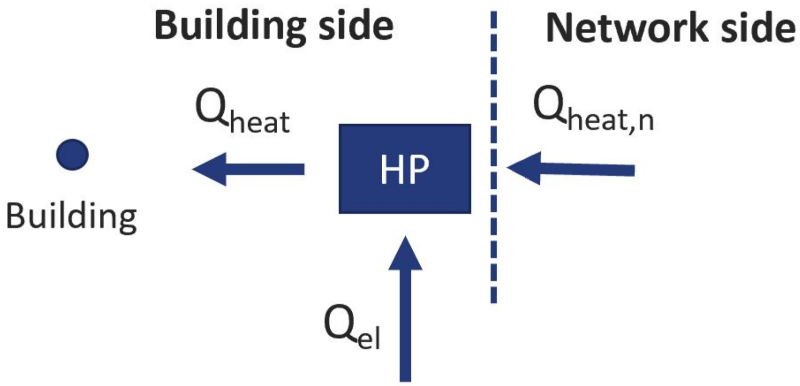

Figure 6.5: Energy flows of building and network side at the consumer building.

$$Q_{\text{heat}} = Q_{\text{heat,n}} + Q_{\text{el}} \tag{6.2}$$

$$COP = \frac{Q_{\text{heat,n}}}{Q_{\text{el}}} + 1 \tag{6.3}$$

Comsof Heat requires the COP of the heat pump as input for all the buildings in this configuration. The input demand for this design is split into three categories: space heating demand, domestic hot water demand, and space cooling demand, and hence it is possible to specify 3 COP input values for these three categories. This configuration is capable of providing cooling to the buildings since it has heat pumps on the building side. However, cooling is not considered in this study. Using the demand data and the COP input, the electricity required and the heat required from the network are calculated for all the buildings.

6.2.4.2 Pipe dimensioning method

The pipe dimensioning method is similar to that of other configurations, except that this configuration can have both heating and cooling demand for a building. Therefore, simultaneity factors can be specified for both heating and cooling. The users can specify the demand selection that they want to consider for the network design. If heating and cooling demand selection is made, the pipe is dimensioned for the dominant demand (the maximum of heating and cooling) in the whole network. In this study, cooling is not considered, so the network is designed for heating only. The space heating and domestic hot water simultaneity factors are calculated using equation 2.3 and equation 2.4 respectively.

6.2.5 Scenarios

In this section, several scenarios, such as different COP scenarios, free waste heat source scenarios, and electricity price scenarios, are explained.

6.2.5.1 Different COP scenarios

In these scenarios, the COP of the distributed heat pump at all buildings will be varied. Two scenarios with average COP of 2.5 and 3.5 are used to design the network. The COP value varies based on the temperature requirements of each building. These scenarios will aid in the comparison of traditional network designs.

6.2.5.2 Free waste heat source scenario

As mentioned in section 6.2.4, the 5GDH networks with distributed heat pumps still require a centralized heat pump because river water is used as a source. However, if the low-temperature waste heat is available at a temperature of 15 °C, the centralized heat pump can be avoided. It can be from sewage water, data centers, or other low temperature waste heat sources. In that case, the investment requirement of an additional centralized source can be avoided. This scenario will be compared against the traditional network design and the 5GDH network design with a centralized source.

6.2.5.3 Electricity price scenarios

The use of heat pumps in the network requires electricity in addition to the heat supply. So, the price of electricity affects the cost of heat produced. Hence, it is important to analyze how different electricity prices affect the viability of the networks. In these scenarios, the electricity

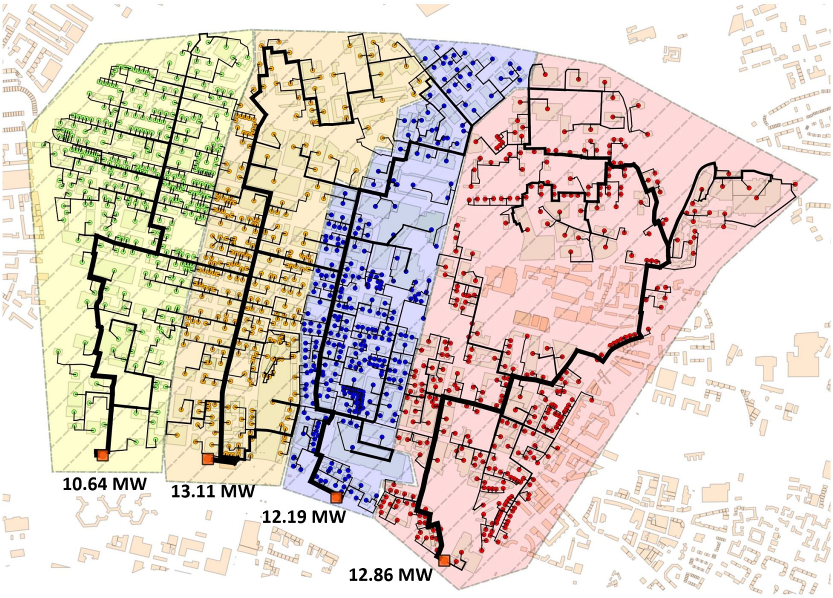

Figure 6.6: Designed network using Comsof Heat.

price is varied between 100 £/MWh to 150 £/MWh for the distributed heat pumps. For the centralized heat pumps, the electricity can be obtained at a special price, and 50 £/ MWh is used for the traditional centralized network design.

6.3 Results and discussion

The total peak power of the case study area is estimated to be 48.8 MW. Several scenarios are simulated, including various COP scenarios, a free waste heat source scenario, and electricity price variation scenarios, to determine their impact on total network cost. The designed network using Comsof Heat is shown in Figure 6.6).

6.3.1 Different COP scenarios

Table 6.3 shows the peak heat demand before and after simultaneity and the electricity required at the building side for the traditional network design (hereafter called the base case scenario) and the 5GDH network with a distributed heat pump COP of 2.5 and 3.5. For the 5GDH networks with distributed heat pump COP of 2.5 and 3.5, the peak heat demand is calculated as 29.28 MW and 34.85 MW, respectively, whereas it is 48.8 MW for the base case. The electricity demand at the building side for these two cases is estimated to be 19.52 MW and 13.95 MW, respectively, whereas there is no electricity required at the building side for the base case. The largest pipe diameter for these two cases is calculated at DN450, whereas it is DN300 for the base case.

Table 6.3: Total demand and electricity required for base case and 5GDH networks

Description	Base case design	COP - 2.5	COP - 3.5
Peak heat demand without simultaneity [MW]	78.56	78.56	78.56
Network temperatures [°C]	80/50	15/5	15/5
Peak heat demand after simultaneity [MW]	48.8	29.28	34.85
Electricity demand at building side after simultaneity [MW]	0	19.52	13.95
Largest pipe diameter	DN300	DN450	DN450

The peak heat demand is decreased from the base case to 5GDH networks with a COP of 3.5, and then it is further reduced in the COP of 2.5 case. This is due to an increase in the use of heat pumps, which is accompanied by an increase in electricity demand. The largest pipe diameter is increased from the base case design to the 5GDH network case. This is caused by the low network temperature difference in the latter case (10 °C) compared to the base case (30 °C).

Figure 6.7 shows the network pipe dimensions of the base case, 5GDH networks with distributed heat pump COP of 2.5 and 3.5 cases. The network pipe dimensions are larger for the 5GDH networks, as shown in Figure 6.7. For example, the proportion of smaller pipes (DN25 and DN32) is much higher in the base case when compared with the 5GDH

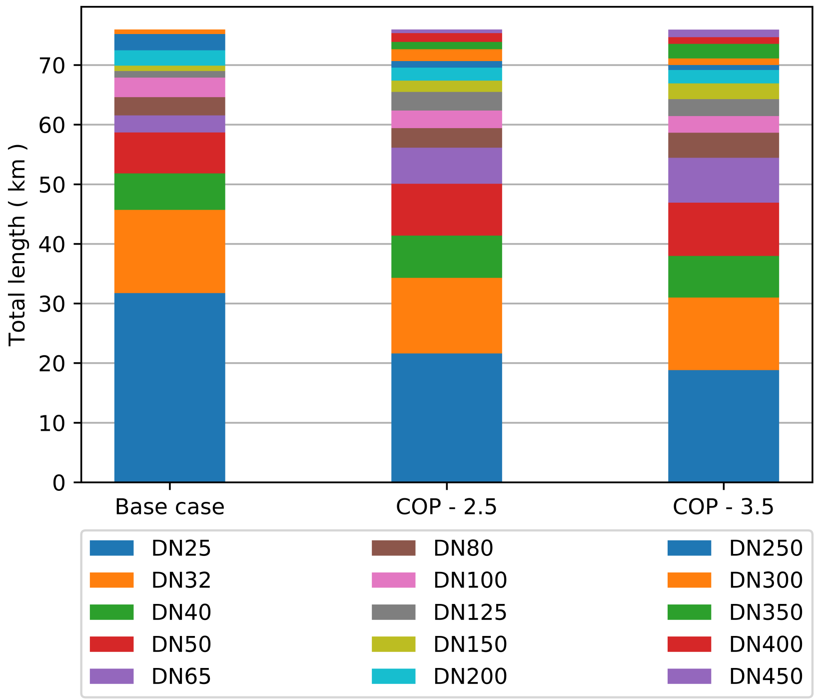

Figure 6.7: Network pipe dimensions of base case, 5GDH networks with COP of 2.5, and COP of 3.5.

networks. This is caused by the low network temperature difference (10 ˚C) in the case of 5GDH temperature networks.

Figure 6.8 shows the network heat loss of base case, 5GDH networks with distributed heat pump COP of 2.5 and 3.5 cases. The network heat loss is way higher in the base case design when compared with 5GDH networks. The heat loss calculation is done with a ground temperature of 10 ˚C. Since the base case design has high network temperature levels, network heat loss is also higher. In the case of 5GDH networks, there is a heat loss only from the supply pipe. Since the return temperature of the network (5 ˚C) is lower than the ground temperature, there will be a heat gain instead of heat loss, which is not considered in this study. So, the reported heat loss for the 5GDH network consists only of supply pipe

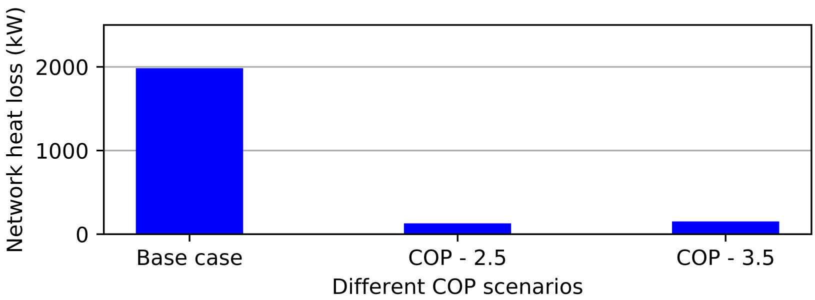

Figure 6.8: Network heat loss of base case, 5GDH networks with COP of 2.5, and COP of 3.5.

heat loss, whereas base case heat loss involves both supply and return pipe heat losses.

Table 6.4: Distributed heat pump cost at the building side – Average and high costs

Power [kW]	Average cost [£]	High cost [£]
0 to 50	10,000	20,000
50 to 100	20,000	40,000
100 to 400	80,000	160,000
400 to 1000	200,000	400,000
1000 to ∞	300,000	500,000

Figure 6.9 shows the total investment cost of the base case, 5GDH network with a distributed heat pump COP of 2.5 and 3.5 for both average and high heat pump costs. The average and high distributed heat pump costs are calculated with the specific distributed heat pump investment cost of 400 £/kW and using the average power from the power range and the high power from the power range, respectively. Table 6.4 shows the average and high-distributed heat pump costs used for this scenario.

The investment cost of 5GDH networks is calculated using both the average and high costs of distributed heat pumps. These investment costs are compared against the base-case scenario in Figure 6.9. The total invest-

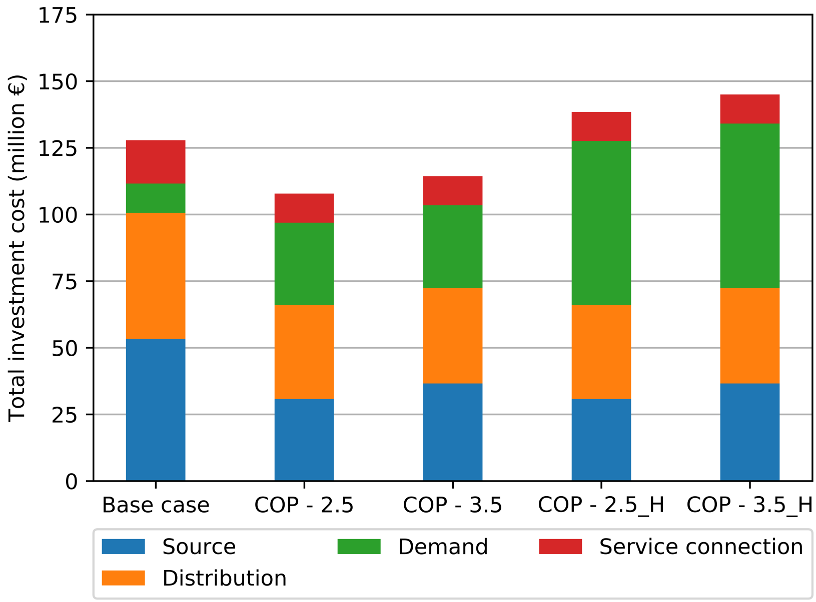

Figure 6.9: Total investment cost of base case, 5GDH networks with COP of 2.5, and COP of 3.5 for average and high distributed heat pump cost.

ment is lower for the 5GDH network case with a COP of 2.5 using average heat pump costs when compared to the base case. The investment cost of an 5GDH network with a COP of 3.5 using average heat pump costs is higher than that of a network with a COP of 2.5 but still less than the base case scenario. However, the 5GDH cases calculated with high distributed heat pump costs are higher than the base case.

The reduction in total investment cost of 5GDH networks is mainly due to their lower source and distribution network costs. The source cost (centralized heat pump) is reduced because of the lesser power requirement due to the additional heat production using distributed heat pumps at the building side. The distribution network cost is reduced because of the cheaper pipes (shown in Table 6.1) required for 5GDH networks. As seen in Figure 6.8, network heat loss is very low for 5GDH networks, and there is no insulation required for the pipes. The demand cost is in-

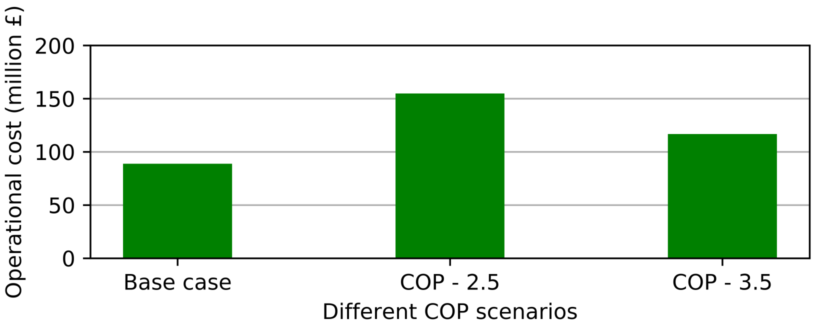

Figure 6.10: Operating cost of base case, 5GDH networks with COP of 2.5, and COP of 3.5.

creased because of the higher investment cost of distributed heat pumps on the building side when compared with the base case scenario. The service connection cost is reduced a bit due to cheaper pipes, as mentioned above. The 5GDH network calculated with high distributed heat pump cost shows an increase in demand cost as a result of the higher heat pump cost.

Figure 6.10 shows the network operating cost of base case, 5GDH networks with COP of 2.5 and 3.5 cases. The operating cost is calculated for the network lifetime of 35 years. The operating cost consists mainly of the heat production cost and the electricity cost of the heat pumps. The operating cost is lower in the base case scenario when compared with the 5GDH network case. This is because the base case has only centralized heat pumps and can fetch cheaper electricity (50 £/MWh) by means of a private wire. The distributed heat pump has to obtain electricity from the grid (100 £/MWh) which is usually more expensive than the private wire price. The case with the COP of 3.5 has a lower operating cost when compared with the COP of 2.5 case. This is because of the better COP.

Figure 6.11) shows the total cost (operational plus investment) of the base case, 5GDH network with a distributed heat pump COP of 2.5 and 3.5 for both average and high heat pump costs. In terms of total network cost over the network lifetime of 35 years, the base case scenario (one with

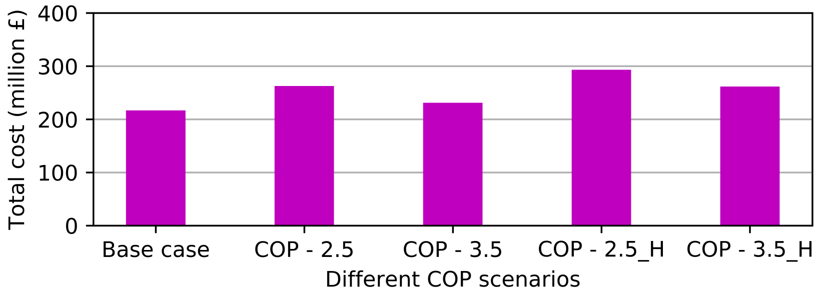

Figure 6.11: Total cost (operational and investment) of base case, 5GDH networks with COP of 2.5, and COP of 3.5 for average and high distributed heat pump costs.

a high-temperature centralized source) is the cheapest when compared to 5GDH networks with distributed heat pumps. This is because the latter case has a higher operating cost.

6.3.2 Free waste heat source scenario

Figure 6.12 shows the total investment cost of base case, 5GDH networks with COP of 2.5 and COP of 3.5 for average and high distributed heat pump with the assumption of free heat source availability. When compared to the base case scenario, the total investment cost for 5GDH networks with average heat pump costs is significantly lower. The reduction in the investment cost of 5GDH networks is mainly because of the reduction in source costs. Since the heat is available for free in this scenario, the source investment cost is negligible. However, harnessing and accessing the free source typically requires additional investment costs. Even 5GDH networks with high distributed heat pump costs are less expensive than the base case scenario. This is possible because of the assumption of free low-temperature source availability.

Figure 6.13 shows the operating cost of base case, 5GDH networks with COP of 2.5 and COP of 3.5. The operating cost is lower in the base case scenario, whereas it is higher in the case of 5GDH networks. This is due to the lower cost of electricity in the base case scenario, as explained in the previous section.

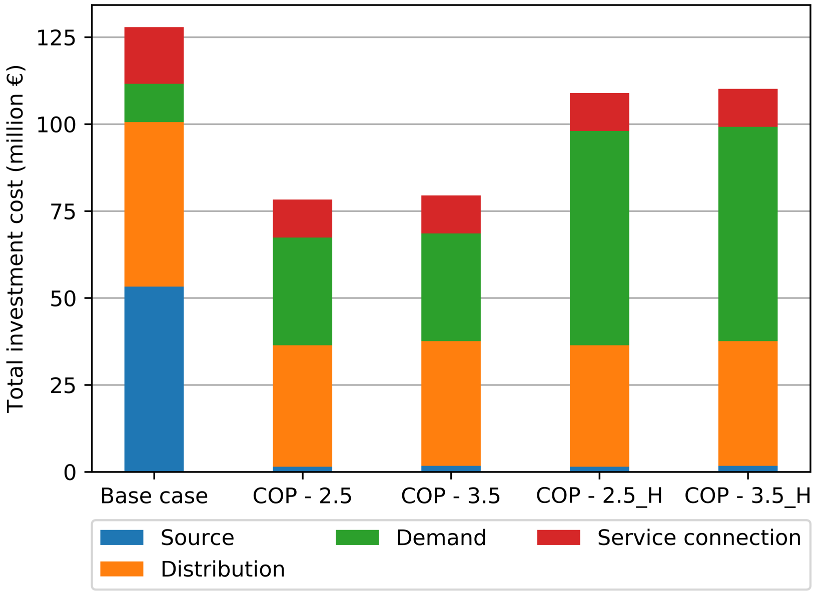

Figure 6.12: Total investment cost of base case, 5GDH networks with COP of 2.5, and COP of 3.5 for average and high distributed heat pump cost with the assumption of free heat source availability.

Figure 6.14 shows the total cost of base-case, 5GDH networks with COP of 2.5 and COP of 3.5 for average and high distributed heat pump costs. The 5GDH network with the COP of 3.5 with the average heat pump cost is the cheapest in terms of total cost. Even the COP of 3.5 scenario with high distributed heat pump costs beats the base case slightly in terms of total cost. The case with a COP of 2.5 using average heat pump costs is on par with the base case scenario. This is mainly because of the very low source cost due to the use of low-temperature waste heat at no cost.

6.3.3 Electricity price scenarios

Figure 6.15 shows the total cost of base case, 5GDH networks with COP of 3.5 using different electricity price. The total cost of 5GDH network with COP of 5 is still lower at 125 £/MWh when compared with the

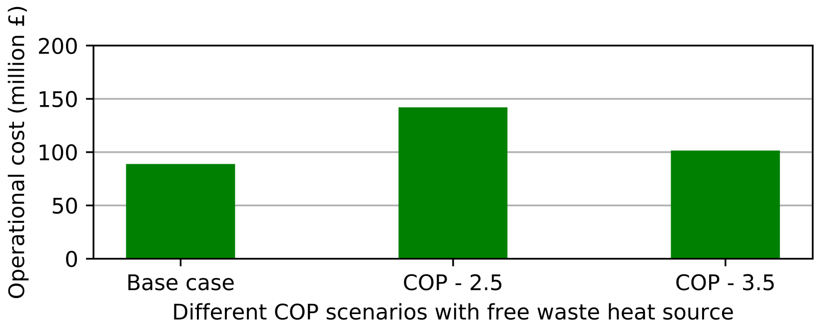

Figure 6.13: Operating cost of base case, 5GDH networks with COP of 2.5, and COP of 3.5 with the assumption of free heat source availability.

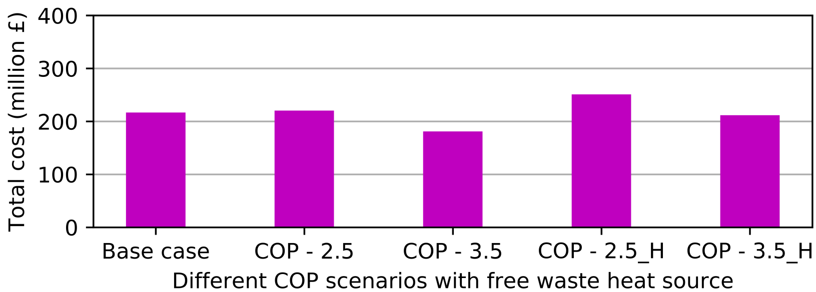

Figure 6.14: Total cost of base case, 5GDH networks with COP of 2.5, and COP of 3.5 for average and high distributed heat pump cost with the assumption of free heat source availability.

base case. The base case is calculated with the electricity price of 50 £/MWh.

6.4 Conclusion

This chapter studied the 5GDH network with a distributed heat pump configuration and compared it with the traditional district heating network in terms of network cost and heat loss. Glasgow City Center is selected as a case study area. The district heating network is designed to supply heat to the buildings in the case study area using both traditional and 5GDH networks with a distributed heat pump configuration.

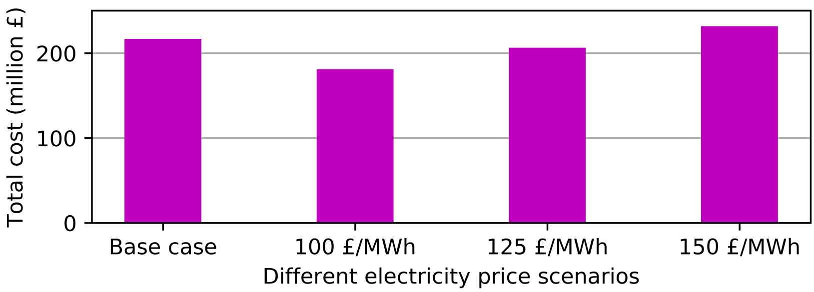

Figure 6.15: Total cost of base case, 5GDH networks with COP of 3.5 using different electricity prices.

The peak heat demand is reduced for the 5GDH network with a distributed heat pump configuration with a COP of 2.5 (29.28 MW) and 3.5 (34.85 MW) when compared with the base case scenario (48.8 MW). However, the electricity demand required at the building side is increased proportionally for the 5GDH network cases. The network heat loss for the base case scenario (1983 kW) is much higher when compared with the 5GDH network cases (129 kW and 151 kW). If the average heat pump cost is used, the 5GDH network with the requirement of centralized and distributed heat pumps has a lower investment cost when compared to the traditional base case scenario. If it is calculated using the high heat pump cost, the base-case scenario has a lower investment cost when compared with 5GDH network cases. Though the investment cost is lower in the average heat pump cost scenario for an 5GDH network, the operating cost is much higher when compared with the base case scenario. This is due to the higher electricity price for the 5GDH networks because of the electricity usage from the grid. Therefore, the higher operating cost offsets the lower investment cost of the 5GDH network case calculated with the average heat pump cost. So, the total cost is lower for the base case scenario when compared with the 5GDH network cases with the required centralized source.

The total investment cost of 5GDH network cases with the free waste heat source at 15 °C is much lower when compared with the base case scenario. Though the operating cost is higher for the 5GDH networks, the total cost is lower for the 5GDH with a COP of 3.5 when compared with the base case scenario. This is because of the utilization of free low-temperature waste heat. As a conclusion, the 5GDH network with distributed heat pumps is financially suitable when there is free low temperature waste heat available (at least 12 to 15 °C). Otherwise, this configuration is not financially attractive, and traditional district heating networks can be designed instead.

In the case of free low-temperature waste heat being available, the 5GDH network with a distributed heat pump COP of 3.5 is attractive even at the electricity price of 100 to 125 £/MWh and beats the base case scenario (at the electricity price of 50 £/MWh). Therefore, it is very important to utilize a low-temperature waste heat source.

Because this study is being conducted in 2021, the information on the used electricity price, network pipe cost, and equipment cost is out of date due to high inflation and a sharp increase in energy prices. However, the results remain valid because prices for both the base case and the 5GDH network cases have risen.

Chapter 7

Conclusion

Contents

7.1 Conclusions

This thesis described a method for automatically creating DH networks under predefined network restrictions. In chapter 2, a case study (Hengstdal neighbourhood) is used to draw the following findings. One of the findings is that the cost of trenching dominates the overall cost of network deployment. This trenching expense can be reduced by combining the construction work with that for other services like sewage, gas, roads, etc. We showed that even if space heating requirements are reduced by 50%, network deployment costs are only reduced by 9% and 16%, respectively, with and without DHW load. This demonstrates how challenging it would be for future DH networks to be profitable while reducing heat demand, and we argue that denser areas would be required to achieve it. Another result is that in future demand reduction scenarios, relative heat loss grows dramatically. Low-energy buildings are excellent at maintaining a comfortable temperature. As a result, to accommodate the future decrease in demand, the network supply temperature may be further lowered.

In chapter 3, the impact of centralized and distributed storage on the overall network cost of a district heating network is examined. The case study findings indicate that a 2-day storage capacity (2000 m^3) with centralized storage resulted in a maximum network cost reduction of 3.9 percent as compared to no storage. With one day of storage (1000 m^3), the maximum network cost reduction inch up to 5.1% for substation level storage (4MW substation size). With one day of storage (1000 m^3), the building level storage also offers the highest possible network cost savings of 6.6 percent. This demonstrates that there is an ideal storage size for every scenario and that it varies depending on the storage distribution. Furthermore, when storage is distributed to 7 and 10 locations, the maximum network cost reduction rises, but falls as distribution proceeds. This demonstrates that there is a perfect location to distribute the storage. It is no longer profitable to distribute after that point. The ideal storage distribution in this case study is between seven and ten clusters. Furthermore, for small storage volumes, building-level storage continues to be the least expensive. The combination of daily storage at the building level with centralized seasonal storage continues to be the least expensive network when daily and seasonal storage are compared. In a nutshell, building-level storage is better suited for daily storage whereas centralized to substation-level storage is better suited for seasonal storage.

With building-level storage, the highest network cost reduction for the scenario with a 50% drop in heat demand will only be around 16.4%. Therefore, the decrease in demand does not match the corresponding decrease in total network costs. The relative peak daily profile variation is used to quantify three separate daily profile variations using an evaluation technique from the literature. It has been demonstrated that the greatest network cost reduction increases with the relative peak daily profile variation. Furthermore, for minor variations in the peak daily profile, centralized storage gives the largest cost reductions. Storage at the substation level is advantageous for daily profile fluctuations with high peaks. No matter how the relative peak daily profile changes, building-level storage continues to be the least expensive option. High source costs also translate into significant cost reductions and change the ideal storage size to favor larger storage capacities. The results and conclusions are based on the input network design and cost assumptions, which are specific to the network design and location. As a result, different input assumptions and cost data will produce different outcomes. By examining various demand profile variations, source costs, and storage temperature differences in this study, we attempted to generalize the findings. Furthermore, the costs at the time of this study (2020) are outdated but the conclusions are largely unaffected because costs for both heat sources and storage may have increased. When using the most recent cost data, minor changes are possible.

Moreover, a method for automatically creating a multiple-source district heating network for the provided network restrictions and design options was presented in chapter 4. To construct multiple-source district heating networks for various KPIs and design options, a case study is created using Comsof Heat. The design decisions' impact on investment costs, energy production costs, carbon costs, and emissions are all being researched. The source selection using various KPI scenarios reveals that the costs of energy production and investment are greater for low-carbon sources. Heat pumps and other low-carbon sources are not favored by cost optimization with the chosen carbon cost of 30 €/tonne. The various carbon cost scenarios illustrate that an increasing carbon cost favors low-carbon sources when total costs (investment, energy production, and carbon cost) are optimized. In order to compete with the other available sources in this case study, the carbon cost has to be increased to 80 €/tonne. Although prices have risen since the study's completion in 2020, and the projected cost of carbon has not been updated, the overall findings remain valid, though minor changes are possible.

Furthermore, a ring-topology combined district heating and cooling network is designed to supply heat and cold to buildings using Comsof heat in chapter 5. The third generation network configuration is used, and both branched and ring topologies are compared. The effect of ring topology on total network deployment costs is investigated and compared to branched topology. The total network deployment cost of the third generation ring topology is 8.9% higher than that of the third generation branched network. The ring configuration, on the other hand, provides redundancy, flexibility, and the possibility of prosumer integration. When the transport layer (where the ring is present) is compared, the total network deployment cost of the ring topology is 75% higher than that of the branched network. The fifth generation network configuration is also designed, in addition to the third generation network configuration. 5th generation networks (ultra-low temperature district heating and cooling with building side heat pump) are 22.8 percent more expensive overall to deploy than 3rd generation ring networks.

In this study, the impact of both centralized and decentralized storage on overall network deployment costs for third-generation ring and branched networks was also examined. When compared to the no storage scenario, the minimum overall network deployment cost for the centralized seasonal case can be lowered by 1.8 percent for branched topology and by 1.7 percent for ring topology. For the ring and branched topologies, the minimum total network deployment cost in the centralized multi-day storage situation can be decreased by 2.2 and 2.4 percent respectively. In the substation-level seasonal case, the minimum network deployment cost can be reduced by 3.3% and 2.7% for the ring and the branched topologies, respectively. When comparing the ring topology to the branched architecture for substation-level storage, the cost decrease is larger in the ring topology. For 3^{rd} generation and 5^{th} generation networks with and without a free low temperature waste heat source, the operating and total costs are compared. The findings demonstrate that the fifth generation networks are only financially viable in the presence of a free low-temperature waste heat source. Ring topology is also expensive, although it has some benefits and can be implemented affordably using a free low-temperature waste heat source.

The 5GDH network with a distributed heat pump configuration was examined in chapter 6, and its network costs and heat loss were compared to those of the conventional district heating network. The peak heat demand is reduced for the 5GDH network with a distributed heat pump configuration with a COP of 2.5 (29.28 MW) and 3.5 (34.85 MW) when compared with the base case scenario (48.8 MW). However, in 5GDH network scenarios, there is a correspondingly higher demand for electricity at the building side. Comparing the base case scenario (1983 kW) to the ultra-low temperature situations, the network heat loss is significantly larger (129 kW and 151 kW). The 5GDH network, which requires both centralized and distributed heat pumps, has a lower investment cost than the conventional base case scenario if the average heat pump cost is chosen. The base-case scenario has a lower investment cost as compared to 5GDH network cases if it is estimated using the high heat pump cost. Although the running cost is significantly greater than the base case scenario in the average heat pump cost scenario for a 5GDH network, the investment cost is lower. This is because using electricity from the grid results in increased electricity costs for 5GDH networks. As a result, the lower investment cost of the 5GDH network case estimated using the average heat pump cost is offset by the higher operating cost. Comparing the basic case scenario to the ultra-low temperature instances with the necessary centralized source, the overall cost is cheaper.

When compared to the base case scenario, the overall investment cost of 5GDH network scenarios with the free waste heat source at 15 °C is significantly cheaper. When compared to the base case scenario, 5GDH networks have a COP of 3.5, which means that even though their operating costs are higher, their overall costs are lower. This is because free low-temperature waste heat is being used. As a conclusion, the 5GDH network with distributed heat pumps is financially suitable when there is free low temperature waste heat available (at least 12 to 15 °C). Otherwise, conventional district heating networks can be designed because this arrangement is not financially advantageous. Harnessing and accessing low-temperature waste heat source also requires additional cost and so the probability of finding free low-temperature waste heat is low. The 5GDH network outperforms the base case scenario (at the electricity price of 50 £/MWh) and is attractive in the case of free low-temperature waste heat being available. It has a distributed heat pump COP of 3.5. Therefore, it is very important to utilize a low-temperature waste heat source. Because this study is being conducted in 2021, the information on the used electricity price, network pipe cost, and equipment cost is out of date due to high inflation and a sharp increase in energy prices. However, the results remain valid because prices for both the base case and the 5GDH network cases have risen.

In this thesis, the research goal of creating an automated and integrated district heating design method was effectively accomplished. The storage model is also created and linked with the design methodology. This method is applied to several case studies that assisted in answering the research questions for this thesis. There are advantages to distributing thermal energy storage throughout networks, and doing so can lower the investment costs for networks. While distributing the thermal energy storage, an optimal point can be reached (minimizing the overall network cost). Additionally, the goal of creating a design method for networks with multiple sources using branching and ring topologies is accomplished. In accordance with the specified source selection criteria, this method may also be used to choose the heat sources. The ring topology networks are about 9% costlier than branched networks and this comparison will help in conducting the cost benefit analysis. In addition, a case study is used to illustrate the process for designing 5GDH networks and to address the research question of evaluating their economic viability with the current state-of-the-art network. In most instances, 5GDH networks are more expensive than conventional networks. It can only be less expensive if an inexpensive heat pump is utilized or if a free waste heat source is provided. The analysis/study was done few years ago and all equipment prices are increased considerably due to high inflation in the past years. Additionally, it costs more to extract heat from a free waste heat source.

7.2 Limitations

The source, substation, and building locations are the only storage options in the storage model described in chapter 3. Additionally, the storage location is not optimal, and it is not possible to locate the storage anywhere else outside the places mentioned above.

In chapter 4, the design approach for multiple source networks is developed using a combination of the assignment and routing algorithms. The drawback of this strategy is that it will take a lot of calculation time to check for all conceivable combinations as the number of substations increases. The only way to get the best results is to test every possible combination. Another limitation is that the transport network's simultaneity is assumed to be 1. As a result, expanding this strategy to the distribution network is difficult.

The approach to designing 5GDH networks with distributed DH networks is developed in chapter 6. However, it is not possible to reintroduce heat into the network using the heat pumps in the buildings. Therefore, heat pumps are unable to function as prosumers. Prosumers are not supported in the established model, despite the development of the necessary building blocks, because it is outside the scope of this PhD.

7.3 Perspectives

In the future energy system, distributed and integrated district heating networks will be crucial. As a result, the DHC networks will be connected to more prosumers. The two-way network design needs to be created in order to support prosumers in the network. Ring networks, storage, heat pumps, and decentralized pumps can do this; nevertheless, sophisticated operation strategies are required. This thesis developed the structural elements to support prosumers in the network. This can be extended in the future work by modelling decentralized pumps and supporting heat delivery from heat pumps back to the network.

Integration of DH networks with the electrical grid is also crucial. DH networks will assist in balancing fluctuations in the power system brought on by unpredictable renewable energy sources. Thermal energy storage is less expensive than battery storage. Electric boilers, heat pumps, and CHP plants will all contribute to the balancing of electrical networks thanks to thermal energy storage. This thesis includes the development of a heat pump model that will calculate how much electricity heat pumps will need at each demand point in a building. The connection to the electrical grid, however, is not modeled. The task at hand in the future would be to pair this heat pump model with an electricity grid connectivity and capacity model.

Furthermore, the storage location optimization is not developed as part of this thesis as stated in the section 7.2. To determine whether or not there is an ideal storage place, additional investigation will be needed. If so, how might the network's storage locations be optimized?

Finally, the branched multi-source connection algorithms can be enhanced as mentioned in the section 7.2. Even if the performance of the generated algorithm is impressive after some reworking by the Comsof development team, the performance of the flow algorithms can be compared. As a result, further research will be needed to enhance connection algorithms and explore the potential for using flow algorithms to create various networks.

List of Publications

Journal publications

1. Jebamalai, Joseph Maria, Kurt Marlein, and Jelle Laverge. ”Design and cost comparison of district heating and cooling (DHC) network configurations using ring topology–A case study.” Energy 258 (2022): 124777.

2. Jebamalai, Joseph Maria, Kurt Marlein, and Jelle Laverge. ”Influence of centralized and distributed thermal energy storage on district heating network design.” Energy (2020): 117689.

3. Jebamalai, Joseph Maria, Kurt Marlein, Jelle Laverge, Lieven Vandevelde, and Martijn van den Broek. ”An automated GIS-based planning and design tool for district heating: Scenarios for a Dutch city.” Energy 183 (2019): 487-496.

Conference publications

1. Jebamalai, Joseph Maria, Kurt Marlein, and Jelle Laverge. “Design and Cost Comparison between Ultra Low Temperature Networks with Distributed Heat Pumps and Traditional District Heating Networks” 17th International Symposium on District Heating and Cooling (DHC), Nottingham, UK, September 2021.

2. Jebamalai, Joseph Maria, Kurt Marlein, and Jelle Laverge. “ An automated method to design multi-source district heating networks with integrated thermal energy storage – A case study” 6th International conference on Smart Energy Systems, October 2020. (No proceedings, only presentation).

3. Jebamalai, Joseph Maria, Kurt Marlein, and Jelle Laverge. “A method for automated routing and designing of multi-source district heating networks” 15th conference on sustainable development of energy, water and environment systems, September 2020.

Bibliography

[1] Climate change: What the eu is doing? https://www.consilium.europa.eu/en/policies/climate-change/. Accessed: 2022-11-26. 46

[2] Di Bella Gabriel, Flanagan Mark, Foda Karim, Maslova Svitlana, Pienkowski Alex, Stuermer Martin, and Toscani Frederik. Natural gas in europe: The potential impact of disruptions to supply, 2022. 33, 47

[3] Gas factsheet. https://www.acer.europa.eu/gas-factsheet. Accessed: 2022-11-26. 47, 51

[4] Urban Persson, Bernd Möller, and Sven Werner. Heat roadmap europe: Identifying strategic heat synergy regions. *Energy Policy*, 74:663–681, 2014. 47

[5] Eurostat data. https://ec.europa.eu/eurostat/cache/infographs/energy/bloc-2c.html. Accessed: 2022-11-26. 33, 48

[6] Eurostat data. https://ec.europa.eu/eurostat/web/products-eurostat-news/-/ddn-20220419-1. Accessed: 2022-11-26. 33, 48, 49

[7] Euractiv. https://rb.gy/hfcs0. Accessed: 2022-11-26. 49

[8] Mason Inman, Greig Aitken, and Scott Zimmerman. Europe gas tracker report. 2021. 49

[9] Ilkka Jokinen, Andreas Lund, Janne Hirvonen, Juha Jokisalo, Risto Kosonen, and Matti Lehtonen. Coupling of the electricity and district heat generation sectors with building stock energy retrofits as a measure to reduce carbon emissions. *Energy Conversion and Management*, 269:115961, 2022. 49

[10] Luc Van Nuffel, João Gorenstein Dedecca, Tycho Smit, and Koen Rademaekers. *Sector coupling: how can it be enhanced in the EU to foster grid stability and decarbonise?* European Parliament Brussels, Belgium, 2018. 50

[11] Majority of eu household energy comes from natural gas. `https://www.brusselstimes.com/241931/majority-of-eu-household-energy-comes-from-natural-gas`. Accessed: 2022-11-26. 33, 50, 51

[12] Konstantinos Kavvadias, Georg Thomassen, Matija Pavičević, and Sylvain Quoilin. Electrifying the heating sector in europe: The impact on the power sector. In *ECOS 2019*. ECOS Association, 2019. 50

[13] David Connolly, Henrik Lund, Brian Vad Mathiesen, Sven Werner, Bernd Möller, Urban Persson, Thomas Boermans, Daniel Trier, Poul Alberg Østergaard, and Steffen Nielsen. Heat roadmap europe: Combining district heating with heat savings to decarbonise the eu energy system. *Energy policy*, 65:475–489, 2014. 51

[14] Lorenzo Di Lucia and Karin Ericsson. Low-carbon district heating in sweden–examining a successful energy transition. *Energy Research & Social Science*, 4:10–20, 2014. 52

[15] Danish Energy Agency. Regulation and planning of district heating in denmark, 2015. 52

[16] City of Copenhagen. Copenhagen district heating system, 2009. 52

[17] Statkraft: Facts about district heating. `https://www.statkraft.com/energysources/district-heating/district-heating-briefly-explained/`. Accessed: 2019-09-14. 33, 53

[18] Yi Dou, Lu Sun, Minoru Fujii, Yasunori Kikuchi, Yuichiro Kanematsu, and Jingzheng Ren. Towards a renewable-energy-driven district heating system: key technology, system design and integrated planning. *Renewable-Energy-Driven Future*, pages 311–332, 2021. 33, 54

[19] Henrik Lund, Sven Werner, Robin Wiltshire, Svend Svendsen, Jan Eric Thorsen, Frede Hvelplund, and Brian Vad Mathiesen. 4th generation district heating (4gdh): Integrating smart thermal grids into future sustainable energy systems. *Energy*, 68:1–11, 2014. 54, 56, 74, 114

[20] Adbioresources. `https://adbioresources.org/about-ad/using-biogas/heat/`. Accessed: 2022-11-26. 33, 55

[21] Lisa Brand, Alexandra Calvén, Jessica Englund, Henrik Landersjö, and Patrick Lauenburg. Smart district heating networks–a simulation study of prosumers' impact on technical parameters in distribution networks. *Applied Energy*, 129:39–48, 2014. 55, 78

[22] Lisa Brange, Jessica Englund, and Patrick Lauenburg. Prosumers in district heating networks–a swedish case study. *Applied Energy*, 164:492–500, 2016. 55, 62, 65, 78

[23] Henrik Lund, Poul Alberg Østergaard, David Connolly, and Brian Vad Mathiesen. Smart energy and smart energy systems. *Energy*, 137:556–565, 2017. 56

[24] Felix Schmid. Sewage water: interesting heat source for heat pumps and chillers. In *Proceedings of the 9th International IEA Heat Pump Conference, Zürich, Switzerland*, pages 20–22, 2008. 33, 57

[25] Marco Pellegrini and Augusto Bianchini. The innovative concept of cold district heating networks: a literature review. *Energies*, 11(1):236, 2018. 57, 58, 64

[26] Svend Frederiksen and Sven Werner. *District heating and cooling.* Studentlitteratur, 2013. 34, 58, 60, 77, 82, 83

[27] Aec online. https://www.aeconline.ae/13/pdcnewsitem/00/98/45/index_13.html. Accessed: 2022-11-26. 33, 59

[28] Gustavo Franco Barbosa, Jonas de Carvalho, et al. A proper framework for design of aircraft production system based on lean manufacturing principles focusing to automated processes. *The International Journal of Advanced Manufacturing Technology*, 72(9):1257–1273, 2014. 61

[29] Joseph Maria Jebamalai, Kurt Marlein, Jelle Laverge, Lieven Vandevelde, and Martijn van den Broek. An automated gis-based planning and design tool for district heating: Scenarios for a dutch city. *Energy*, 2019. 61, 114, 120, 130, 186

[30] Mohammad Sameti and Fariborz Haghighat. Optimization of 4th generation distributed district heating system: Design and planning of combined heat and power. *Renewable Energy*, 130:371–387, 2019. 62, 65

[31] Eugenia D Mehleri, Haralambos Sarimveis, Nikolaos C Markatos, and Lazaros G Papageorgiou. A mathematical programming approach for optimal design of distributed energy systems at the neighbourhood level. *Energy*, 44(1):96–104, 2012. 62, 63

[32] Yaran Wang, Shijun You, Huan Zhang, Wandong Zheng, Xuejing Zheng, and Qingwei Miao. Hydraulic performance optimization of meshed district heating network with multiple heat sources. *Energy*, 126:603–621, 2017. 62, 63

[33] Netsim. https://www.vitecsoftware.com/en/productareas/energy/products/netsim-grid-simulation/. Accessed: 2022-11-26. 62

[34] Termis. https://www.se.com/il/en/product-range/61613-termis-engineering/#overview. Accessed: 2022-11-26. 62

[35] Mattias Vesterlund and Jan Dahl. A method for the simulation and optimization of district heating systems with meshed networks. *Energy conversion and management*, 89:555–567, 2015. 63

[36] Jonathan Chambers, Kapil Narula, Matthias Sulzer, and Martin K Patel. Mapping district heating potential under evolving thermal demand scenarios and technologies: a case study for switzerland. *Energy*, 2019. 74, 99, 128

[37] Hanne Kauko, Karoline Husevåg Kvalsvik, Daniel Rohde, Natasa Nord, and Åmund Utne. Dynamic modeling of local district heating grids with prosumers: A case study for norway. *Energy*, 151:261–271, 2018. 74

[38] Reducing the capital cost of district heat network infrastructure. Technical report, AECOM and Energy Technology Institute (ETI), 2017. 33, 75, 76

[39] Hakan Ibrahim Tol and Svend Svendsen. Improving the dimensioning of piping networks and network layouts in low-energy district heating systems connected to low-energy buildings: A case study in roskilde, denmark. *Energy*, 38(1):276–290, 2012. 75, 76, 77, 78, 82

[40] Stanislav Chicherin, Anna Volkova, and Eduard Latõšov. Gis-based optimisation for district heating network planning. *Energy Procedia*, 149:635–641, 2018. 75, 78

[41] Julien F Marquant, L Andrew Bollinger, Ralph Evins, and Jan Carmeliet. A new combined clustering method to analyse the potential of district heating networks at large-scale. *Energy*, 156:73–83, 2018. 75, 85

[42] Jérémy Unternährer, Stefano Moret, Stéphane Joost, and François Maréchal. Spatial clustering for district heating integration in urban energy systems: Application to geothermal energy. *Applied energy*, 190:749–763, 2017. 75, 86

[43] Guidelines for low temperature district heating. Technical report, Danish Energy Agency, 2014. 76

[44] Helge Averfalk and Sven Werner. Essential improvements in future district heating systems. *Energy Procedia*, 116:217–225, 2017. 76

[45] A Dalla Rosa, R Boulter, K Church, and S Svendsen. District heating (dh) network design and operation toward a system-wide methodology for optimizing renewable energy solutions (smores) in canada: A case study. *Energy*, 45(1):960–974, 2012. 43, 78, 81, 82

[46] Axelle Delangle, Romain SC Lambert, Nilay Shah, Salvador Acha, and Christos N Markides. Modelling and optimising the marginal expansion of an existing district heating network. *Energy*, 140:209–223, 2017. 78

[47] Gerald Schweiger, Per-Ola Larsson, Fredrik Magnusson, Patrick Lauenburg, and Stéphane Velut. District heating and cooling systems–framework for modelica-based simulation and dynamic optimization. *Energy*, 137:566–578, 2017. 78

[48] Alessandro Dalla Rosa and Jørgen Erik Christensen. Low-energy district heating in energy-efficient building areas. *Energy*, 36(12):6890–6899, 2011. 78

[49] Nijmegen - european green capital 2018. `https://greencapital2018.nl/en/`. Accessed: 2019-05-07. 80

[50] Isabelle Best, Janybek Orozaliev, and Klaus Vajen. Impact of different design guidelines on the total distribution costs of 4th generation district heating networks. *Energy Procedia*, 149:151–160, 2018. 82

[51] Specifications for installations inside buildings conveying water for human consumption, pipe sizing, simplified method. Technical report, BSI and CEN, 2006. 82, 83

[52] Code of practice for domestic water supply installations. Technical report, Dansk Standardiseringsrad (DS), 2009. 82

[53] Design and installation of preinsulated bonded pipe systems for district heating. Technical report, BSI and CEN, 2010. 43, 85, 96

[54] Design manual. Technical report, Logstor, 2015. 43, 44, 85, 122, 185

[55] James MacQueen et al. Some methods for classification and analysis of multivariate observations. In *Proceedings of the fifth Berkeley symposium on mathematical statistics and probability*, volume 1, pages 281–297. Oakland, CA, USA, 1967. 86

[56] Fionn Murtagh and Pedro Contreras. Methods of hierarchical clustering. *arXiv preprint arXiv:1105.0121*, 2011. 86

[57] Kohei Arai and Ali Ridho Barakbah. Hierarchical k-means: an algorithm for centroids initialization for k-means. *Reports of the Faculty of Science and Engineering*, 36(1):25–31, 2007. 86

[58] Franco Robledo Amoza. *GRASP heuristics for Wide Area Network design*. PhD thesis, Universidad de la República, 2005. 88

[59] Thomas H Cormen, Charles E Leiserson, Ronald L Rivest, and Clifford Stein. *Introduction to algorithms*. MIT press, 2009. 88

[60] Edsger W Dijkstra. A note on two problems in connexion with graphs. *Numerische mathematik*, 1(1):269–271, 1959. 88

[61] Robert Clay Prim. Shortest connection networks and some generalizations. *Bell system technical journal*, 36(6):1389–1401, 1957. 88

[62] Joseph B Kruskal. On the shortest spanning subtree of a graph and the traveling salesman problem. *Proceedings of the American Mathematical society*, 7(1):48–50, 1956. 88

[63] Stuart J Russell and Peter Norvig. *Artificial intelligence: a modern approach*. Malaysia; Pearson Education Limited, 2016. 88

[64] Zbigniew Michalewicz and David B Fogel. Traditional methods—part 1. In *How to Solve It: Modern Heuristics*, pages 55–81. Springer, 2004. 88

[65] Milan Stanojevic and Mirko Vujoševic. An exact algorithm for steiner tree problem on graphs. *International Journal of Computers Communications & Control*, 1(1):41–46, 2006. 88

[66] Eduardo Uchoa and Renato F Werneck. Fast local search for steiner trees in graphs. In *Proceedings of the Meeting on Algorithm Engineering & Expermiments*, pages 1–10. Society for Industrial and Applied Mathematics, 2010. 88

[67] Hazen-willams pipe roughness coefficient. `https://www.engineeringtoolbox.com/hazen-williams-coefficients-d_798.html`. Accessed: 2022-11-30. 43, 89, 90

[68] Glenn O Brown. The history of the darcy-weisbach equation for pipe flow resistance. *Environmental and Water Resources History*, 38(7):34–43, 2002. 89

[69] PK Swanee and Akalank K Jain. Explicit equations for pipeflow problems. *Journal of the hydraulics division*, 102(5), 1976. 90

[70] Lewis F Moody. Friction factors for pipe flow. *Trans. Asme*, 66:671–684, 1944. 34, 90, 91

[71] Frank M White. *Fluid mechanics*. Tata McGraw-Hill Education, 1979. 34, 92

[72] Chyr Pyng Liou. Limitations and proper use of the hazen-williams equation. *Journal of Hydraulic Engineering*, 124(9):951–954, 1998. 91

[73] Srbislav Genić, Ivan Aranđelović, Petar Kolendić, Marko Jarić, Nikola Budimir, and Vojislav Genić. A review of explicit approximations of colebrook's equation. *FME transactions*, 39(2):67–71, 2011. 91

[74] Bram van der Heijde. Optimal integration of thermal energy storage and conversion in fourth generation thermal networks. 2019. 91, 122

[75] Petter Wallentén. *Steady-state heat loss from insulated pipes*. PhD thesis, Division of Building Physics, 1991. 97

[76] Giovanni Manente, Andrea Lazzaretto, Ivan Molinari, and Federico Bronzini. Optimization of the hydraulic performance and integration of a heat storage in the geothermal and waste-to-energy district heating system of ferrara. *Journal of Cleaner Production*, 230:869–887, 2019. 113, 116

[77] Russell McKenna, D Fehrenbach, and E Merkel. The role of seasonal thermal energy storage in increasing renewable heating shares: A techno-economic analysis for a typical residential district. *Energy and Buildings*, 187:38–49, 2019. 113

[78] M Köfinger, RR Schmidt, D Basciotti, O Terreros, I Baldvinsson, J Mayrhofer, S Moser, R Tichler, and H Pauli. Simulation based evaluation of large scale waste heat utilization in urban district heating networks: Optimized integration and operation of a seasonal storage. *Energy*, 159:1161–1174, 2018. 113

[79] Nicholas Good, Lingxi Zhang, Alejandro Navarro-Espinosa, and Pierluigi Mancarella. High resolution modelling of multi-energy domestic demand profiles. *Applied Energy*, 137:193–210, 2015. 114

[80] Henrik Gadd and Sven Werner. Daily heat load variations in swedish district heating systems. *Applied Energy*, 106:47–55, 2013. 114, 129

[81] Michal Turski and Robert Sekret. Buildings and a district heating network as thermal energy storages in the district heating system. *Energy and Buildings*, 179:49–56, 2018. 114, 116

[82] Elisa Guelpa and Vittorio Verda. Thermal energy storage in district heating and cooling systems: A review. *Applied Energy*, 252:113474, 2019. 114

[83] Vittorio Verda and Francesco Colella. Primary energy savings through thermal storage in district heating networks. *Energy*, 36(7):4278–4286, 2011. 116, 117

[84] Dmytro Romanchenko, Johan Kensby, Mikael Odenberger, and Filip Johnsson. Thermal energy storage in district heating: Centralised storage vs. storage in thermal inertia of buildings. *Energy conversion and management*, 162:26–38, 2018. 116, 117

[85] Charlotte Marguerite, Gorm Bruun Andresen, and Magnus Dahl. Multi-criteria analysis of storages integration and operation solutions into the district heating network of aarhus–a simulation case study. *Energy*, 158:81–88, 2018. 117

[86] Thomas Nuytten, Bert Claessens, Kristof Paredis, Johan Van Bael, and Daan Six. Flexibility of a combined heat and power system with thermal energy storage for district heating. *Applied Energy*, 104:583–591, 2013. 117

[87] Georg K Schuchardt. Integration of decentralized thermal storages within district heating (dh) networks. *Environmental and Climate Technologies*, 18(1):5–16, 2016. 117

[88] Synthetic load profiles of belgium gas and electricty grids. `http://www.synergrid.be/index.cfm?PageID=16896`. Accessed: 2019-10-25. 35, 119, 121, 129

[89] Technology brief e16, energy technology systems analysis programme. Technical report, International Energy Agency (IEA), 2013. 43, 44, 120, 122, 185, 186

[90] Jan Erik Nielsen. Iea-shc task 45: Large solar heating/cooling systems, seasonal storage, heat pumps. *Energy Procedia*, 30:849–855, 2012. 35, 124

[91] D Connolly, D Drysdale, K Hansen, and T Novose. Creating hourly profiles to model both demand and supply, 2015. 129

[92] Chiara Bordin, Angelo Gordini, and Daniele Vigo. An optimization approach for district heating strategic network design. *European Journal of Operational Research*, 252(1):296–307, 2016. 153

[93] Théophile Mertz, Sylvain Serra, Aurélien Henon, and Jean-Michel Reneaume. A minlp optimization of the configuration and the design of a district heating network: Academic study cases. *Energy*, 117:450–464, 2016. 153

[94] Mattias Vesterlund and Jan Dahl. A method for the simulation and optimization of district heating systems with meshed networks. *Energy conversion and management*, 89:555–567, 2015. 153

[95] Boran Morvaj, Ralph Evins, and Jan Carmeliet. Optimising urban energy systems: Simultaneous system sizing, operation and district heating network layout. *Energy*, 116:619–636, 2016. 153

[96] Tingting Fang and Risto Lahdelma. Genetic optimization of multi-plant heat production in district heating networks. *Applied Energy*, 159:610–619, 2015. 153

[97] Yaran Wang, Shijun You, Huan Zhang, Wandong Zheng, Xuejing Zheng, and Qingwei Miao. Hydraulic performance optimization of meshed district heating network with multiple heat sources. *Energy*, 126:603–621, 2017. 153

[98] Joakim Widén et al. Development, validation and application of a fixed district heating model structure that requires small amounts of input data. *Energy Conversion and Management*, 75:74–85, 2013. 153

[99] Kevin Sartor, Sylvain Quoilin, and Pierre Dewallef. Simulation and optimization of a chp biomass plant and district heating network. *Applied Energy*, 130:474–483, 2014. 154

[100] Marouf Pirouti, Audrius Bagdanavicius, Janaka Ekanayake, Jianzhong Wu, and Nick Jenkins. Energy consumption and economic analyses of a district heating network. *Energy*, 57:149–159, 2013. 154

[101] Kamal Kuriyan and Nilay Shah. A combined spatial and technological model for the planning of district energy systems. *International Journal of Sustainable Energy Planning and Management*, 21, 2019. 154

[102] Joseph Maria Jebamalai, Kurt Marlein, and Jelle Laverge. Influence of centralized and distributed thermal energy storage on district heating network design. *Energy*, 202:117689, 2020. 157, 162

[103] Joseph Maria Jebamalai, Kurt Marlein, Jelle Laverge, Lieven Vandevelde, and Martijn van den Broek. An automated gis-based planning and design tool for district heating: Scenarios for a dutch city. *Energy*, 183:487–496, 2019. 158

[104] Edsger W Dijkstra. A note on two problems in connexion with graphs. In *Edsger Wybe Dijkstra: His Life, Work, and Legacy*, pages 287–290. 2022. 160

[105] Glenn O Brown. The history of the darcy-weisbach equation for pipe flow resistance. In *Environmental and water resources history*, pages 34–43. 2003. 161

[106] Prabhata K Swamee and Akalank K Jain. Explicit equations for pipe-flow problems. *Journal of the hydraulics division*, 102(5):657–664, 1976. 161

[107] Rémi Patureau, Cong Toan Tran, Valentin Gavan, and Pascal Stabat. The new generation of district heating & cooling networks and their potential development in france. *Energy*, 236:121477, 2021. 178

[108] Michele Tunzi, Dorte Skaarup Østergaard, Svend Svendsen, Rabah Boukhanouf, and Edward Cooper. Method to investigate and plan the application of low temperature district heating to existing hydraulic radiator systems in existing buildings. *Energy*, 113:413–421, 2016. 178

[109] Saleh S Meibodi and Fleur Loveridge. The future role of energy geostructures in fifth generation district heating and cooling networks. *Energy*, page 122481, 2021. 179

[110] Michael-Allan Millar, Neil M Burnside, and Zhibin Yu. District heating challenges for the uk. *Energies*, 12(2):310, 2019. 179

[111] Laurent Gagné-Boisvert and Michel Bernier. Integrated model for comparison of one-and two-pipe ground-coupled heat pump network configurations. *Science and Technology for the Built Environment*, 24(7):726–742, 2018. 179

[112] Ankita Singh Gaur, Desta Z Fitiwi, and John Curtis. Heat pumps and our low-carbon future: A comprehensive review. *Energy Research & Social Science*, 71:101764, 2021. 180

[113] J Barco-Burgos, JC Bruno, U Eicker, AL Saldaña-Robles, and V Alcántar-Camarena. Review on the integration of high-temperature heat pumps in district heating and cooling networks. *Energy*, page 122378, 2021. 180

[114] Tobias Sommer, Matthias Sulzer, Michael Wetter, Artem Sotnikov, Stefan Mennel, and Christoph Stettler. The reservoir network: A new network topology for district heating and cooling. *Energy*, 199:117418, 2020. 180

[115] Simone Buffa, Marco Cozzini, Matteo D'antoni, Marco Baratieri, and Roberto Fedrizzi. 5th generation district heating and cooling systems: A review of existing cases in europe. *Renewable and Sustainable Energy Reviews*, 104:504–522, 2019. 180

[116] Hakan Ibrahim Tol and Svend Svendsen. Improving the dimensioning of piping networks and network layouts in low-energy district heating systems connected to low-energy buildings: A case study in roskilde, denmark. *Energy*, 38(1):276–290, 2012. 182, 183

[117] Hakan İbrahim Tol and Svend Svendsen. Effects of boosting the supply temperature on pipe dimensions of low-energy district heating networks: A case study in gladsaxe, denmark. *Energy and Buildings*, 88:324–334, 2015. 182, 183

[118] Felix Bünning, Michael Wetter, Marcus Fuchs, and Dirk Müller. Bidirectional low temperature district energy systems with agent-based control: Performance comparison and operation optimization. *Applied Energy*, 209:502–515, 2018. 182, 183

[119] Rasmus Lund, Dorte Skaarup Østergaard, Xiaochen Yang, and Brian Vad Mathiesen. Comparison of low-temperature district heating concepts in a long-term energy system perspective. *International Journal of Sustainable Energy Planning and Management*, 12:5–18, 2017. 182, 183, 199

[120] Dorte Østergaard and Svend Svendsen. Space heating with ultra-low-temperature district heating–a case study of four single-family houses from the 1980s. *Energy Procedia*, 116:226–235, 2017. 182, 183

[121] Jing Zeng, Jie Han, and Guoqiang Zhang. Diameter optimization of district heating and cooling piping network based on hourly load. *Applied Thermal Engineering*, 107:750–757, 2016. 183

[122] Michele Tunzi, Matthieu Ruysschaert, Svend Svendsen, and Kevin Michael Smith. Double loop network for combined heating and cooling in low heat density areas. *Energies*, 13(22):6091, 2020. 183

[123] Cordin Arpagaus, Frederic Bless, Michael Uhlmann, Jurg Schiffmann, and Stefan S Bertsch. High temperature heat pumps: Market overview, state of the art, research status, refrigerants, and application potentials. *Energy*, 152:985–1010, 2018. 44, 184, 186

[124] Steven Meyers, Bastian Schmitt, and Klaus Vajen. The future of low carbon industrial process heat: A comparison between solar thermal and heat pumps. *Solar Energy*, 173:893–904, 2018. 44, 184, 186

[125] Oddgeir Gudmundsson, Ralf-Roman Schmidt, Anders Dyrelund, and Jan Eric Thorsen. Economic comparison of 4gdh and 5gdh systems–using a case study. *Energy*, 238:121613, 2022. 44, 184, 186

[126] Joseph Maria Jebamalai, Kurt Marlein, and Jelle Laverge. Influence of centralized and distributed thermal energy storage on district heating network design. *Energy*, 202:117689, 2020. 187, 193

[127] Brian Vad Mathiesen and Henrik Lund. Comparative analyses of seven technologies to facilitate the integration of fluctuating renewable energy sources. *IET Renewable Power Generation*, 3(2):190–204, 2009. 203

[128] David Connolly and Brian Vad Mathiesen. A technical and economic analysis of one potential pathway to a 100% renewable energy system. *International Journal of Sustainable Energy Planning and Management*, 1:7–28, 2014. 203

[129] Rasmus Lund and Urban Persson. Mapping of potential heat sources for heat pumps for district heating in denmark. *Energy*, 110:129–138, 2016. 203

[130] Jacopo Vivian, Giuseppe Emmi, Angelo Zarrella, Xavier Jobard, Dirk Pietruschka, and Michele De Carli. Evaluating the cost of heat for end users in ultra low temperature district heating networks with booster heat pumps. *Energy*, 153:788–800, 2018. 204

[131] Poul Alberg Østergaard and Anders N Andersen. Booster heat pumps and central heat pumps in district heating. *Applied Energy*, 184:1374–1388, 2016. 204

[132] Torben Ommen, Jan Eric Thorsen, Wiebke Brix Markussen, and Brian Elmegaard. Performance of ultra low temperature district heating systems with utility plant and booster heat pumps. *Energy*, 137:544–555, 2017. 204

[133] Wiebke Meesenburg, Torben Ommen, Jan Eric Thorsen, and Brian Elmegaard. Economic feasibility of ultra-low temperature district heating systems in newly built areas supplied by renewable energy. *Energy*, 191:116496, 2020. 204

[134] Xiaochen Yang and Svend Svendsen. Ultra-low temperature district heating system with central heat pump and local boosters for low-heat-density area: Analyses on a real case in denmark. *Energy*, 159:243–251, 2018. 204

A small neighbourhood with district heating network supplied by renewable energy sources.